Modulation of FGF pathway signaling and vascular differentiation using designed oligomeric assemblies

Ashish Phal

A dissertation
submitted in partial fulfillment of the
requirements for the degree of

Doctor of Philosophy

University of Washington
2024

Reading Committee:
Hannele Ruohola-Baker, Chair
David Mack
Julie Mathieu

Program Authorized to Offer Degree:
Bioengineering

©Copyright 2024
Ashish Phal

University of Washington

ABSTRACT

Modulation of FGF pathway signaling and vascular differentiation using designed oligomeric assemblies

Ashish Phal

Chair of the Supervisory Committee:
Hannele Ruohola-Baker
Department of Biochemistry

During embryonic development, cell fate decisions are orchestrated through spatiotemporal modulation of extracellular cues. The precise molecular mechanisms by which cells decode these signals to regulate lineage commitment remain an outstanding question in developmental biology. Growth factors and cytokines initiate intracellular signaling cascades by engaging the extracellular domains of receptor tyrosine kinases (RTKs), facilitating receptor oligomerization and transphosphorylation of intracellular kinase domains. The Fibroblast Growth Factor (FGF) signaling axis, in particular, is a key determinant of cell fate and survival, yet the isoform-specific functions of alternatively spliced FGF receptor variants during development remain poorly understood. To systematically interrogate the role of FGFR valency and geometry in signaling dynamics, we engineered synthetic cyclic homo-oligomers derived from repeat protein building blocks. These scaffolds were functionalized with a *de novo* designed binding module specific for the c-splice variant of FGFR1/2, enabling controlled activation. These synthetic FGFR1/2c signaling ligands exhibited potent valency- and geometry- dependent Ca^{2+} release and MAPK pathway activation. We also showed that these synthetic agonists have a capacity to drive endothelial cell differentiation through an FGF-mimetic trajectory. By leveraging these tools, we delineated isoform-specific roles of FGFR variants in early vascular development. Selective activation of the c-isoform promoted endothelial cell specification, with a marked bias toward arterial endothelial cell fate, whereas antagonists selective for the b-isoform preferentially directed differentiation toward perivascular cell lineages. Endothelial cells derived from human iPSCs using the c-isoform agonists were functionally mature, integrating seamlessly into vascular networks in vivo. These findings demonstrate the capability of engineered FGFR1/2c agonists to dissect FGFR variant functions in development, offering a tool to untangle signaling complexities during critical developmental transitions. Furthermore, leveraging computationally designed PRC2 inhibitors fused to dCas9, we demonstrate the targeted upregulation of p16 in diffuse midline gliomas, resulting in a significant reduction in tumor cell viability. These findings underscore the therapeutic potential of epigenetic reprogramming in cancer.

TABLE OF CONTENTS

LIST OF ABBREVIATIONS

ABBREVIATION	DEFINITION
AKT	Alpha Serine/Threonine-Protein Kinase
BBB	Blood-Brain Barrier
BMP4	Bone Morphogenetic Protein 4
BSA	Bovine Serum Albumin
CHO	Chinese Hamster Ovary
DAG	Diacylglycerol
DAPI	4',6-Diamidino-2-Phenylindole
DNA	Deoxyribonucleic Acid
ECGS	Endothelial Cell Growth Supplement
EGFR	Epithelial Growth Factor Receptor
EGM2	Endothelial Growth Media 2
EMT	Epithelial-to-Mesenchymal Transition
ERK	Extracellular Signal Regulated Kinase
FACS	Fluorescence-Activated Cell Sorting
FBS	Fetal Bovine Serum
FGF	Fibroblast Growth Factor
FGFR	Fibroblast Growth Factor Receptor
FRS2	Fibroblast Growth Factor Receptor Substrate 2
GFP	Green Fluorescent Protein
GSK3	Glycogen Synthase Kinase 3
HDAC	Histone Deacetylase
HEPES	2-[4-(2-Hydroxyethyl) Piperazin-1-yl] Ethane Sulfonic Acid
HER2	Human Epithelial Growth Factor Receptor 2
HRP	Horseradish Peroxidase
HUVEC	Human Umbilical Vein Endothelial Cell
Ig	Immunoglobulin

IP3	Inositol Triphosphate
iPSC	Induced Pluripotent Stem Cell
KOSR	Knock-Out Serum Replacement
LDL	Low Density Lipoprotein
MAPK	Mitogen Activated Protein Kinase
MTG	1-Thioglycerol
NOD-SCID	Nonobese Diabetic / Severe Combined Immunodeficiency
PBS	Phosphate Buffered Saline
PCA	Principal Component Analysis
PDGF-B	Platelet Derived Growth Factor beta
PFA	Paraformaldehyde
PI3K	Phosphoinositide 3-Kinase
PIP2	Phosphatidylinositol 4,5-Bisphosphate
PKC	Protein Kinase C
PLC-γ	Phospholipase C Gamma
PRC2	Polycomb Repressive Complex 2
PTB	Phospho-Tyrosine-Binding
PTP	Protein Tyrosine Phosphatase
RAF	Rapidly Accelerated Fibrosarcoma
RNA	Ribonucleic Acid
RTK	Receptor Tyrosine Kinase
SDS	Sodium Dodecyl Sulfate
SH2	Src Homology 2
SHH	Sonic Hedgehog
SOS	Son of Sevenless
TGF-β	Transforming Growth Factor beta
TNF-α	Tumor Necrosis Factor alpha
UMI	Unique Molecular Identifier
VEGF	Vascular Endothelial Growth Factor
VEGFR	Vascular Endothelial Growth Factor Receptor

VSMC	Vascular Smooth Muscle Cell

INTRODUCTION

CELLULAR SIGNALING AS A DRIVER OF DEVELOPMENT

GROWTH FACTORS AND CYTOKINE SIGNALING

Cellular signaling is a fundamental process that enables cells to sense and respond to extracellular cues, facilitating coordinated behaviors essential for development, tissue homeostasis, and repair. Growth factors and cytokines act as primary extracellular messengers, binding to specific receptors on the cell's surface to initiate intracellular signaling cascades that regulate key processes such as cell division, migration, differentiation, and apoptosis.[1] For example, fibroblast growth factors (FGFs) are growth factors that are essential regulators of mesoderm induction and limb development, as evidenced by Fgf8 knockout studies, which demonstrated severe defects in mesoderm formation and limb bud outgrowth.[2, 3] Similarly, the transforming growth factor-beta (TGF-β) signaling pathway is crucial for epithelial-to-mesenchymal transitions (EMT), which drive processes like gastrulation and organogenesis. TGF-β1-mediated EMT has been shown to regulate mesenchymal marker expression, including Snail and Twist, during heart valve and neural crest development.[4, 5] Another critical pathway, the Wnt/β-catenin signaling axis, is indispensable for axis specification during early embryogenesis. Genetic studies in Xenopus and mice have shown that Wnt3 is essential for anterior-posterior axis formation, with β-catenin functioning as a transcriptional co-activator to regulate gene expression in this context.[6, 7]

In addition to regulating individual cells, signaling via secreted ligands enables crosstalk between different cell types within the same tissue. This intercellular communication ensures that cells develop in tandem to form functional tissues and organs. For example, during lung bud development, mesenchymal cells secrete FGF-10, which binds to FGFR2b receptors on the endodermal epithelium, promoting epithelial proliferation and branching morphogenesis. In turn, the endodermal epithelium secretes Sonic Hedgehog (SHH), which acts on mesenchymal cells to spatially restrict FGF-10 expression, ensuring balanced and patterned outgrowth of lung buds.[8, 9] Another

example of ligand-mediated crosstalk is seen in angiogenesis, where endothelial and perivascular cells exchange signals to maintain vessel stability. Endothelial cells secrete PDGF-B to recruit pericytes, which stabilize nascent vessels by depositing extracellular matrix and producing TGF-β, a factor that reinforces endothelial barrier integrity. Such reciprocal signaling ensures the proper morphogenesis and maintenance of blood vessels.[10] Such crosstalk establishes reciprocal feedback loops that synchronize cell fate decisions and spatial organization. This dynamic interplay exemplifies the complexity of signaling during development and underscores its importance in tissue morphogenesis.

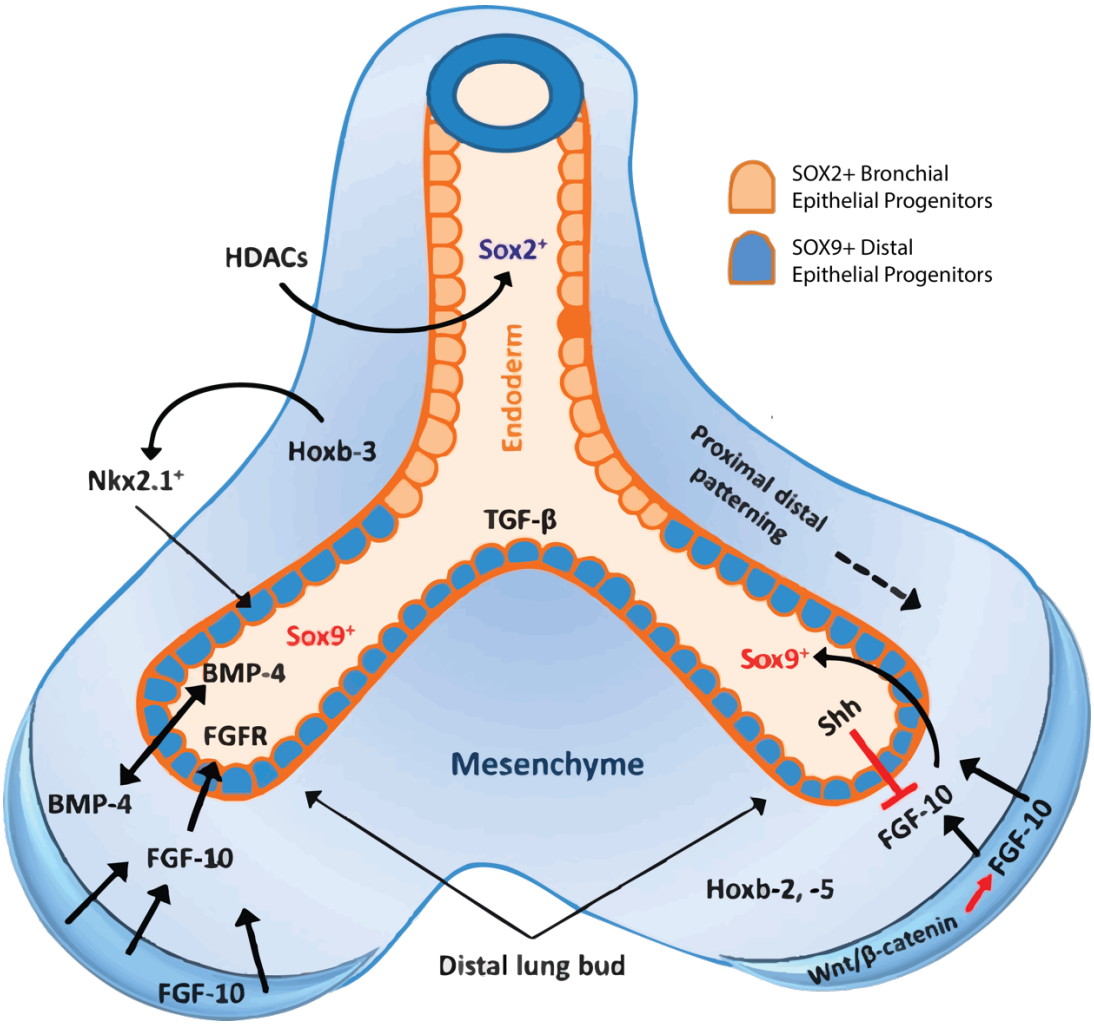

Fig 1: Signaling interactions between the endoderm and mesenchyme during lung bud development. FGFs, BMP-4, and Wnt/β-catenin pathways coordinate proximal-distal patterning, with SOX2+ cells marking the proximal endoderm and SOX9+ cells marking the distal regions. TGF-β signaling and feedback loops, including SHH and FGF-10, regulate mesenchymal and epithelial crosstalk. These pathways collectively drive tissue specification, branching morphogenesis, and organogenesis. *(adapted from [8])*

ROLE OF RECEPTOR TYROSINE KINASES IN DEVELOPMENT

Receptor tyrosine kinases (RTKs) are integral components of cellular signaling networks, mediating the effects of numerous growth factors and cytokines.[1] These transmembrane proteins are activated when extracellular ligands bind to their receptor domains, inducing receptor dimerization or oligomerization. For instance, fibroblast growth factor (FGF) binding to FGFR triggers receptor dimerization, a prerequisite for downstream signaling.[11] This structural rearrangement brings intracellular kinase domains into close proximity, enabling transphosphorylation of specific tyrosine residues within the cytoplasmic domain. These phosphorylated residues serve as docking sites for adaptor proteins, triggering downstream signaling cascades such as the mitogen-activated protein kinase (MAPK) pathway, phosphoinositide 3-kinase (PI3K)-AKT pathway, and phospholipase C-gamma (PLCγ) pathway.[1, 11]

The mitogen-activated protein kinase (MAPK) pathway is one such effector pathway, activated via Grb2 and SOS-mediated recruitment of RAS, which triggers a phosphorylation cascade involving RAF, MEK, and ERK. This pathway regulates gene expression and promotes cellular proliferation and differentiation.[12] The PI3K-AKT pathway, initiated by recruitment of PI3K to the receptor, is critical for cell survival and metabolism, as AKT activation leads to inhibition of pro-apoptotic factors.[13] Meanwhile, the PLC-γ pathway generates inositol triphosphate (IP3) and diacylglycerol (DAG), mobilizing intracellular calcium and activating protein kinase C (PKC), which governs cytoskeletal dynamics and vesicle trafficking.[14] Collectively, these pathways regulate gene expression, cytoskeletal organization, and cell survival, processes that are essential for proper embryonic development and tissue homeostasis.

The spatial and temporal regulation of receptor tyrosine kinase (RTK) signaling is critical for achieving specificity in developmental outcomes. The precise activation and downstream signaling of RTKs ensure that cells respond appropriately to extracellular cues during processes such as organogenesis, patterning, and differentiation. Dysregulation of RTK signaling, whether through mutations, overactivation, or impaired feedback mechanisms, often results in severe developmental disorders and diseases. For example, activating mutations in FGFR2 and FGFR3 are implicated in craniofacial defects, where premature fusion of cranial sutures disrupts skull development.[15] Similarly, mutations in EGFR or aberrant HER2 signaling are frequently associated with cancer progression, where unchecked RTK activity drives proliferation, invasion, and metastasis.[16]

DYNAMICS OF SIGNALING: BINDING, DIMERIZATION AND DOWNSTREAM CASCADES

The dynamics of receptor-ligand interactions underpin the initiation of cellular signaling, with receptor tyrosine kinases (RTKs) serving as a canonical model for this process. In their inactive state, RTKs typically exist as monomers, with their kinase domains maintained in an inactive conformation due to steric and conformational constraints.[1] This autoinhibition prevents premature activation of downstream signaling pathways, ensuring spatial and temporal specificity in cellular responses. The binding of a growth factor or cytokine to the extracellular ligand-binding domain induces receptor dimerization, a critical structural event required for signaling initiation. For example, the binding of epidermal growth factor (EGF) to EGFR induces conformational changes in the extracellular domain, exposing dimerization arms that facilitate receptor pairing.[17]

Growth factors such as fibroblast growth factors (FGFs) and epidermal growth factor (EGF) bind to specific sites on the extracellular domain of receptor tyrosine kinases (RTKs), stabilizing receptor dimer formation. This binding typically involves multiple contact points between the ligand and receptor, creating a high-affinity interaction that is essential for signaling activation.[18] For example, FGFs interact not only with their receptors but also with heparin or heparan sulfate proteoglycans (HSPGs), which serve

as co-factors to stabilize the receptor-ligand complex and promote dimerization.[1, 19] These co-factors bridge FGFs and their receptors, increasing binding specificity and enhancing downstream signaling efficiency. The stabilization of receptor dimers through ligand binding aligns the two extracellular domains in a conformation that facilitates subsequent steps in signaling activation. This alignment propagates structural changes across the transmembrane domain, bringing the intracellular kinase domains into proximity for transphosphorylation. In FGFRs, the interaction with HSPGs has been shown to not only stabilize the receptor-ligand complex but also increase the local concentration of ligand, further enhancing signaling fidelity and efficiency.[11] These intricate interactions highlight the critical role of extracellular co-factors in fine-tuning RTK activation and downstream signaling cascades.

The dimerization of receptor tyrosine kinases (RTKs) induces conformational changes that propagate across the transmembrane domain to the intracellular kinase domain. The transmembrane domain undergoes slight rotational and translational movements, which are critical for aligning the intracellular domains of the receptor pair in an orientation that facilitates activation. These structural rearrangements bring the kinase domains into close proximity, allowing them to overcome autoinhibitory mechanisms and enabling transphosphorylation.[20]

In the active dimer, the intracellular kinase domains phosphorylate specific tyrosine residues on the opposite receptor monomer in a process known as transphosphorylation. These phosphorylated tyrosines serve two primary functions:

- **Activation of Kinase Activity**: Initial phosphorylation events occur within the activation loop of the kinase domain, stabilizing it in an open and active conformation. Structural studies of insulin receptor kinase revealed that phosphorylation of tyrosines within the activation loop induces a conformational shift, increasing the accessibility of the active site and enhancing catalytic efficiency.[21]
- **Docking Sites for Adaptor Proteins**: Phosphorylated tyrosines outside the kinase domain act as docking sites for downstream signaling proteins. These

proteins typically recognize phospho-tyrosine residues through Src homology 2 (SH2) or phospho-tyrosine-binding (PTB) domains, initiating signaling cascades.[1]

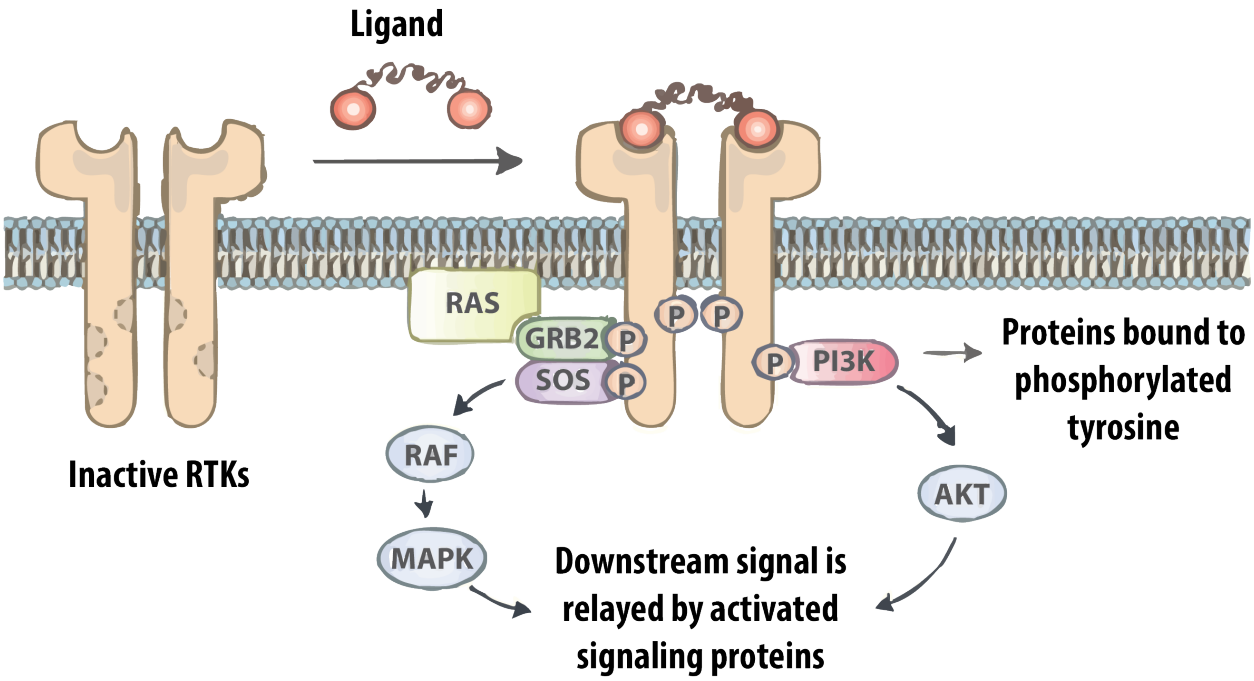

Fig 2: Simplified schematic of receptor tyrosine kinase (RTK) signaling. Ligand binding induces receptor dimerization, leading to the phosphorylation (P) of specific tyrosine residues within the intracellular domains. Phosphorylated tyrosines serve as docking sites for adaptor proteins such as GRB2 and SOS, which activate the MAPK pathway (via RAF) and the PI3K-AKT pathway. These downstream signaling cascades regulate cell proliferation, survival, and differentiation. *(adapted from [23])*

Once adaptor proteins bind to phosphorylated tyrosines on receptor tyrosine kinases (RTKs), they recruit and activate downstream effector proteins that propagate the signal through canonical pathways such as MAPK, PI3K-AKT, and PLC-γ. RTK signaling is tightly regulated to prevent aberrant activation and maintain cellular homeostasis. Negative feedback mechanisms play a crucial role in terminating or modulating the signal. One such mechanism is receptor internalization via clathrin-mediated endocytosis. Once internalized, RTKs can follow distinct fates: they may be recycled back to the plasma membrane for reuse, or they may be targeted to lysosomes for

degradation, permanently terminating the signal.[22] This sorting decision is influenced by factors such as the duration of ligand binding and receptor ubiquitination status.

In addition to receptor trafficking, protein tyrosine phosphatases (PTPs) dephosphorylate activated receptors, counteracting kinase activity and attenuating signaling. For example, PTP1B has been shown to dephosphorylate EGFR and insulin receptor kinase, thereby modulating the intensity and duration of signaling.[23] The temporal dynamics of these regulatory processes—such as the balance between phosphorylation and dephosphorylation—dictate the duration, strength, and spatial localization of the signaling response, ensuring proper cellular behavior during development and tissue repair.

EPIGENETIC REGULATION

While growth factors and cytokines serve as essential extracellular cues orchestrating cellular behavior during development, their effects are profoundly shaped by epigenetic mechanisms that regulate gene expression. Epigenetic modifications, including DNA methylation, histone modifications, chromatin remodeling, and non-coding RNA-mediated processes, alter the chromatin landscape to control transcriptional activity without modifying the underlying DNA sequence.[121, 122, 123] These mechanisms ensure the spatiotemporal coordination of gene expression, which is critical for lineage specification, maintenance of cell identity, and repression of alternative developmental programs.[124, 125] For instance, Polycomb Repressive Complex 2 (PRC2) catalyzes the tri-methylation of histone H3 at lysine 27 (H3K27me3), a hallmark repressive mark that silences key regulatory genes, thereby guiding cellular differentiation and maintaining stemness in progenitor cells.[126]

Epigenetic regulation also provides a layer of adaptability, enabling cells to integrate and sustain responses to transient signaling inputs. Dynamic modifications, such as histone acetylation and phosphorylation, act as molecular switches that either activate or repress gene expression in response to extracellular signals like fibroblast growth factor (FGF) or transforming growth factor-beta (TGF-β).[127, 128] Additionally, epigenetic

modulators facilitate crosstalk between neighboring cells by stabilizing gene expression patterns that coordinate tissue morphogenesis. For example, during neural development, histone deacetylases (HDACs) and PRC2 repress genes promoting alternative cell fates, ensuring proper lineage specification and structural integrity of the developing brain.[129]

These same epigenetic mechanisms, however, are frequently dysregulated in cancer, including gliomas, where they contribute to tumorigenesis and therapy resistance. Aberrant PRC2 activity and H3K27me3 patterns, for instance, can silence tumor suppressor genes or promote a stem-like phenotype that enables cellular plasticity and invasion.[130, 131] Gliomas, particularly diffuse midline gliomas (DMGs), often exhibit mutations in genes encoding histone H3.3, leading to a lysine-to-methionine substitution at position 27 (H3K27M) that dominantly inhibits PRC2 function, resulting in a global reduction of H3K27me3.[132, 133] This epigenetic reprogramming creates a permissive chromatin environment for oncogenic transcriptional programs while simultaneously repressing differentiation pathways.

VASCULAR DEVELOPMENT

VASCULOGENESIS AND ANGIOGENESIS

The formation of the vascular system is one of the earliest and most critical events in embryonic development, providing the growing embryo with essential oxygen and nutrients while facilitating waste removal. Vascular development is broadly categorized into two processes: vasculogenesis and angiogenesis. Vasculogenesis is the de novo formation of blood vessels from mesoderm-derived endothelial progenitor cells, also known as angioblasts. These progenitors migrate and aggregate to form primitive vascular structures such as the dorsal aorta and cardinal veins.[25] This process requires tightly regulated signaling cues, such as vascular endothelial growth factor (VEGF), which guides the differentiation and migration of angioblasts into functional endothelial cells.[26] The assembly of endothelial cells is accompanied by the recruitment of

perivascular cells, including pericytes and vascular smooth muscle cells (VSMCs), which provide structural support and functional specialization as vessels mature.[27]

Endothelial cells, which line the interior surface of blood vessels, primarily arise from the lateral plate mesoderm. This mesodermal region gives rise to progenitor cells that differentiate into the endothelial lining of the circulatory system, forming the initial vascular structures during embryogenesis.[31] Pericytes, the mural cells that envelop endothelial cells and provide structural support to blood vessels, have a more heterogeneous origin. In the central nervous system, pericytes are predominantly derived from neural crest cells. Lineage-tracing studies have demonstrated that neural crest cells migrate and differentiate into pericytes, contributing to the formation and stabilization of the blood-brain barrier.[32] In contrast, pericytes in other tissues, such as skeletal muscle and the retina, can originate from mesodermal sources, including the lateral plate mesoderm. This diversity in origin reflects the complex developmental pathways that converge to establish a functional vascular system.[33] Vasculogenesis primarily occurs during early embryogenesis, setting the foundation for the vascular system.

Angiogenesis, in contrast, involves the sprouting of new blood vessels from pre-existing ones, enabling the vascular network to expand and meet the metabolic demands of growing tissues. This process is driven by endothelial cell proliferation, migration, and remodeling, often in response to hypoxia-induced VEGF expression.[28] Angiogenesis can be further subdivided into two distinct mechanisms. In sprouting angiogenesis, endothelial tip cells extend filopodia toward angiogenic signals, such as VEGF-A, leading the migration of stalk cells and the formation of new vessel branches.[29] Alternatively, in branching angiogenesis, existing vessels undergo longitudinal splitting by forming intraluminal pillars that divide and remodel the vascular lumen, increasing vascular complexity without endothelial proliferation.[30] These mechanisms work in tandem to refine and adapt the vascular network to the requirements of specific tissues. Together, vasculogenesis and angiogenesis form the basis of vascular development,

ensuring the proper delivery of oxygen and nutrients and the removal of waste throughout the organism.

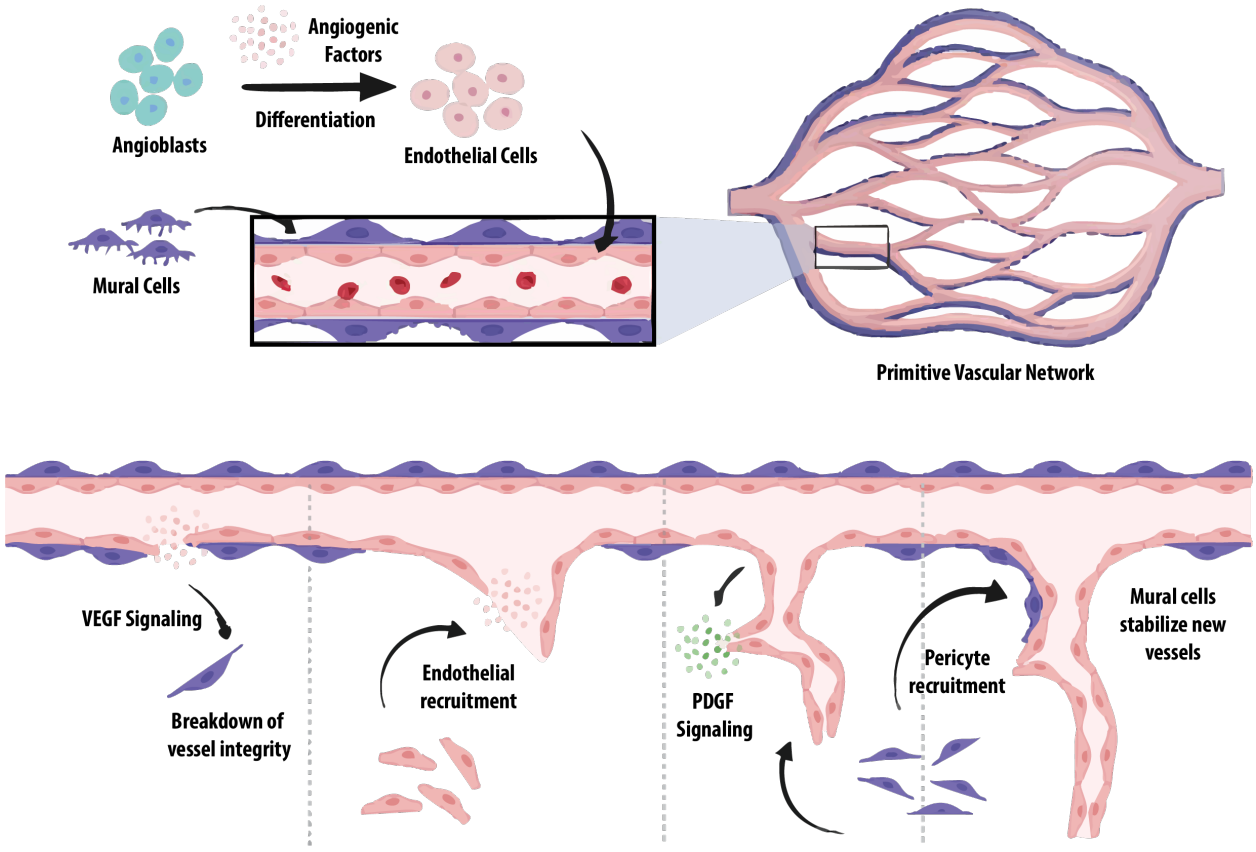

Fig 3: Overview of vasculogenesis and angiogenesis. The top panel illustrates vasculogenesis, where endothelial progenitor cells aggregate and differentiate to form the initial vascular plexus. The bottom panel depicts angiogenesis, which involves the sprouting of new vessels from pre-existing ones. Endothelial cells migrate and proliferate in response to angiogenic signals, followed by lumen formation, stabilization by pericytes, and integration into the vascular network. These processes are critical for establishing and remodeling the vascular system during development and tissue repair. *(adapted from [34])*

ROLE OF ENDOTHELIAL AND PERIVASCULAR CELLS

The vascular system is composed of multiple specialized cell types that work in concert to maintain vascular integrity and functionality. Endothelial cells form the inner lining of blood vessels and are derived from angioblasts, mesodermal progenitors that

differentiate into arterial, venous, or lymphatic endothelial subtypes. These subtypes are distinguished by their unique gene expression profiles and functions, such as the high expression of Ephrin-B2 in arterial endothelial cells and Ephrin-B4 in venous endothelial cells, which guide vessel specification during development.[35] Lymphatic endothelial cells, marked by the expression of Prox1, arise from a subset of venous endothelial cells and contribute to fluid homeostasis and immune surveillance.[35, 36] Endothelial cells regulate vascular permeability, mediate leukocyte trafficking during immune responses, and produce vasoactive molecules such as nitric oxide, which maintains vessel tone and prevents thrombosis.[37]

Perivascular cells, including vascular smooth muscle cells (VSMCs) and pericytes, provide structural and functional support to the vascular network. Pericytes, which are more abundant in capillaries, are primarily derived from mesenchymal progenitors and form an integral component of vessel stabilization.[38] These cells envelop endothelial tubes, providing mechanical support, regulating blood flow, and maintaining vascular tone. Pericytes also regulate endothelial barrier function, ensuring tight junction integrity and preventing vascular leakage. For example, in the blood-brain barrier, pericytes limit permeability by modulating endothelial cell gene expression, and their loss has been linked to neurodegenerative conditions such as Alzheimer's disease.[39]

The development and maturation of the vascular system rely on intricate crosstalk between endothelial cells and perivascular cells, mediated by multiple signaling pathways that coordinate their growth, differentiation, and stabilization. Endothelial cells, which form the inner lining of blood vessels, secrete platelet-derived growth factor-BB (PDGF-BB), a critical signal that recruits pericytes to nascent vessels. PDGF-BB binds to PDGFR-β receptors on perivascular cells, promoting their migration and attachment to endothelial structures, an essential step for vessel maturation.[10] The recruited pericytes, in turn, secrete transforming growth factor-beta (TGF-β), which enhances endothelial junction integrity and promotes the deposition of a mature vascular basement membrane.[38] TGF-β also regulates the differentiation of VSMCs, contributing to vessel stability and tone. Fibroblast growth factors (FGFs), secreted by mesenchymal

cells, play a dual role in vascular development. FGFs stimulate endothelial cell proliferation through FGFR-mediated signaling, promoting angiogenesis. Simultaneously, FGFs drive perivascular cell differentiation, ensuring the concurrent development of both cell types and the formation of structurally robust vessels.[40] Angiopoietins, particularly Ang1 and Ang2, further refine this interplay through their interactions with the Tie2 receptor on endothelial cells. Ang1 strengthens endothelial-pericyte interactions by stabilizing vessel walls and enhancing basement membrane formation, while Ang2 acts as a context-dependent antagonist. Ang2 facilitates vascular remodeling by disrupting Ang1-Tie2 signaling under certain conditions, such as during angiogenesis or vascular regression.[41] Additionally, endothelial cells produce vascular endothelial growth factor (VEGF), a central driver of angiogenesis. VEGF primarily acts on endothelial cells, stimulating their proliferation and migration. However, VEGF also modulates perivascular cell behavior indirectly by influencing the expression of signaling molecules such as Ang2 and PDGF-BB.[25] This bidirectional communication ensures that endothelial cells form functional vessels while perivascular cells provide the structural support and regulatory cues necessary for vascular integrity. The combined activity of these pathways creates a dynamic feedback loop, enabling precise spatial and temporal regulation of vessel formation, remodeling, and stabilization.

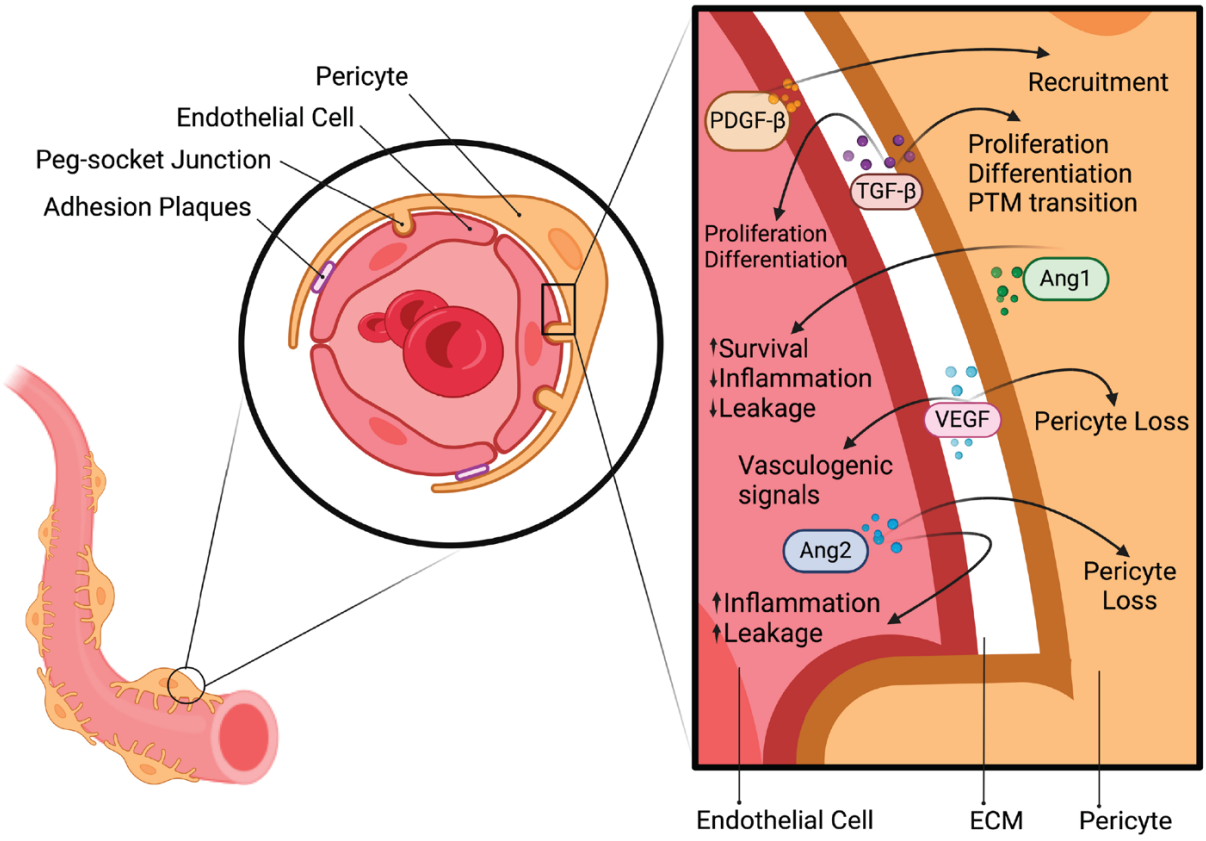

Fig 4: Crosstalk between endothelial cells and pericytes during vascular development. Endothelial cells secrete PDGF-B to recruit pericytes, while pericytes release TGF-β to promote endothelial differentiation and extracellular matrix (ECM) stabilization. Angiopoietin-1 (Ang1) facilitates vessel maturation and reduces inflammation and leakage, whereas Ang2 antagonizes this effect, promoting vascular remodeling under specific conditions. VEGF signals enhance endothelial proliferation and survival, but imbalances can lead to pericyte loss and vessel instability. The interaction between these cell types is critical for maintaining vascular integrity and function. *(adapted from [42])*

The interplay between endothelial and perivascular cells ensures that blood vessels not only form but also acquire the structural integrity required for efficient blood flow. These interactions are essential for vessel stabilization, regulation of permeability, and the maintenance of vascular tone. Disruptions in endothelial-perivascular crosstalk are linked to a range of vascular pathologies, including aneurysms, hemorrhages, and aberrant angiogenesis, such as that observed in tumor vascularization. Together, these cell types orchestrate the formation and specialization of blood vessels during

embryonic development, responding to finely tuned signaling cues to form an organized vascular system capable of sustaining physiological demands postnatally. Variations in the abundance, structure, and developmental signaling of these cell types reflect the distinct functional requirements of arteries, veins, and capillaries across the vascular system. Arteries, for instance, are characterized by a thick smooth muscle layer to withstand high blood pressure, while veins rely on valves to prevent backflow in a low-pressure system. Capillaries, by contrast, are designed for exchange and rely heavily on pericytes for stabilization and regulation of permeability.[43] The ratio of endothelial cells to pericytes varies significantly across tissues, further illustrating their specialized functional demands. For instance, the blood-brain barrier has a high pericyte density—estimated at one pericyte for every two endothelial cells—to maintain its selective permeability and support the integrity of tight junctions.[44] Conversely, the kidney, where rapid filtration occurs, has a much lower pericyte density, reflecting its need for higher permeability to facilitate filtration.[38] These regional differences highlight how cellular ratios and interactions within vessel walls are precisely adapted to meet the unique physiological needs of each tissue type.[25]

VASCULAR DISEASE AND REGENERATION

Degenerative vascular diseases, including atherosclerosis, aneurysms, and diabetic vasculopathy, are among the leading causes of global morbidity and mortality, profoundly impacting vascular integrity and function.[45] These conditions progressively weaken vessel walls, disrupt blood flow, and elevate the risk of ischemia, thrombosis, and hemorrhage, often with organ-specific consequences. Notably, these diseases disproportionately affect different vessel types, reflecting the distinct structural and functional characteristics of arteries, veins, and capillaries. For instance, atherosclerosis predominantly affects large- and medium-sized arteries, where lipid deposition, endothelial dysfunction, and chronic inflammation lead to plaque formation, vessel stenosis, and the risk of rupture or thrombosis.[46] Veins, in contrast, are more commonly affected by conditions such as venous thrombosis, which arises from endothelial activation, stasis, and hypercoagulability.[47] Capillaries, with their unique reliance on pericyte stabilization, are especially vulnerable to degenerative changes in diseases

such as diabetic vasculopathy, where loss of pericyte coverage exacerbates vascular leakage and permeability.

Diabetic vasculopathy exemplifies the systemic effects of vascular disease, particularly in small vessels within the retina, kidneys, and peripheral circulation. Chronic hyperglycemia initiates oxidative stress in endothelial cells, impairing their ability to maintain vascular barrier function. This dysfunction promotes an inflammatory cascade, characterized by the recruitment of immune cells and the deposition of inflammatory proteins into the vessel wall, further damaging the endothelium and amplifying vascular instability.[48, 49] Pericytes, which play a key role in maintaining capillary integrity and regulating blood-retina and blood-brain barriers, are particularly vulnerable to hyperglycemia-induced apoptosis.[50] Their loss creates structural gaps in the capillary network, resulting in increased vascular permeability, leakage, and the risk of hemorrhage, as observed in diabetic retinopathy.[51] However, recent studies have demonstrated that transplantation of human blood vessel organoids into diabetic mice led to the regeneration of functional, perfused blood vessels at the site of injection, highlighting their potential as a regenerative strategy for restoring vascular integrity in diabetic vasculopathy.[52]

The structural and functional specificity of arteries, veins, and capillaries in health and disease underscores the need for regenerative strategies tailored to their unique cellular compositions and signaling requirements. For instance, arteries rely heavily on the mechanical strength provided by smooth muscle cells and fibroblasts, while capillaries are more dependent on endothelial-pericyte interactions to maintain permeability and stability. Effective regenerative therapies must therefore incorporate an understanding of how these vascular cell types—and their subtypes—develop, differentiate, and interact during both embryonic and postnatal vascular formation. By unraveling the signaling pathways that regulate these processes, researchers can better design targeted strategies to repair or replace damaged vasculature, taking into account the unique demands of each tissue and vessel type.

KEY SIGNALING PATHWAYS IN VASCULAR DEVELOPMENT

VEGF is one of the most critical drivers of endothelial cell differentiation and proliferation. During development, VEGF signaling directs mesodermal progenitors toward an endothelial cell fate, initiating vasculogenesis and the formation of the first vascular networks.[53] VEGF binds to VEGFR2 on endothelial progenitors, triggering a cascade that promotes cell survival, proliferation, and migration, enabling these cells to organize into tubular structures that prefigure blood vessels.[54] *In vitro*, differentiation protocols frequently incorporate VEGF to generate endothelial cells from human pluripotent stem cells (hPSCs), recapitulating its role in directing lineage commitment and promoting tubular morphogenesis.[55]

FGF signaling also plays a crucial role in endothelial cell development, particularly during angiogenesis, where it facilitates the formation of new vessels from pre-existing ones.[40] FGF2, a major factor in vascular development, binds to FGFRs on endothelial cells, stimulating proliferation and sprouting.[11] Differentiation protocols frequently combine FGF2 with VEGF to enhance endothelial cell proliferation and promote vascular network expansion. For instance, Palpant et al. utilized a protocol where FGF2, in combination with VEGF, significantly improved endothelial cell differentiation from hPSCs, resulting in high-purity endothelial cells.[56]

Once endothelial cells have formed nascent vessels, pericytes are recruited to stabilize and mature these structures. PDGF-BB signaling, secreted by endothelial cells, plays a central role in attracting pericytes, guiding their migration, and promoting their association with nascent vessels.[10] Once endothelial cells have formed nascent vessels, pericytes are recruited to stabilize and mature these structures. Pericyte recruitment is regulated primarily by PDGF-β signaling from endothelial cells, which acts as an attractant, guiding pericytes to wrap around the new vessels. The presence of pericytes is critical, especially in tissues where the vascular barrier must be tightly controlled, such as the brain and retina. The interaction between pericytes and endothelial cells supports vessel stability and maintains the integrity of selective barriers like the blood-brain barrier. VEGF and FGF signaling further influence this endothelial-

pericyte interaction by modulating factors that affect endothelial cell permeability and pericyte coverage. In addition to these, several other signaling pathways play critical roles in the development and maturation of endothelial cells and pericytes, including Notch and TGF-β.[10]

However, the field faces significant challenges in precisely dissecting the roles of these pathways during vascular development due to the promiscuity of ligand-receptor interactions within these signaling systems. VEGF ligands, for example, bind to multiple receptor subtypes, including VEGFR1, VEGFR2, and VEGFR3, each of which triggers distinct but sometimes overlapping signaling pathways. VEGFR2 is primarily associated with endothelial cell proliferation and migration, while VEGFR1 has a higher ligand-binding affinity but a weaker signaling output, often acting as a decoy receptor in some contexts.[54] Similarly, FGF ligands, such as FGF2, bind to multiple FGFR isoforms with variable affinities, leading to diverse downstream effects depending on the receptor isoform and cellular environment.[11] This receptor-ligand promiscuity complicates efforts to delineate specific signaling outcomes, as both VEGF and FGF signaling pathways frequently exhibit redundancy and crosstalk.

The context-dependent nature of these interactions further adds to the complexity. For instance, VEGF can induce angiogenesis in hypoxic tissues, but the signaling response is heavily influenced by co-factors such as neuropilins, heparan sulfate proteoglycans, and integrins, which modulate ligand binding and receptor activation.[58] Similarly, FGF signaling requires interactions with heparin or heparan sulfate to stabilize receptor dimerization and enhance signaling fidelity.[11] These co-factors contribute to the cellular and tissue specificity of signaling but also make it challenging to isolate the direct contributions of individual ligands and receptors during vascular development. Consequently, while much progress has been made in identifying these signaling mechanisms, developing tools that can selectively manipulate individual pathways without unintended cross-activation remains an important goal for advancing our understanding of vascular development.

ARTERIO-VENOUS SPECIFICATION

The vascular system is composed of arteries, veins, and capillaries, each with distinct structural and functional properties. Arteries transport oxygenated blood from the heart to peripheral tissues under high pressure, supported by thick walls composed of smooth muscle cells and elastic fibers that provide both strength and flexibility. In contrast, veins return deoxygenated blood to the heart under lower pressure, characterized by thinner walls and the presence of valves to prevent backflow. Capillaries, the smallest vessels, are specialized for exchange and consist of a single layer of endothelial cells supported by pericytes. The developmental specification of arterial and venous endothelial cells is tightly regulated by signaling pathways that operate early during vasculogenesis and angiogenesis, ensuring proper vascular patterning.

Arterial specification is primarily driven by the Notch signaling pathway, which plays a pivotal role in establishing arterial identity. Activation of Notch receptors by ligands such as Delta-like ligand 4 (DLL4) induces the expression of arterial markers, including Ephrin-B2, a transmembrane protein essential for arterial differentiation and boundary formation.[58] Downstream of Notch activation, transcription factors such as HES1 and HEY2 suppress venous identity by inhibiting venous-specific markers, ensuring commitment to the arterial program.[59] Notch signaling also interacts with other pathways, such as VEGF, to further refine arterial specification. High VEGF-A levels enhance Notch activity in arterial progenitors, promoting arterial-specific gene expression and vessel sprouting.[60] Additionally, FGF signaling contributes to arterial specification by activating MAPK pathways that enhance Notch signaling. For example, studies have shown that FGF2 synergizes with VEGF to induce arterial fate in zebrafish and mouse models, emphasizing the complementary roles of these pathways.[58]

Venous specification, in contrast, is governed by the transcription factor COUP-TFII (NR2F2), which actively suppresses Notch signaling and arterial marker expression, thereby facilitating venous identity.[61] COUP-TFII inhibits the expression of arterial-specific genes such as Ephrin-B2, while promoting the expression of venous markers like EphB4, a receptor critical for venous endothelial cell function and identity. VEGF

also plays a role in venous specification, but in a concentration-dependent manner. Lower VEGF levels, compared to the high concentrations required for arterial development, are sufficient to support venous identity.[60] Hemodynamic forces, including shear stress, further influence venous development, as regions exposed to low shear stress tend to adopt venous characteristics.[59]

Beyond VEGF, Notch, and FGF, additional pathways contribute to arterial-venous specification. Sonic hedgehog (SHH) signaling indirectly supports arterial specification by upregulating VEGF expression in mesenchymal cells, which enhances Notch-mediated arterial differentiation.[62] Similarly, bone morphogenetic proteins (BMPs), particularly BMP4, have been implicated in arterial fate by modulating Notch signaling and promoting the expression of arterial-specific genes.[63] Transforming growth factor-beta (TGF-β) signaling also contributes to arterial-venous specification, acting through Smad-dependent and independent pathways to regulate endothelial differentiation and stabilize vessel identity.[64]

The Ephrin-B2/EphB4 system further reinforces arterial-venous boundaries. Ephrin-B2 is predominantly expressed in arterial endothelial cells, while its receptor EphB4 is restricted to venous endothelial cells. Their bidirectional signaling ensures proper segregation and prevents inappropriate connections between arterial and venous vessels.[65] This interplay between signaling pathways establishes the distinct identities of arterial and venous endothelial cells, enabling the functional specialization required for an organized and efficient vascular system.

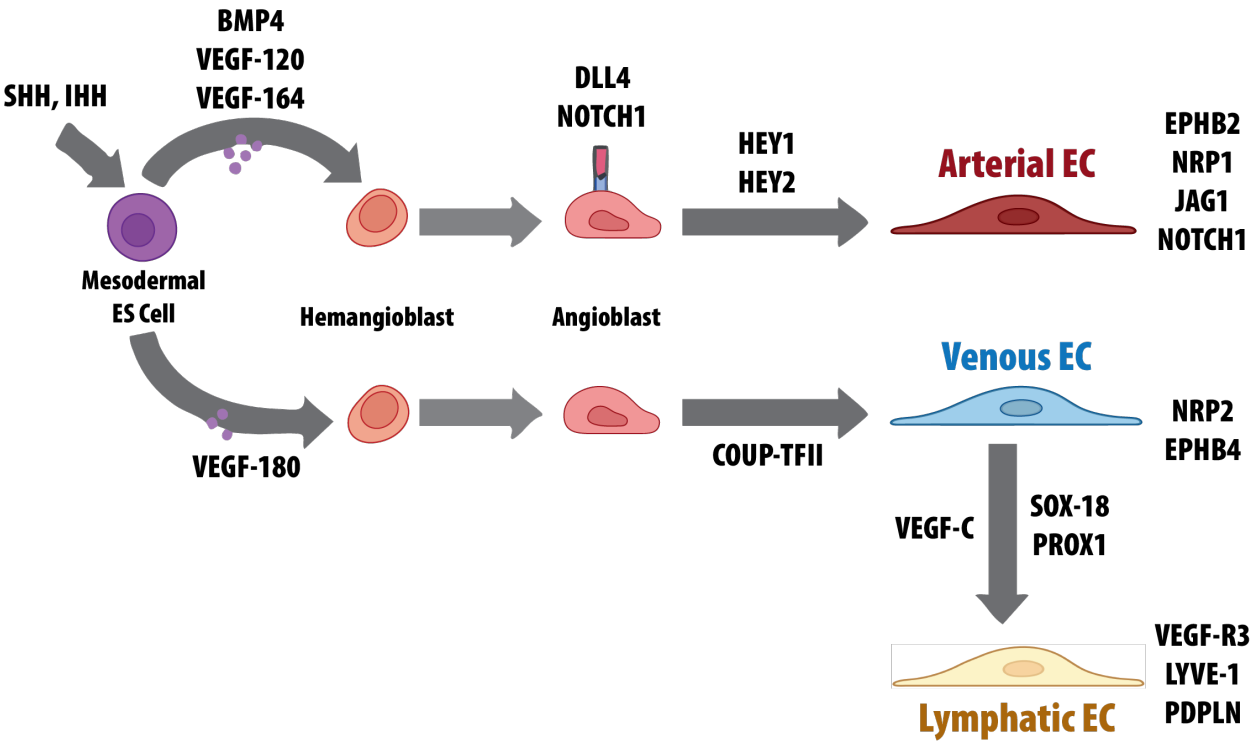

Fig 5: Arteriovenous specification during vascular development. Endothelial progenitor cells differentiate into arterial or venous endothelial cells (ECs) in response to distinct signaling cues. Notch signaling, activated by ligands such as DLL4, promotes arterial specification, inducing the expression of arterial markers like Ephrin-B2. In contrast, venous endothelial cells arise under the influence of COUP-TFII, which suppresses Notch signaling and upregulates venous markers like EphB4. Lymphatic endothelial cells differentiate from a subset of venous endothelial cells, driven by Prox1 expression and VEGF-C signaling. *(adapted from [66])*

FGF SIGNALING

THE FGF FAMILY: LIGANDS AND RECEPTORS

Fibroblast growth factor (FGF) signaling is a cornerstone of developmental and regenerative processes, orchestrating cell proliferation, differentiation, migration, and survival. The FGF family in humans comprises 22 ligands (FGF1–FGF23, excluding FGF15 and FGF19, which are murine and human orthologs, respectively) and four receptor tyrosine kinases (FGFR1–FGFR4), each contributing to unique and overlapping signaling functions.[67] These ligands are categorized into paracrine and

endocrine subfamilies based on their mode of action. Paracrine FGFs, such as FGF2 and FGF8, are among the most extensively studied and are critical for embryonic development. FGF8, for instance, is essential for mesoderm induction and anterior-posterior patterning, while FGF2 is involved in angiogenesis and wound healing.[68] Endocrine FGFs, such as FGF21 and FGF23, act systemically, regulating metabolic processes including phosphate homeostasis and lipid metabolism.[69]

FGF receptors (FGFRs) are characterized by an extracellular domain containing three immunoglobulin (Ig)-like loops (D1–D3), a single transmembrane domain, and an intracellular tyrosine kinase domain. The D2 and D3 regions are critical for ligand binding, with additional specificity conferred by interactions with heparan sulfate proteoglycans (HSPGs).[11] These interactions stabilize the FGF-FGFR complex, facilitating receptor dimerization and downstream signaling activation. Each FGFR can bind multiple FGF ligands, but the affinity and specificity of FGF-FGFR interactions are modulated by alternative splicing, which generates two major isoforms—IIIb and IIIc—for FGFR1, FGFR2, and FGFR3. These isoforms differ in the sequence of their D3 region, resulting in distinct ligand-binding preferences and tissue-specific expression patterns.[70] For example, FGFR2-IIIb predominantly binds FGF7 and FGF10 and is expressed in epithelial tissues, whereas FGFR2-IIIc binds FGF2 and FGF8 and is expressed in mesenchymal tissues.[74] This splicing-driven specificity underpins the diverse biological functions of FGF signaling across different developmental and physiological contexts.

The broad functional versatility of FGF signaling is further enhanced by crosstalk with other signaling pathways. In development, paracrine FGFs establish gradients that regulate tissue patterning, such as in limb bud development, where FGF8 from the apical ectodermal ridge directs proximal-distal growth.[71] Similarly, FGF signaling integrates with Wnt and BMP pathways during mesoderm induction, underscoring its role as a central hub in developmental biology.[72] Dysregulation of FGF signaling, whether through receptor mutations, overactivation, or aberrant ligand expression, is implicated in numerous pathologies, including craniofacial syndromes, cancer, and

metabolic disorders.[73] Understanding the molecular mechanisms of FGF-FGFR interactions and their downstream effects remains critical for elucidating their roles in both normal development and disease.

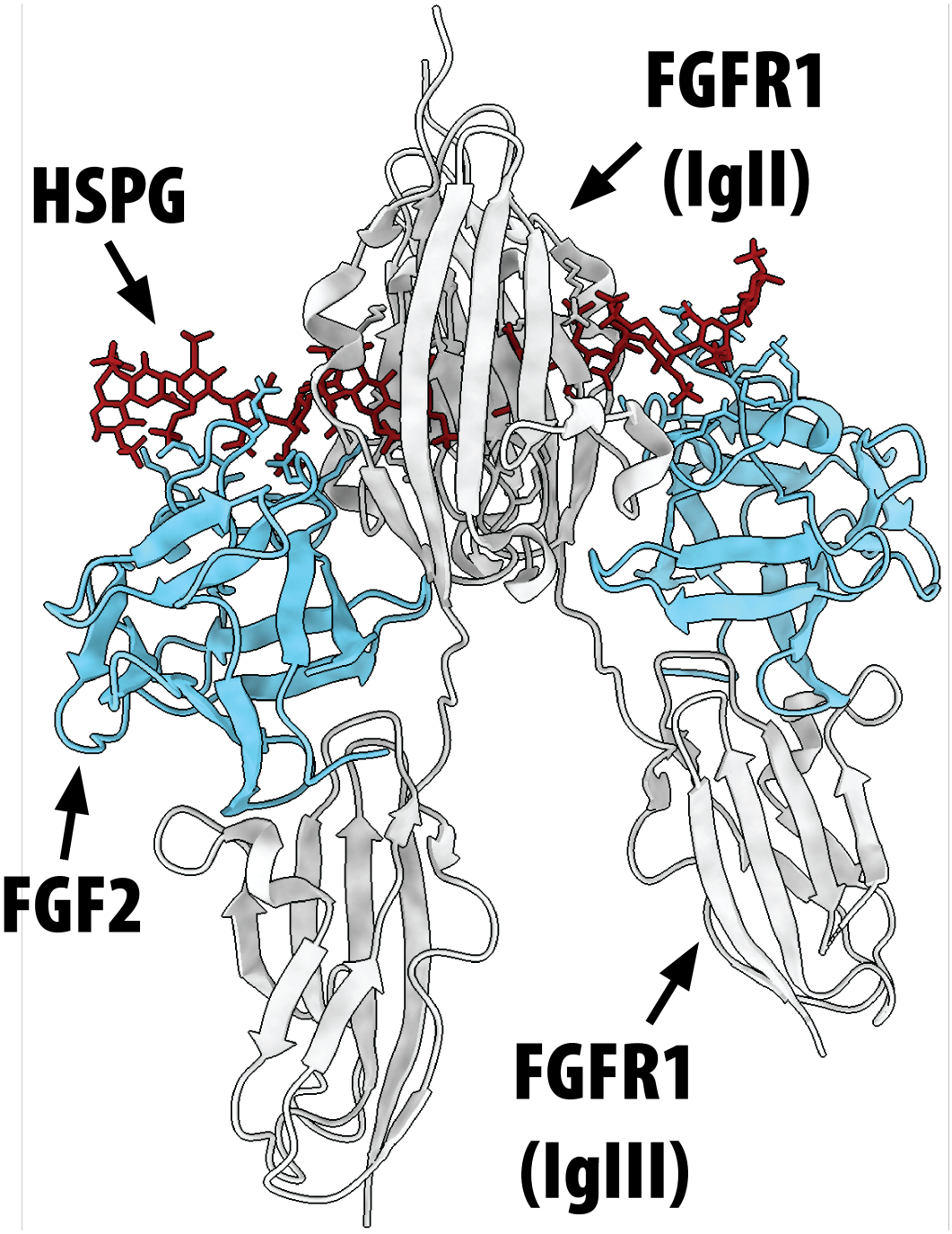

Fig 6: Structure of the FGF2-FGFR1-heparan sulfate proteoglycan (HSPG) complex. The fibroblast growth factor receptor 1 (FGFR1) is shown with its Ig-like domains II and III, which mediate FGF2 binding. FGF2 (cyan) interacts with both FGFR1 and HSPG (red), forming a ternary complex. The HSPG stabilizes the receptor-ligand interaction, facilitating FGFR1 dimerization and downstream signaling activation. This complex exemplifies the role of co-factors in modulating FGF signaling. *(adapted from [75])*

DOWNSTREAM PATHWAYS: MAPK, PLCγ AND OTHERS

FGF signaling activates several canonical pathways that regulate distinct cellular processes, each tailored to specific biological roles during development and tissue repair. Upon FGF binding, FGFRs undergo dimerization and transphosphorylation, creating docking sites for adaptor proteins such as FGFR substrate 2 (FRS2). FRS2 serves as a central scaffold, recruiting SH2 domain-containing proteins like Grb2 and Shp2, which initiate the MAPK cascade (RAF-MEK-ERK). This pathway is the primary effector of FGF signaling, promoting gene expression changes that drive cell proliferation, differentiation, and survival. In embryonic development, the MAPK pathway is essential for processes such as mesoderm induction, limb bud formation, and neural patterning, where rapid and spatially regulated cell division is critical.[11, 68]

The phospholipase C-gamma (PLC-γ) pathway represents another key branch of FGF signaling, responsible for cytoskeletal dynamics and vesicle trafficking. Activated PLC-γ hydrolyzes PIP2 into IP3 and DAG, triggering intracellular calcium release and the activation of protein kinase C (PKC). This pathway is particularly relevant in cellular migration, where calcium fluxes coordinate the reorganization of actin filaments and the formation of lamellipodia and filopodia. For example, during angiogenesis, PLC-γ-mediated signaling enables endothelial cells to migrate toward VEGF and FGF gradients, forming new vascular structures.[76]

The PI3K-AKT pathway, another downstream effector of FGF signaling, is crucial for cell survival and metabolic homeostasis. PI3K activation leads to phosphorylation of AKT, which inhibits pro-apoptotic factors and promotes cell growth. In the context of

wound healing, PI3K-AKT signaling enhances fibroblast survival and collagen deposition, ensuring proper tissue repair. Additionally, this pathway plays a role in maintaining stem cell pluripotency, where AKT-mediated signals prevent differentiation under specific conditions.[73]

Crosstalk between these pathways adds complexity to FGF signaling outcomes. For example, the duration and intensity of MAPK activation are critical for determining cell fate. Sustained MAPK activation is associated with differentiation, as seen in neural crest cell lineage specification, whereas transient activation favors proliferation, such as during early mesodermal expansion.[77] The relative activation of these pathways is also influenced by factors such as receptor isoform expression, ligand concentration, and interactions with heparan sulfate proteoglycans (HSPGs). These co-factors not only stabilize receptor-ligand complexes but also modulate the spatial and temporal dynamics of pathway activation, fine-tuning FGF's effects across various biological contexts.[78]

ALTERNATIVELY SPLICED VARIANTS: B VS C ISOFORMS

FGF receptors (FGFRs) undergo alternative splicing, producing distinct isoforms that adapt FGF signaling to specific cellular contexts. Of particular importance are the “b” and “c” splice variants of FGFR1, FGFR2, and FGFR3. These isoforms exhibit unique ligand-binding affinities and tissue-specific expression patterns, allowing fibroblast growth factors (FGFs) to elicit context-dependent effects. Specifically, alternative splicing of exon 8 versus exon 9 within the FGF receptor genes alters the third immunoglobulin (Ig)-like domain (D3) of the receptor, producing two main isoforms known as IIIb and IIIc (referred to as "b" and "c" isoforms). This D3 domain is an essential part of the FGF-binding region, and the choice between exon 8 and exon 9 determines whether the receptor variant will favor certain FGF ligands over others. The IIIb isoform (FGFR-b) generally binds ligands such as FGF7 and FGF10, while the IIIc isoform (FGFR-c) primarily binds FGF2, FGF4, and FGF9, reflecting distinct roles for these isoforms in development and physiology.[67, 70]

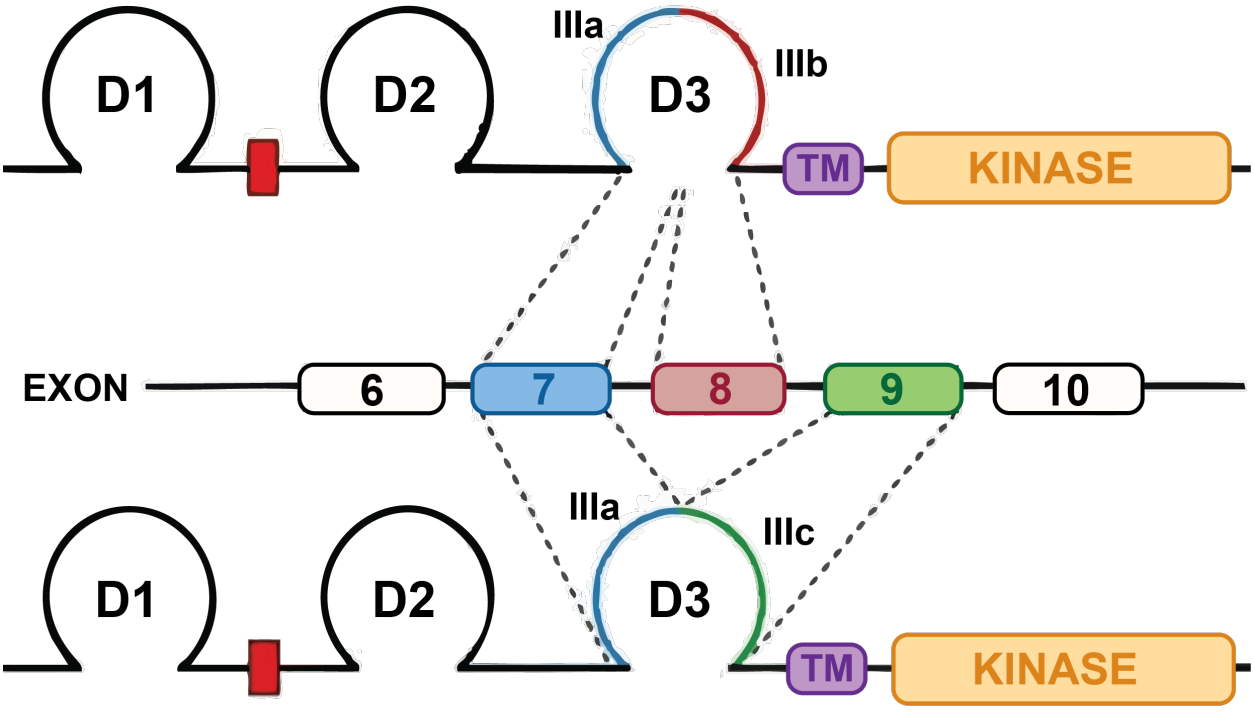

Fig 7: Structural organization of FGFR (Fibroblast Growth Factor Receptor) highlighting alternative splicing in the ligand-binding domain. The extracellular region comprises Ig-like domains (IgI, IgII, and IgIII), with the IgIII domain undergoing alternative splicing to form isoforms IgIIIb (red) and IgIIIc (green), which determine ligand-binding specificity. The figure illustrates the functional diversity introduced by alternative splicing and its role in tissue-specific signaling.

The FGFR-b isoforms are predominantly expressed in epithelial cells, where they mediate epithelial-mesenchymal interactions essential for organogenesis. For example, FGFR2b interacts with FGF7 and FGF10 to regulate branching morphogenesis during the development of organs such as the lungs, kidneys, and salivary glands. In FGFR2b knockout mice, severe defects in epithelial branching and organ formation highlight the indispensability of this isoform in epithelial tissue development.[79] Although the role of FGFR-b isoforms in vascular development are unknown, their presence in epithelial cells influences surrounding vasculature through paracrine signaling. Epithelial cells expressing FGFR2b release growth factors and extracellular signals that stimulate endothelial proliferation and vascularization, a mechanism particularly relevant during

tissue repair and regeneration. For instance, epithelial-mesenchymal interactions mediated by FGFR2b indirectly support angiogenesis in tissues undergoing repair.[73]

In contrast, the FGFR-c isoforms are expressed predominantly in mesenchymal and endothelial cells, where they play direct roles in vascular development and angiogenesis. FGFR2c and FGFR3c isoforms bind ligands such as FGF2 and FGF9, which are critical for endothelial cell proliferation, migration, and differentiation during vessel formation. In endothelial cells, FGFR-c isoforms mediate FGF2-driven sprouting angiogenesis, promoting the formation of new capillaries and vascular networks. FGFR-c isoforms are also essential for pericyte recruitment, a process mediated by FGF9 signaling, which stabilizes nascent vessels and ensures vascular integrity.[80] These isoforms coordinate endothelial-pericyte interactions that are critical during both development and in adult tissues requiring vascular remodeling, such as wound healing and tumor vascularization.[67]

The differential binding affinities of FGFR-b and FGFR-c isoforms provide a mechanism for FGF signaling specificity across various tissues and developmental stages. This selectivity is crucial in contexts where tightly regulated FGF signaling is required, such as in the spatial organization of epithelial and vascular structures. However, the promiscuity of FGF ligands, which can bind to multiple FGFR isoforms, complicates efforts to isolate the functions of each splice variant in vivo. This binding promiscuity highlights a need for further research to develop tools that can precisely target and manipulate specific FGFR isoforms, which could advance both our understanding of vascular biology and the development of targeted regenerative therapies.

ROLE IN VASCULAR DEVELOPMENT

FGF signaling plays a multifaceted role in vascular development, acting at multiple stages to regulate the growth, stability, and functional specialization of blood vessels and their constituent cell types. In the early stages of vascular development, ligands such as FGF2 are critical for the proliferation and migration of endothelial cells, which form the innermost lining of blood vessels. By binding to FGFR1 and FGFR2 on

endothelial cells, FGF2 activates downstream MAPK/ERK and PI3K/AKT signaling pathways. These pathways stimulate endothelial cell division, enhance survival, and guide cells to organize into vessel-like structures. This process is fundamental to both vasculogenesis, the de novo formation of the primary vascular network, and angiogenesis, the sprouting of new vessels from pre-existing ones.[11, 40]

Beyond endothelial cells, FGF signaling also influences pericytes, the supportive cells that stabilize endothelial cells, particularly in micro vessels such as capillaries and venules. While PDGF-BB signaling is primarily responsible for recruiting pericytes to nascent vessels, FGF signaling plays a complementary role in promoting pericyte survival and function. FGF signaling supports the differentiation of mesenchymal progenitors into pericytes and enhances their proliferation, ensuring an adequate supply of these stabilizing cells.[81] In specialized vascular beds, such as the blood-brain and blood-retina barriers, where pericyte density is particularly high, FGFs are essential for maintaining selective permeability. Pericytes interact with endothelial cells through FGF-mediated signaling, which encourages them to secrete matrix proteins and stabilizing factors such as laminins and collagen, reinforcing the vascular barrier and contributing to vessel maturation.[38] This crosstalk is vital for maintaining vascular homeostasis and integrity.

FGF signaling also shapes the hierarchical organization of the vascular network, ensuring the coordinated formation and maturation of both large and small vessels to meet tissue-specific demands. FGF signaling acts synergistically with VEGF, where VEGF provides directional cues for endothelial migration, while FGFs promote cellular proliferation and sprouting. This interaction is particularly evident during angiogenesis, where the two signaling pathways cooperate to expand vascular networks in a balanced manner.[82] For example, during tissue regeneration, VEGF gradients guide endothelial cells toward hypoxic regions, while FGF signaling maintains the proliferative capacity of these migrating cells to sustain vessel growth.

At a more specialized level, FGF signaling contributes to the specification of arterial and venous identity, a key aspect of vascular patterning. FGF2 has been shown to induce Notch signaling in endothelial cells, which is necessary for arterial specification. By enhancing the expression of arterial markers such as Ephrin-B2, FGF signaling interacts with other pathways like VEGF and BMP to establish distinct arterial and venous territories. This arterial-venous patterning is critical for the functional differentiation of the vascular system, ensuring that each vessel type is structurally and functionally suited to its role.[83]

COMPUTATIONAL DESIGN OF SIGNALING LIGANDS

Clustering of cell surface receptors is a critical mechanism for enhancing and sustaining signal transduction in response to extracellular stimuli, with growing interest in developing technologies to manipulate receptor clustering for therapeutic and research applications.[84, 85, 86] Advances in nanotechnology and multivalent ligands have further highlighted the potential of receptor clustering to improve signaling precision and efficiency, particularly in targeted drug delivery.[87, 88] Emerging tools, including transmembrane peptides, have also provided insights into the biophysical processes underlying receptor clustering and activation at the plasma membrane.[89]

Designed protein assemblies have been employed to drive receptor clustering by incorporating naturally occurring receptor-binding domains, demonstrating the ability to modulate signaling pathways with high specificity.[90, 91] Additionally, geometrically tunable dimeric ligands have been used to probe the influence of dimerization geometry on signaling output, revealing that precise spatial control over receptor alignment can dictate downstream signaling responses.[90, 92] These approaches, including the use of “synthekines” that compel signaling through non-natural receptor dimers, highlight the potential of engineered assemblies to dissect and manipulate complex receptor-mediated processes.[93, 94]

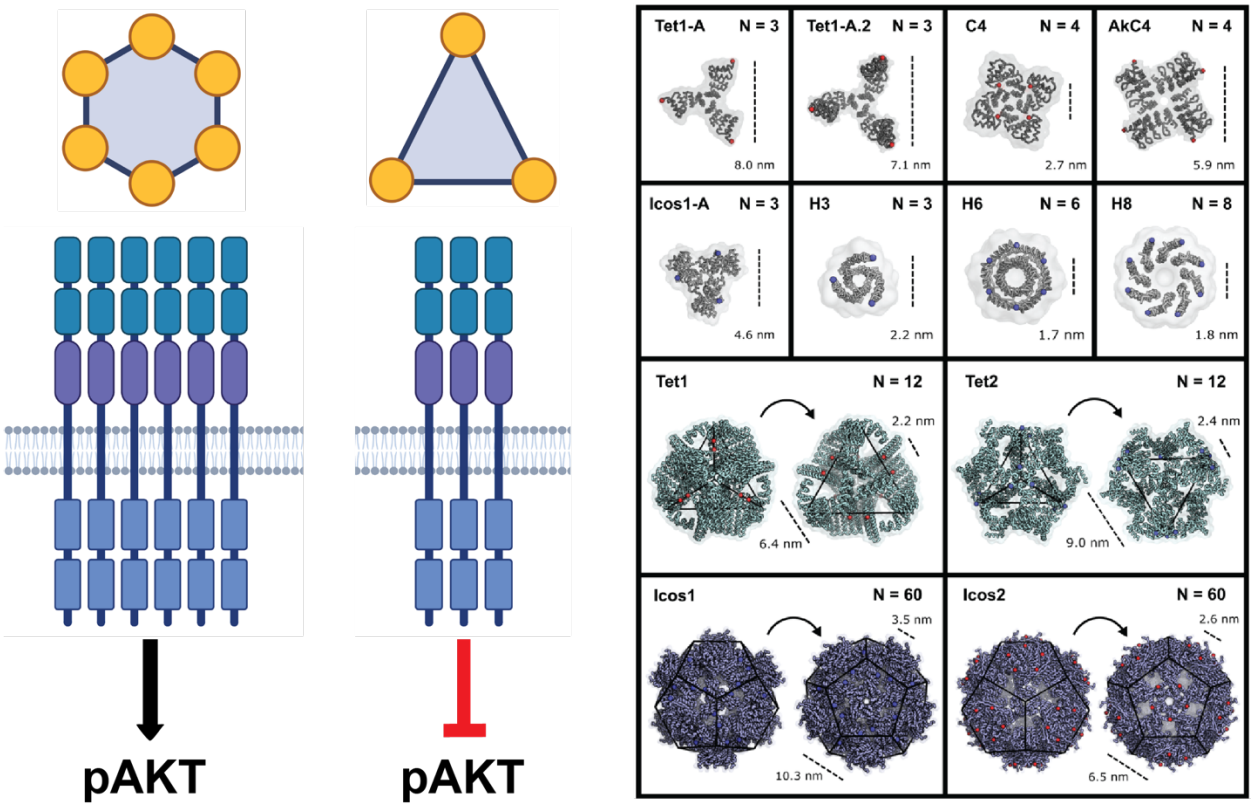

Fig 8: Valency-dependent Tie2 receptor clustering modulates signaling. Left: High-valency (≥6) complexes activate pAKT, promoting vascular stability, cell migration and FOXO1 translocation, while low-valency (≤3) complexes inhibit pAKT, promoting destabilization. Right: Structural models of oligomeric scaffolds used in the study to control valency. *(adapted from [90])*

Higher-order receptor assemblies are involved in a variety of signaling systems, facilitating complex cellular responses by organizing receptors into functional clusters.[95, 96] A tunable oligomeric scaffold presenting receptor-binding domains could advance the study of how angstrom-level topology influences receptor output, particularly in systems where spatial arrangement determines signaling dynamics.[97] Previous efforts in protein design have produced oligomers with diverse cyclic symmetries, enabling the creation of precise, modular scaffolds. For example, recent developments using computational design tools like RFdiffusion have generated cyclic homo-oligomers with customizable architectures, although these designs have not yet achieved the flexibility required for distinct receptor-binding configurations.[98, 99, 100, 101]

OBJECTIVES

The goal of this study is to engineer and evaluate synthetic signaling ligands that selectively manipulate receptor tyrosine kinase (RTK) pathways, specifically fibroblast growth factor receptors (FGFRs), to control cellular fate and vascular development. By leveraging isoform-specific targeting and modular protein design, we aim to gain insights into RTK signaling dynamics and their applications in vascular biology and regenerative medicine.

Aim 1: Design and Characterization of Isoform-Specific Synthetic Ligands
To develop *de novo* protein-based ligands that selectively bind to the FGFR1/2c isoforms with high affinity and specificity. This aim includes engineering cyclic homo-oligomeric scaffolds with tunable valency and geometry to enhance receptor clustering, stabilize signaling complexes, and direct specific downstream pathway activation.

Aim 2: Functional Analysis of Synthetic Ligands in Vascular Development
To evaluate how FGFR1/2c-specific ligands influence vascular development, including endothelial and perivascular cell differentiation. This aim involves studying the roles of synthetic ligands in early vascular morphogenesis using an iPSC-derived 2D differentiation protocol and understanding their contribution to vascular stability and maturation.

Aim 3: Manipulating Arterial-Venous Specification Using Synthetic Ligands
To investigate the ability of FGFR1/2c-specific ligands to direct arterial-venous specification of endothelial cells. This aim focuses on determining the role of isoform-specific signaling in establishing arterial and venous endothelial fates during vascular development using a 3D organoid system, as well as testing their ability to regenerate vascular networks *in vivo*.

MATERIALS AND METHODS

CELL CULTURE

Human umbilical vein endothelial cells (HUVECs) were obtained from Lonza, Germany (#CC-2519). Cells were grown in EGM2 media (20% Fetal Bovine Serum [BioWest, #S1620], 1% Penicillin-Streptomycin [Gibco, #1514012], 1% GlutaMAX [Gibco #35050061], 1% ECGS (Endothelial Cell Growth Supplement), 1mM Sodium Pyruvate [Gibco, #11360070], 7.5mM HEPES [Gibco, #15630130], 0.08mg/mL Heparin [Fisher BioReagents, #9041-08-1], 0.01% Amphotericin B [Gibco, #15290018], a mixture of 1X RPMI 1640 +/- glucose [Gibco, #1187902] for a final concentration of 5.6mM glucose; filtered through 0.2-mm filter) on 0.1% gelatin-coated [Sigma, #G1890-100] 35mm cell culture dishes. Cells were cryopreserved at passage 4 for later thawing and use in Western blots. ECGS was extracted from 25 mature whole bovine pituitary glands [Pel-Freeze, #57133-2]. Pituitary glands were homogenized with ice-cold 0.15M NaCl [Fisher Chemical, #CAS 7647-14-5] and adjusted to pH 4.5 with HCl [Sigma-Aldrich, 320331]. Following 1hr centrifugation at 4°C, the supernatant (wine colored) was collected and adjusted to pH 7.6, followed by addition of 0.5g/ 100 mL of Streptomycin Sulfate [Sigma, #S9137]. The following day, the supernatant was centrifuged at 4,000 RPM for 1hr at 4°C. The supernatant was sterile filtered using a 0.45-mm filter and stored at -20°C. Parental heparan-deficient Chinese hamster ovary (CHO) cells [pgsD-677 cells; ATCC, #CRL-2244] stably expressing human FGFR1c were maintained in F-12K medium [ATCC, #30-2004] supplemented with 10% Fetal Bovine Serum, 1% Penicillin-Streptomycin, and 10 mg/mL Puromycin [Gibco, #A11138-03]. Rat myoblast (L6) cells [ATCC, #CRL-1458] stably expressing either human FGFR1c (L6-R1c) or FGFR1b (L6-R1b)[102] were maintained in DMEM medium [Gibco, #10566] supplemented with 10% Fetal Bovine Serum, 1% Penicillin-Streptomycin, and 10 mg/mL Puromycin.

TREATMENTS AND PROTEIN ISOLATION FOR WESTERN BLOTTING AND PROTEOMICS

For activation assays, cells were seeded onto 12-well plates and grown to ~80% confluence. Cells were serum-starved overnight in their respective media (F-12K for

CHO cells, DMEM low glucose (1 g/L) [Gibco, 11885-084] for HUVEC, L6 cells). The following day, cells were stimulated with different concentrations of either recombinant FGF2 [Peprotech, #100-18B] or designed scaffolds at 37°C for 15 min. Concentration is reported as the concentration of the oligomeric particle, not the mb7 domain; for example, 10 nM of C4-71C_mb7 corresponds to 10 nM of C4 oligomer and 40 nM of mb7. Following treatment, cells were washed once with 1X PBS before harvesting total protein for analysis. Cells were lysed with lysis buffer containing 20 mM Tris–HCl [Sigma-Aldrich, #1185-53-1] (pH 7.5), 150 mM NaCl, 15% Glycerol [Sigma-Aldrich, #G5516], 1% Triton-X [Sigma-Aldrich, #9002-93-1], 3% SDS [Sigma-Aldrich, #151-21-3], 25 mM b-Glycerophosphate [Sigma-Aldrich, #50020-100G], 50 mM NaF [Sigma-Aldrich, #7681-49-4], 10 mM Sodium Pyrophosphate [Sigma-Aldrich, #13472-36-1], 0.5% Sodium Orthovanadate [Sigma-Aldrich, #13721-39-6], 1% PMSF [Roche Life Sciences, #329-98-6], 25 U benzonase nuclease [EMD, #70664], protease inhibitor cocktail [Pierce Protease Inhibitor Mini Tablets, Thermo Scientific, #A32963], and phosphatase inhibitor cocktail 2 [Sigma-Aldrich, #P5726] in a tube. 4X Laemmli Sample Buffer [Bio-Rad, #1610747] containing 10% beta-mercaptoethanol [Sigma-Aldrich, #M7522-100] was added to the cell lysate and then heated at 95°C for 10 min. The boiled samples were either used immediately for Western blot analysis or stored at -80°C.

WESTERN BLOTTING

If frozen, protein samples were thawed and heated at 95°C for 10 minutes. A 4-10% SDS-PAGE gel was loaded with 30uL of protein per well and separated for 30 min at 250V. Proteins were transferred onto a nitrocellulose membrane for 12 minutes using the semidry turbo transfer Western blot apparatus [Bio-Rad]; the membrane was then blocked in 5% bovine serum albumin (BSA) [VWR, #0332-500G] for 1 hour. The membrane was incubated with the appropriate primary antibodies on a rocker at 4°C overnight. The antibodies used in this study were pERK1/2 p44/42 [Cell Signaling, #4370S] at 1:1,000 dilution, S6 [Cell Signaling, #2217S] at 1:1,000 dilution, ERK1/2 p44/42 [Cell Signaling, #9102] at 1:1,000 dilution, Phospho-FGF Receptor (Tyr 653/654) [Cell Signaling, #3471] at 1:1,000 dilution, and FGF Receptor 1 (D8E4) [Cell Signaling,

#9740] at 1:1,000 dilution. The next day, membranes were washed with 1X TBS-T (3 times, 10 min intervals) and incubated with the respective HRP-conjugated secondary antibody [BioRad, #1706515] (1:10,000 dilution in 5% BSA) at room temperature for 1 hour. All the membranes were washed with 1X TBS-T (3 times, 10 min intervals) after secondary antibody incubation, developed using a Chemiluminescence developer, and imaged using a BioRad ChemiDoc Imager.

CALCIUM RELEASE ASSAY

CHO-R1c cells were seeded on 96-well flat bottom microplates [Corning, #3603] and grown to ~70-80% confluence. Cells were starved in serum-free F12-K medium for 3 hours. Following starvation, the cells were incubated in serum-free media containing 5mM Calbryte 520 AM fluorescent intracellular calcium indicator [AAT Bioquest, #20651] for 30 min at 37°C. Cells were washed 3X with serum-free media and treated with various concentrations of recombinant FGF2 (with or without 40mg/mL Heparin [Iduron, #H010]) or designed scaffolds. Confocal live imaging was done on a Nikon Yokogawa W1 spinning disk confocal microscope using a 20X objective. Parameters for each live frame: Excitation/Emission filters for GFP fluorescence, Exposure time of 150ms, Acquisition rate of 5 sec/frame, and total recording time of 20 minutes (5 min baseline recording + 15 min ligand treatment time). Images were processed with Fiji software distribution of ImageJ v1.52i[103] and frame-by-frame cellular fluorescence intensity was tracked and quantified with CellProfiler.[104] Dose-specific average calcium release was calculated by tracking each individual cell's response during the recording time and computing the mean peak fluorescence achieved by all cells in the frame. An average of 50-100 cells were tracked per recording.

BULK TRANSCRIPTOMICS

HUVEC endothelial cells were seeded at a density of 80,000 cells/well in a 0.1% gelatin-coated 12-well tissue culture dish and allowed to grow to ~80% confluence. Cells were washed 3X with 1X PBS and serum-starved overnight in DMEM low glucose (1 g/L). Following starvation, cells were treated with either recombinant FGF2 or C6-79C_mb7 at 10 nM or 100 nM in serum-free media for 6 hours. Concentration is

reported as the concentration of the oligomeric particle, not the mb7 domain. After treatment, cells were enzymatically detached using Tryp-LE [Thermo-Fisher Scientific, #12563011] and washed once with cold 1X PBS. Cells from each treatment were then counted and loaded at a concentration of 10,000 cells/lane on the 10x 3' gene expression platform [10X Genomics, PN-1000121]. After library preparation, libraries were sequenced on the Nextseq 550 with a 75-cycle high-output kit (Read1: 26bp, Index1:8bp, Read2:58). Processed reads were then mapped using the 10x cell-ranger pipeline and mapped to the hg38 reference genome. Transcriptomes from treated samples (recombinant FGF2 or C6-79C_mb7) were then compared to serum starved cells using the fit_models() function in the Monocle3 software suite.

IN VITRO ENDOTHELIAL DIFFERENTIATION

Briefly, hiPSCs (WTC-11 human induced pluripotent stem cells) [Coriell, #GM25256] were seeded on 24-well plates coated with growth factor-reduced Matrigel [Corning, #356231] and cultured in mTeSR1 stem cell medium [StemCell Technologies, #85850] until cells reach confluence with media changes daily. One day before differentiation (deemed Day (-1)), cells were pre-treated with mTeSR1 supplemented with 1mM of GSK3-Inhibitor (CHIR99021) [Cayman Chemicals, #13122]. On the first day of differentiation (D0), stem cell media was replaced with cardiogenic mesoderm media consisting of RPMI 1640 Medium [Thermo, #11875093] supplemented with 1X B27(-) [Fisher Scientific, #A1895601], 100 ng/mL Activin A [Peprotech, #120-14P] and 1X Matrigel for 17 hrs. The next day, media was replaced with RPMI supplemented with 1mM of GSK3-Inhibitor (CHIR99021), B27 (-), and 5 ng/mL bone morphogenetic protein-4 (BMP-4) [R&D systems, #314-BP-010] for 24 hours. On Day 2 of differentiation, cells were washed with 1X PBS and media was replaced with vascular differentiation media consisting of StemPro [Thermo Fisher, #10639011] supplemented with 1X GlutaMAX, 1X Penicillin-Streptomycin, 300 ng/mL vascular endothelial growth factor (VEGF) [R&D systems, #293- VE-050], 10 ng/mL BMP-4, 5 ng/mL FGF2, 50 ug/mL Ascorbic Acid [Sigma-Aldrich, #A8960], and 40 mM monothioglycerol (MTG) [Sigma-Aldrich, #M6145]. On Day 5, cells were dissociated with Accutase [Thermo, #A1110501] and replated on 12-well 0.1% gelatin-coated tissue culture dishes in

endothelial growth media (EGM) consisting of EGM basal media [Lonza, #CC-3121] supplemented with 20 ng/mL VEGF, 20 ng/mL FGF2 and 1mM GSK3-Inhibitor (CHIR99021). EGM media was replaced every 48 hours until the final harvest at Day 28. After harvest, samples from each day were exposed to a hypotonic lysis buffer (10mM Tris-HCl Ph7.4, 10 mM NaCl, 3 mM MgCl2, 0.05% IGEPAL), labeled with hash oligos, chemically fixed, and then stored at -80°C until cells from all experimental timepoints had been collected. Following collection, cells were processed using the sci-RNA-seq as described previously.[105] Following library preparation, libraries were sequenced on 2 Nextseq2000 100 cycle kit with standard sequencing chemistry: Read1: 34bp, Index1: 10bp, and Read2: 66bp. Reads were then demultiplexed, assigned to cells and mapped to the hg38 reference genome. Sample barcodes were matched to a corresponding experimental condition only if a sample barcode was significantly enriched (Chi-squared test; q-value < 0.05) and displayed a 4-fold enrichment ratio in that cell. All low-quality reads were removed from the data by setting UMI cutoff to greater than 100 and removing all mitochondrial reads. To eliminate effects of cell-cycle heterogeneity, we used Seurat's[106] workflow for cell-cycle scoring and regression. Following Monocle3's workflow, the data were normalized by size factor, preprocessed using PCA, embedded in 2 dimensions with UMAP, and clustered. Differential gene expression analysis was performed to identify genes that were specifically expressed in each cluster, and this information was used to annotate each cluster based on the relative expression of canonical marker genes. The two clusters obtained at Day 14 were compared across conditions to determine the relative contribution of each treatment to either the endothelial or pericyte cluster.

IMMUNOSTAINING

Cells were seeded on glass coverslips coated with 0.1% gelatin on Day 5 and cultured until confluency on Day 14 following the process described below. The cells were then fixed in 4% paraformaldehyde (PFA) for 15 minutes. The fixed cells were washed three times for 5 min each in 1X PBS before blocking for 1hr with 3% BSA and 0.1% Triton X-100 in 1X PBS while on nutation. Primary antibody incubation was carried out at a 1:100 dilution in blocking buffer overnight at 4C: CD31 (Cell Signaling, Catalog #3528), and

PDGFR-B (Cell Signaling, Catalog #3169). Following overnight incubation, the cells were washed three times for 5 min each in 1X PBS while on nutation. The cells were then incubated with secondary antibodies (Invitrogen, A21050 and Invitrogen, A11008; 1:200 each) diluted in blocking buffer for 1.5hrs at 37°C. Secondary antibodies were then removed, and cells were washed three times for 10 min each in 1X PBS on nutation. Coverslips were sealed using VECTASHIELD with DAPI [Vector laboratories, #H-2000-2] upside-down on glass slides for analysis in confocal microscopy. Images were taken on a Nikon Yokogawa W1 spinning disk confocal microscope using a 20X objective.

FLOW CYTOMETRY

Cells derived using FGF2, C6-79C_mb7, and mb7 in combination with FGF2 (at Day 14 of differentiation) were harvested as a single cell suspension, adjusted to a concentration of 0.5 x 10^6 cells/mL in ice-cold FACS Buffer (1X PBS, 1% BSA, 0.1% NaN3 sodium azide [Millipore-Sigma, #26628-22-8], and blocked for 30 minutes on ice. Primary (unlabeled) antibodies were added at a dilution of 1:100 in FACS buffer for 30 min at 4°C: CD31, CLDN5 [Abcam, #15106]. Cells were washed 3 times in 1X PBS by centrifugation at 1500 rpm for 5 minutes each, following which primary (labeled) or secondary antibodies were added at a dilution of 1:100 in FACS buffer for 1hr at 4°C in the dark: VE-Cadherin-APC [eBioscience, #17-1449-42], PDGFR-B-APC [BioLegend, #323608], NG2-FITC [EMD Millipore, #AB5320A4] and ACTA2-PE [Abcam, #208844]. Cells were washed 3 times in 1X PBS by centrifugation at 1500 rpm for 5 minutes each and resuspended in 100uL of ice-cold FACS Buffer for subsequent analysis. Unstained controls were included. Samples were run on a FACSCanto II flow cytometer (BD Biosciences) and recorded events were analyzed using the flowCore[107] package for R. FSC and SSC (Unstained control) were used for size gating. Events were analyzed as percentage of cells positive for the given panel of markers, and values are reported as mean ± SEM from 3 independent biological replicates.

CELL MIGRATION ASSAY

Cells derived using no FGF, FGF2, C6-79C_mb7, and mb7 in combination with FGF2 (until Day 14 of differentiation) were grown on 12-well plates coated with 0.1% gelatin. Following the formation of a cell monolayer, with the tip of a 200-uL pipette, a scratch was made to remove cells from the top to bottom of each well. Cells were allowed to grow for 24 hours, and images were captured at the 0-, 6- and 24-hour time points using a Nikon Yokogawa W1 spinning disk confocal microscope at a 20X objective. Images were taken from 3 arbitrarily chosen fields from a total of 3 biological replicates per treatment. The size of the scratch area was quantified using the Wound Healing Size Tool for ImageJ[108] and values are reported as a percentage reduction in wound area from the 0-hour time point.

TUBE FORMATION ASSAY

Cells derived using FGF2, C6-79C_mb7, and mb7 in combination with FGF2 (at Day 14 of differentiation) were seeded on 24-well plates pre-coated (30 minutes before seeding) with ice-cold growth-factor reduced 100% Matrigel. Cells were seeded at a density of 1.5 x 10^5 cells/well, and were incubated at 37°C for 24 hours in serum-free media (DMEM low glucose (1 g/L). Tubular structures were observed after 24 hours, and images were taken from 5 arbitrarily chosen fields from a total of 3 biological replicates per treatment using a Nikon Yokogawa W1 spinning disk confocal microscope at a 20X objective. To quantify their 2D network forming ability, the number of nodes, segments and meshes in each field were quantified using the Angiogenesis Analyzer macro tool[109] for ImageJ. All data were normalized to the FGF2 treatment.

LDL UPTAKE ASSAY

LDL uptake was assessed with the LDL Uptake Assay Kit Cell-Based [Abcam, #287862], using an adapted protocol. Briefly, cells derived using FGF2 and C6-79C_mb7 (at Day 14 of differentiation) were seeded at a density of 3 x 105 cells/well in 96-well plates coated with 0.1% gelatin and allowed to starve overnight in DMEM low glucose (1 g/L). Post-starvation, cells were washed with Uptake Assay Buffer (pre-heated to 37°C) and replaced with a 0.1 mg/mL working solution of Fluorophore-

Labeled LDL (diluted in pre-heated Uptake Assay Buffer). Cells were incubated at 37°C for 4 hours, following which the cells were washed with Uptake Assay Buffer and harvested for analysis. Samples were run on a FACSCanto II flow cytometer (BD Biosciences) and recorded events were analyzed using the flowCore package for R using a similar process to the one described previously.

CYTOKINE CHALLENGE ASSAY

Cells derived using FGF2 and C6-79C_mb7 (until Day 14 of differentiation) were grown on glass coverslips coated with 0.1% gelatin, following which they were treated with 10 ng/mL TNF-α [Gibco, #PHC3011] in DMEM low glucose (1 g/L) for 24 hours. After 24 hours, the cells were fixed with 4% paraformaldehyde (PFA) for analysis. The fixed cells were washed 3 times for 5 min each in 1X PBS before blocking for 1 hour with 3% BSA and 0.1% Triton X-100 in 1X PBS while on nutation. Primary antibody incubation was carried out at a 1:100 dilution in blocking buffer overnight: VCAM1 [Abcam, #134047]. Following overnight incubation, the cells were washed three times for 5 min each in 1X PBS while on nutation. The cells were then incubated with secondary antibody [Invitrogen, #A11008; 1:200] diluted in blocking buffer for 1.5 hours at 37°C. Secondary antibodies were then removed, and cells were washed three times for 10 min each in 1X PBS on nutation. Coverslips were sealed using VECTASHIELD including DAPI upside-down on glass slides for analysis in confocal microscopy. Images were taken from 5 arbitrarily chosen fields from a total of 3 biological replicates per treatment, using a Nikon Yokogawa W1 spinning disk confocal microscope at a 40X objective.

F-ACTIN ASSEMBLY

Contractile potential was assessed by quantifying the assembly of F-actin fibers in the cytoplasm. Cells derived using FGF2, C6- 79C_mb7, and mb7 in combination with FGF2 (until Day 14 of differentiation) were grown on glass coverslips coated with 0.1% gelatin until they reached ~80% confluence. The cells were then fixed with 4% paraformaldehyde (PFA) for analysis. The fixed cells were washed three times for 5 min each in 1X PBS before blocking for 1hr with 3% BSA and 0.1% Triton X-100 in 1X PBS

while on nutation. Primary antibody incubation was carried out at a 1:100 dilution in blocking buffer overnight: PDGFR-B. Following overnight incubation, the cells were washed three times for 5 min each in 1X PBS while on nutation. The cells were then incubated with secondary antibody (Invitrogen, #A11008; 1:200) and Phalloidin (1:100, Invitrogen, #A12380) diluted in blocking buffer for 1.5hrs at 37°C. Secondary antibodies were then removed, and cells were washed three times for 10 min each in 1X PBS on nutation. Coverslips were sealed using VECTASHIELD including DAPI upside-down on glass slides for analysis in confocal microscopy using a Nikon Yokogawa W1 spinning disk confocal microscope with a 20X objective. Images were captured from 7 randomly chosen fields from a total of 3 biological replicates per treatment. Cells in each field were segmented using CellProfiler[104] and the mean intensity of Phalloidin was quantified per cell. All summarized results are normalized to the FGF2 treatment.

BLOOD VESSEL ORGANOIDS

To create iPSC-derived vascular organoids, WTC-11 hiPSCs were passaged, counted, and resuspended in differentiation media (DMEM/F12, 20% KOSR [Gibco, #10828028], 1X GlutaMAX, 1X NEAA [Gibco, #11140050]) supplemented with 50mM Y-27632 [Tocris Bioscience, #1254] and distributed into Ultra Low Attachment 6-well culture plates [Corning, #07-200-601] at a density of 3 x 105 cells/well to allow spheroid formation. At Day 3, cells were fed with fresh differentiation media supplemented with 12mM CHIR99021. At Days 5, 7, 9, cells were fed with fresh differentiation media supplemented with 30ng/ml recombinant BMP-4, 30ng/ml recombinant VEGFA165, and 30ng/ml recombinant FGF2. For Days 11-15, the glucose in the differentiation media was reduced to 2 g/L glucose from 3.15 g/L by using SILAC Advanced DMEM/F12 [Gibco, #A2494301] supplemented with 147.5 mg/mL L-Arginine, 91.25 mg/mL L-Lysine, 2 g/L D-Glucose, 20% KOSR, 1X GlutaMAX and 1X NEAA. On Day 11, cells were given fresh differentiation media supplemented with 30ng/ml VEGFA165, 30ng/mL FGF2, and 10 mM SB431542 [Miltenyi, #130-106-275]. On Day 13, cells were transferred to Ultra Low Attachment U-Bottom 96 well plates [Corning #CLS3474-24EA] at 1 organoid per well, embedded in 1:1 Matrigel: Collagen I matrix, and overlaid with differentiation media supplemented with 100 ng/mL VEGFA165 and 100 ng/mL FGF2.

From Days 15 to 23, the glucose in the differentiation media was reduced to 1g/L glucose (physiological glucose) by making it as described for Days 11-15 but supplemented with 1 g/L glucose. Cells were fed on Day 15 and every 3 days thereafter until Day 37. To test the ability of C6-79C_mb7 to yield arterial vascular organoids, the FGF2 in the media between days 5 and 13 was replaced with an equivalent concentration of C6-79C_mb7. At time of harvest, organoids were fixed in 8% PFA diluted 1:1 in differentiation media (4% final concentration) for 15 minutes and washed 3 times for 5 minutes each in 1X PBS. Prior to immunostaining, cells were stored in 1X PBS at 4°C.

IMMUNOSTAINING

For immunostaining, all processes were done with organoids in suspension and all incubations were done in tubes on a nutator. Organoids were blocked in solution (1X PBS containing 5% normal goat serum and 0.3% Triton-X) overnight at 4°C. They were then suspended in antibody dilution buffer (1X PBS containing 1% BSA and 0.3% Triton-X) and primary antibodies diluted at concentrations recommended by the manufacturer and incubated overnight at 4°C. On the third day, cells were washed 3 times for 5 minutes with 1X PBS, then resuspended in antibody dilution buffer containing secondary antibodies at 1:200 and DAPI (1:50), and then incubated overnight at 4°C. On the fourth day, organoids were washed 3 times for 5 minutes in 1x PBS and mounted in Vectashield Anti-fade Mounting Media on a glass microscope slide equipped with a press-to-seal silicone isolator [Electron Microscopy Sciences], 1 organoid per well. Organoids were imaged on a Leica DMi8 confocal microscope equipped with HyD and PMT spectral detectors and LASX acquisition software [version 3.5.5IR]. Images were processed using Lightning Deconvolution. Images were captured with 10X (NA 0.4 PlanApo) and 20X (NA 0.75 PlanApo) air lenses or a 40X (NA 1.1 PlanApo) water immersion lens. Resulting confocal images were processed with Imaris Microscopy Image Analysis Software (Version 9.9) and FIJI ImageJ Analysis software (Version 2.14.0).

MOUSE KIDNEY CAPSULE IMPLANTATION

Blood vessel organoids were differentiated using the protocol above with either FGF2 or C6-79C_mb7 for 21 days. On the day of transplantation, organoids in suspension were broken down into single organoids and transferred to a beveled, kinked PE50 tubing [BD Intramedic, #427517]. Two experimental groups were created corresponding to two treatment conditions (FGF2 or C6- 79C_mb7, n = 3 mice per group). Adult NOD-SCID mice (8-10 weeks old) were anesthetized using isoflurane supplemented with oxygen within an anesthesia chamber. Animals were then transferred to a nose cone and maintained on 2% isoflurane. To maintain a body temperature of 37°C, mice were placed on a heating pad throughout the transplantation. Mice were shaved and the site was sterilized with betadine and alcohol wipes prior to making a 1-2 cm dorsal flank incision. Kidneys were externalized using a cotton swab and the capsule was nicked near the caudal end using a needle tip (22 gauge). The beveled PE50 tubing was inserted beneath the capsule and cellular material was implanted under the control of a Hamilton syringe. A cotton swab was used to clot and seal the opening in the capsule to hold the implant in place. Next, the kidney was returned to the abdominal cavity, the peritoneum was sutured shut with absorbable sutures, and the skin was closed with surgical staples. Experiment was performed in compliance with ethical regulations, IACUC protocol #4375-01. Mice were placed into a heated recovery cage until they regained consciousness, and then moved back to their home cage and transported back to the vivarium. 20 days after injection, mice were euthanized, kidneys were excised with graft intact and fixed in 4% paraformaldehyde at 4°C for 1.25 hours and transferred to 30% sucrose solution at 4°C overnight. Kidneys were then bisected and embedded in embedding cryo-molds [Sakura, #25608-916] with Tissue-Tek O.C.T. compound [Sakura, #4583]. The embedded tissue was then frozen by placing a cold-resistant beaker of 2-methylbutane solution [EMD, #MX0760-1] into liquid nitrogen, which causes fast cooling to -80°C. Samples were then placed in a -80°C freezer for storage until cryo-sectioning. 10-20 mm-thick sections were made on pre-chilled Superfrost Plus microscope slides [Fisherbrand, #12-550-15] and then stored at -80°C until used for immunofluorescence analysis.

IMMUNOSTAINING

Frozen slides were blocked in blocking buffer (5% Normal Goat Serum, 0.3% Triton X-100 in 1X PBS) for 90 minutes at RT. Primary antibody incubation was carried out in antibody buffer (1% BSA, 0.3% Triton X-100 in 1X PBS) overnight at 4C: anti-hVE-Cadherin (1:100, [Cell Signaling, Catalog #2500]), anti-hCD31, and anti-mCD31 (1:100, [BD Biosciences, #557355]). Following overnight incubation, the cells were washed three times for 5 min each in 1X PBS, followed by incubation with secondary antibodies (1:200 each) diluted in antibody buffer overnight at 4°C. Secondary antibodies were then removed, and cells were washed three times for 5 min each in 1X PBS on nutation. Coverslips were sealed using VECTASHIELD including DAPI upside-down on glass slides for analysis in confocal microscopy.

GUIDE RNA DESIGN, SYNTHESIS & TRANSFECTION

The gRNAs targeting the *p16* gene was designed using the CRISPRscan web prediction tool and ordered as T7-gRNA primers. The T7-gRNA forward primer and the reverse scaffold primer were used in primer extension reaction to synthesize a double stranded DNA fragment by using Q5 High Fidelity-based PCR [New England Biolabs] followed by PCR purification [Qiagen]. The 120 bp dsDNA served as a template for IVT [MAXIscript T7 kit, Applied BioSystems]. The RNA was then purified using Pellet Paint Co-Precipitant [Novagen]. For transfection, $1x10^{\wedge 5}$ WTC EBdCas9 or $1x10^{\wedge 5}$ NCdCas9 cells were seeded at day 0, and treated with Dox (2µg/ml) for 2 days before and during transfection. On day 2 cells were transfected with gRNAs using Lipofectamine RNAiMAX [Life Technologies]. gRNA was added at a 40 nM final concentration when added alone or 20nM in co-gRNA transfection. A second transfection was performed after 24 h. All no guide controls were induced by Dox and harvested with study groups.

CELL VIABILITY

Cell viability assay was measured by AlamarBlue [ThermoFisher Scientific, #DAL1025]. Cells were induced and transfected with gRNA as discussed above. 6h after last transfection, 10× of viability reagent was added to media. Time “0” was measured 4h

after. Fluorescence measurements were read on PerkinElmer Envision plate reader after transferring 50ul of media from each condition to a 96 well microplate reader.

QUANTIFICATION AND STATISTICAL ANALYSIS

Details of the quantification and statistical analysis can be found in the Figure legends and method details sections. Calcium release assays were processed and analyzed with the Fiji software distribution of ImageJ v1.52i[103] and cellular fluorescence was quantified with CellProfiler[104] which was also used for F-actin assembly measurements. Cell migration assays were analyzed with the Wound Healing Size Tool[108] for ImageJ. Tube formation assays were analyzed via the Angiogenesis Analyzer macro tool[109] for ImageJ. Flow cytometry assays were analyzed with FlowJo software or the flowCore package[107] for R and plotted with Origin Pro 9.1. Transcriptomics data was analyzed using the Monocle3[110] software suite. Immunostainings of blood vessel organoids were processed with the Imaris Microscopy Image Analysis Software (Oxford Instruments) and Fiji ImageJ Version 2.14.0.

RESULTS

FGFR PATHWAY INHIBITION

In collaboration with the Institute for Protein Design (IPD), we developed a de novo protein binder specifically targeting the c-isoform of FGFR1 and FGFR2. This effort utilized a generalizable approach for designing proteins that bind to a specific site on a target protein using only its three-dimensional structure. Starting with a broad exploration of possible binding modes across the selected region of the FGFR surface, we intensified the search around the most promising modes to identify high-affinity interactions. The resulting binder (mb7), a 74-amino acid protein with a molecular weight of 7.5 kDa, exhibited a dissociation constant (K_d) of 2.5 nM, indicating a strong binding affinity. Crucially, the binder was designed to target domain D3, the region responsible for conferring isoform specificity, allowing us to create a molecule that binds exclusively to the c-isoform without interacting with the b-isoform. This isoform specificity was confirmed through X-ray crystallography, revealing precise binding to the

D3 domain [Fig 1A]. Functional studies further demonstrated that the binder acts as an FGF-specific, dose-dependent inhibitor in HUVEC cells, effectively blocking FGF activity with an IC_{50} of approximately 31.1 nM in the presence of native FGF ligands [Fig 1B,C].

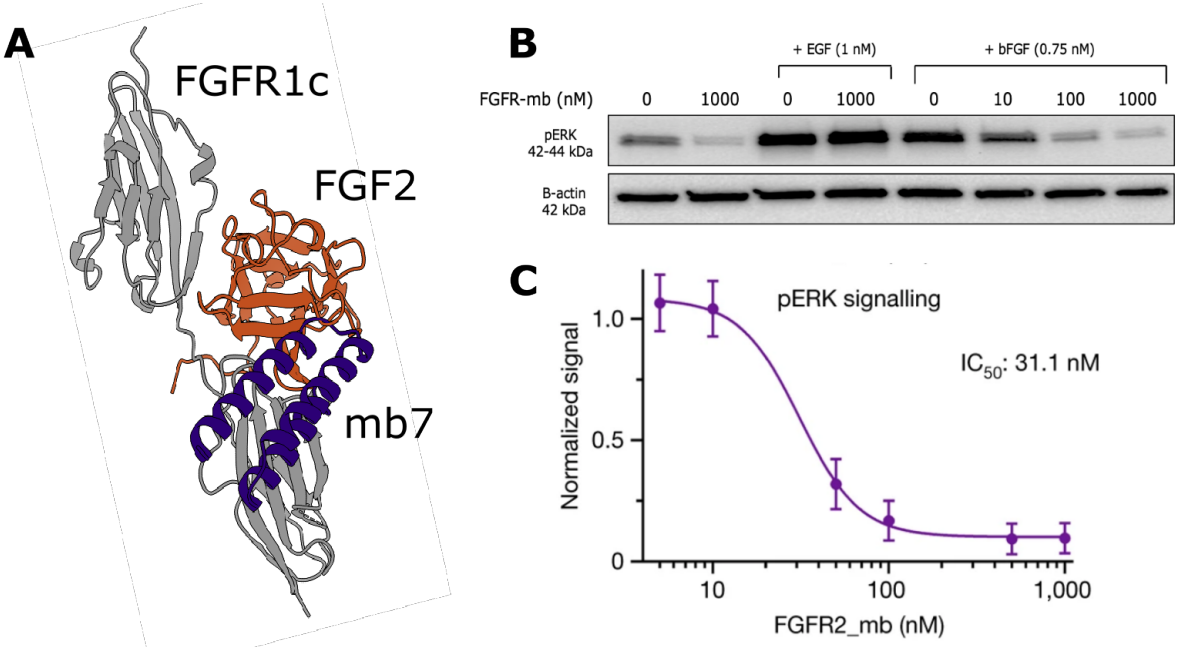

Fig 1: De novo designed FGFRc mini binder exhibits dose-dependent inhibition. A) Design model of natural geometry of signaling competent FGF2 (orange) with FGFR1c (gray) together with superimposed FGFRc mini binder (mb7, purple). B) Serum-starved HUVECs treated with mb7 exhibit dose-dependent inhibition of native FGF signaling. Competitive inhibition with native EGF demonstrates pathway specificity of our binder. C) Dose-response curve, IC_{50} for pERK inhibition in HUVECs.

FGFR PATHWAY ACTIVATION

We next investigated whether clustering receptor tyrosine kinases in higher-order geometries by presenting receptor-binding domains on designed oligomers could drive cross-phosphorylation of their intracellular kinase domains and induce downstream signaling. In collaboration with the IPD, we designed cyclic homo-oligomers with up to 8 subunits using repeat protein building blocks that can be modularly extended. The multiple distinct valencies and geometries of our oligomeric ligands enable exploration of how the geometry and valency of tyrosine kinase receptor association influence

signaling output and cell behavior. We fused the de novo-designed minibinder (mb7) against FGFRc at either the N or C termini of the designed cyclic oligomers with a short glycine-serine linker. Six oligomers were selected for fusion: C2-58, C4-71, C6-71, C6-79, and C8-71. Depending on the fusion terminus and the geometry of the oligomer, the binding domains are displayed at different spacings on adjacent subunits: for example, C6-79C_mb7 displays the minibinders 54 A˚ apart with mb7 on the C terminus of the oligomer, while C6-79N_mb7 displays the binders 18 A˚ apart with mb7 on the N terminus of the oligomer [Fig 2].

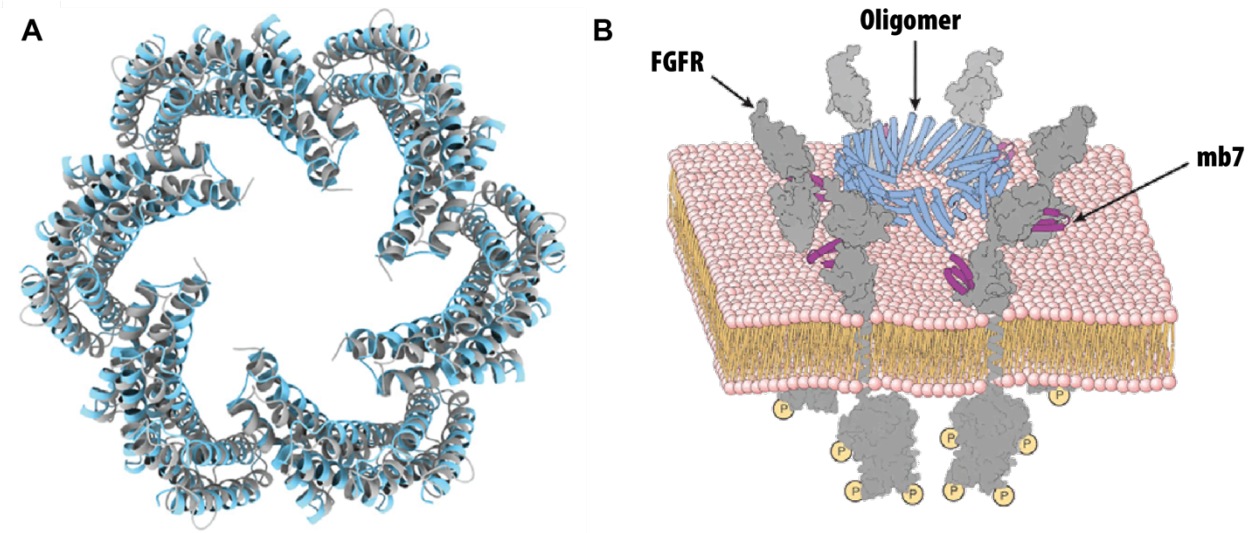

Fig 2: Engineered Cyclic Oligomeric Scaffolds for Receptor Clustering and Signal Modulation. A) C6-79 alignment of design model (gray) with cryo-EM structure (cyan, PDB: 8F6R) in top view. Structures align well with an RMSD of 2.85 A˚. B) Schematic representation of the oligomer integrated into the plasma membrane, illustrating its application in clustering FGF receptors to drive signaling.

FGF-mediated FGFR signaling results in stimulation of the Ras signaling pathway, leading to phosphorylation of extracellular-signal-regulated kinase 1 and 2 (ERK1/2) and activation of phospholipase C-gamma (PLC-ɣ), leading to intracellular calcium release.[73] We evaluated the signaling activity of our designs by screening them in

serum-starved Chinese hamster ovary (CHO) cells stably expressing hFGFR1c (CHO-R1c) at 10 nM each for 15 min at 37°C. Downstream activation through phosphorylation of ERK1/2 and FGFR1 (Y653/654) was analyzed by western blot. Of the designs, we found that C6-79C_mb7, C6- 79N_mb7, C4-71N_mb7, C4-71C_mb7, and C8-71C_mb7 broadly induced strong FGFR activation and ERK1/2 phosphorylation, comparable to that achieved by native FGF2, while C2- 58-2X_mb7, C6-71C_mb7, C6-71N_mb7, and C8-71N_mb7 displayed weaker activity [Fig 3A]. To characterize their dose-dependent activity, we titrated a subset of these designs using western blotting for ERK1/2 phosphorylation in CHO-R1c cells. C2-58-2X_mb7, C4-71C_mb7, C4-71N_mb7, C6-79C_mb7, and C8-71C_mb7 had similar EC50 values of 0.63, 1.33, 0.89, 1.56, and 2.07 nM, respectively, and similar maximal activation (E_{max}) values, while C2-58-2X_mb7 had a lower E_{max} [Fig 3B-G].

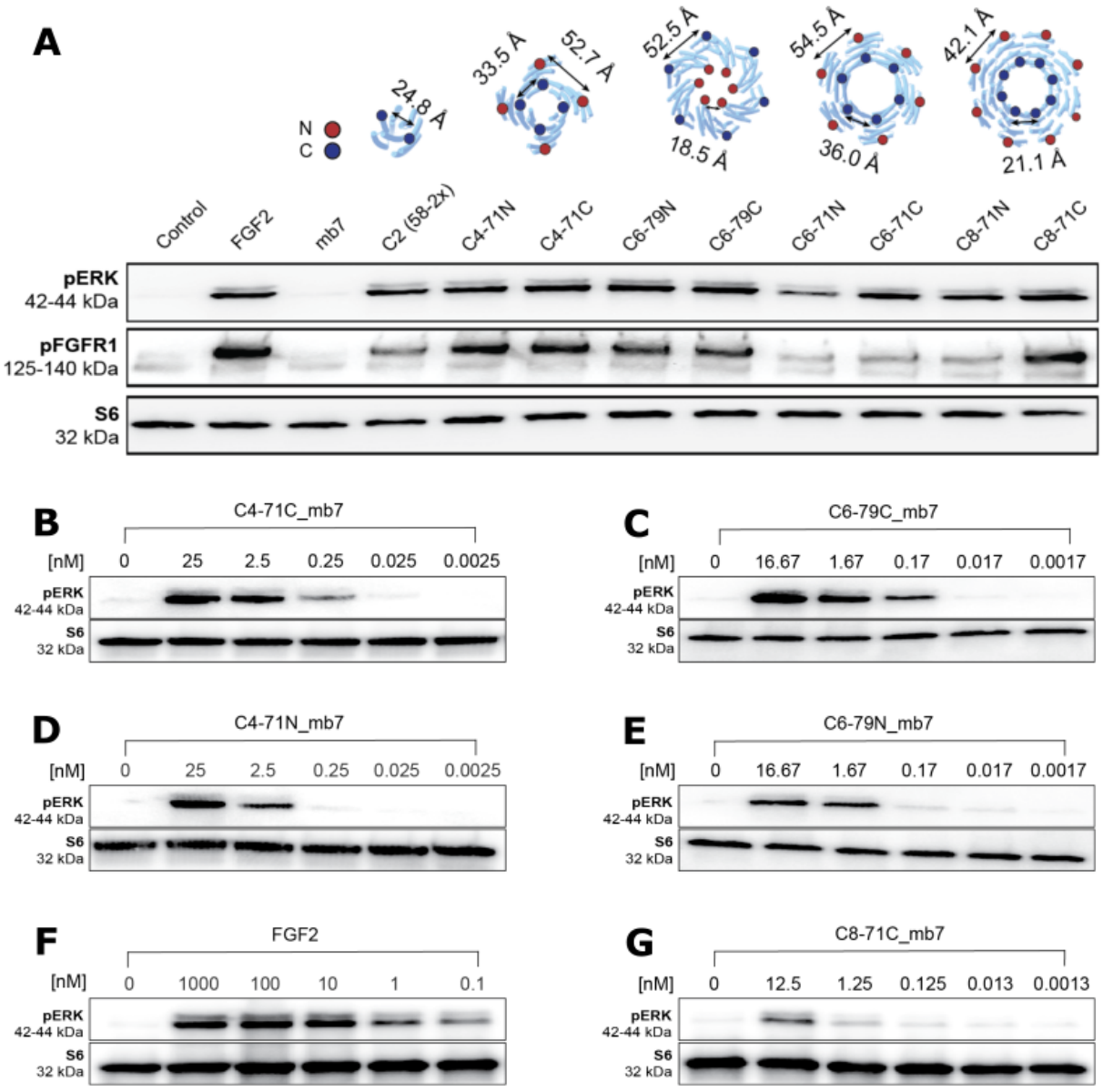

Fig 3: Activation of FGFR signaling by designed agonists. A) Signaling response to a library of oligomers presenting mb7 in CHO-R1c cells, treated at 10 nM each, analyzed through western blot. Top: cartoons of oligomers presenting mb7 at their N or C termini; distances between neighboring chains are shown above their respective treatments. B-G) hFGFR1c-expressing CHO cells were treated with different concentrations of FGF2 or designed scaffolds for 15 min at 37C, followed by western blot analysis for phosphorylated ERK. (B) C4-71C_mb7, (C) C6-79C_mb7, (D) C4-71N_mb7, (E) C6-79N_mb7, (F) FGF2, and (G) C8-71C_mb7.

RECEPTOR CLUSTERING ON CELL SURFACE

To investigate whether FGFR1c activation was due to induced receptor clustering, cells were examined by single-particle tracking with a HaloTag targeting FGFR1c[111] to directly visualize their diffusion in the plasma membrane; receptors engaged in a signaling cluster should exhibit decreased diffusion, manifesting in a decreased diffusion coefficient.[112] Receptors on cells treated with C6-79C_mb7 showed slower diffusion than those treated with FGF1 and heparin [Fig 4C], indicating that C6-79C_mb7 induces an oligomeric state of FGFR1c at the membrane. To probe the presence of local receptor clusters on the cell surface after ligand treatment, intensity levels of single spots in HaloTagged CHO-R1c cells labeled with Alexa488 were evaluated. C6-79C_mb7-treated cells showed signals with an intensity distribution slightly shifted compared with FGF1 supplemented with heparin, with intensity peaks at 500, 1,000, and 2,000 a.u., suggesting that multiple receptors are clustered together by the designed mb7-presenting oligomers. The extent of signaling correlated with the ability of the designs to cluster receptors [Fig 4A,B].

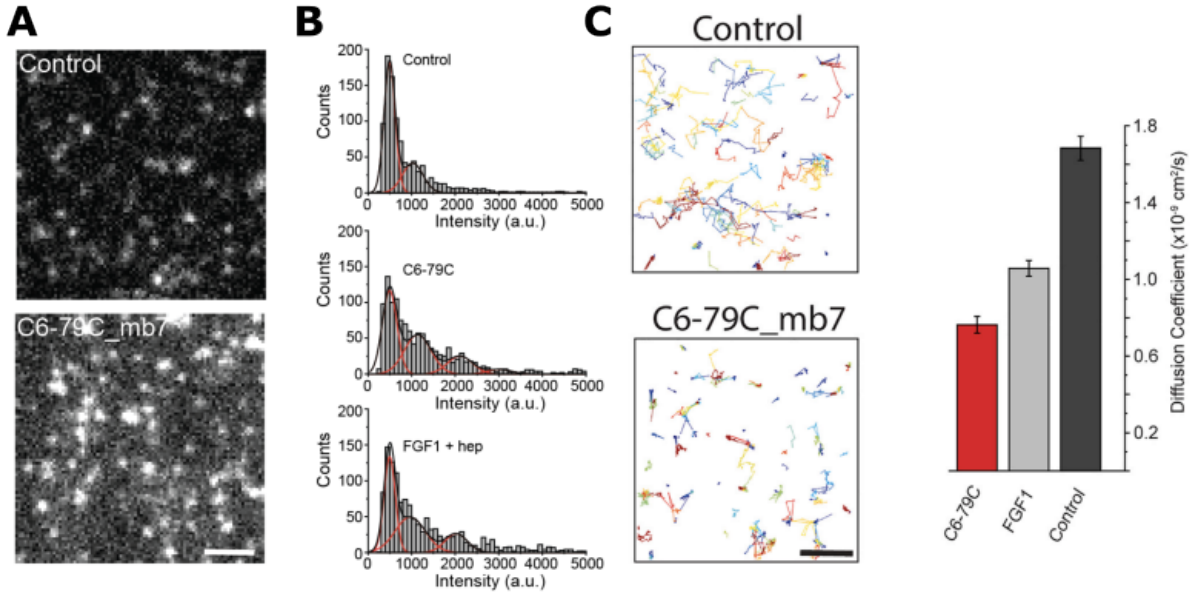

Fig 4: Direct measurement of FGFR diffusion coefficients in the cell membrane. A) Single particle tracking of FGFR1 molecules on the cell surface. B) Intensity histograms of receptor clusters on the cell surface reveals receptor clustering induced via oligomerization. C) CHO-R1c cells were treated with FGF1/heparin or C6-79C_mb7 and fluorescently tagged FGFR1c

(HaloTag-R1c) revealed a strong decrease in the diffusion coefficient values in both conditions. Diffusion coefficients were calculated from analyzing the labeled receptor tracks. Error bars represent SEM from three independent biological repeats. Scale bars: 2μm.

FGFR1C ISOFORM SPECIFICITY

FGFRs 1–3 have two alternatively spliced variants, the ‘‘c’’ and ‘‘b’’ isoforms, which have different third Ig-like domains and variable FGF ligand affinities. Tissue-specific expression of these isoforms and their reciprocal signaling play roles in embryonic development, tissue repair, and cancer. Separating the functions of the FGFR b- and c-isoforms in differentiation has been hindered by a lack of ligands that can selectively bind one isoform or the other. The mb7 minibinder was designed to specifically bind the c-isoform of the FGFR, and it selectively inhibits signaling through this isoform. We evaluated the receptor isoform specificity of our synthetic agonists by treating serum-starved L6 rat myoblast cells stably expressing either the c- or b-isoform of hFGFR1 (L6-R1c or L6-R1b, respectively; overexpression was validated with RT-qPCR), with 10 nM of mb7, FGF2, or C6-79C_mb7 for 15 min at 37°C. Although FGF2 does not discriminate between the two FGFR1 isoforms and activates signaling in both cell types, C6-79C_mb7 stimulates ERK1/2 and FGFR phosphorylation only in L6-R1c cells. We reasoned that it should be possible to specifically activate signaling through the b-isoform by combining FGF2 with the monomeric mb7 (which blocks signaling through the c-isoform); to test this, we stimulated both L6 cell lines with a combination of mb7 and FGF2 at 10 nM each for 15 min. We found that this combination stimulates ERK1/2 phosphorylation in L6-R1b cells only; thus, our designs enable selective activation of signaling through either isoform [Fig 5].

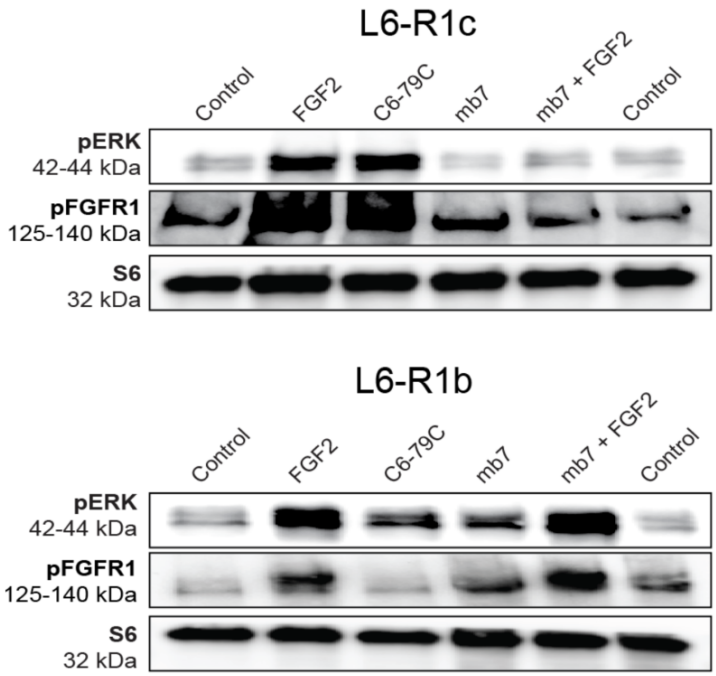

Fig 5: FGFR isoform specificity. Signaling response (pERK and pFGFR1) to FGF2, mb7, C6-79C_mb7, or mb7 + FGF2 in L6-R1c (top) or L6-R1b (bottom) cells, analyzed through western blot.

We next investigated the ability of the designs to activate FGF signaling through the PLC-ɣ downstream branch of signaling by measuring the levels of intracellular calcium release following treatment of serum-starved CHO-R1c cells with varying concentrations of the designs. These results show a similar trend: C6- 79C_mb7, C4-71C_mb7, and C8-71C_mb7 induce strong intracellular calcium release, with EC_{50} values of 0.38, 0.72, and 3.09, respectively, while C2-58-2X_mb7 displays lower activity, with an EC_{50} of 26.02 nM [Fig 6A]. Although the peak magnitude of calcium release was similar between FGF2 at 10 nM and the synthetic agonist C6-79C_mb7 at 10 nM, there was a pronounced difference in the duration of the response: the higher valency synthetic ligand, C6-79C_mb7, generated longer-duration calcium transients [Fig 6B,C], similar to a control condition in which we supplemented FGF2 together with heparin. This strong, heparin-independent signaling effect of our designed agonist likely reflects the slow off rates of the high avidity multivalent agonists.

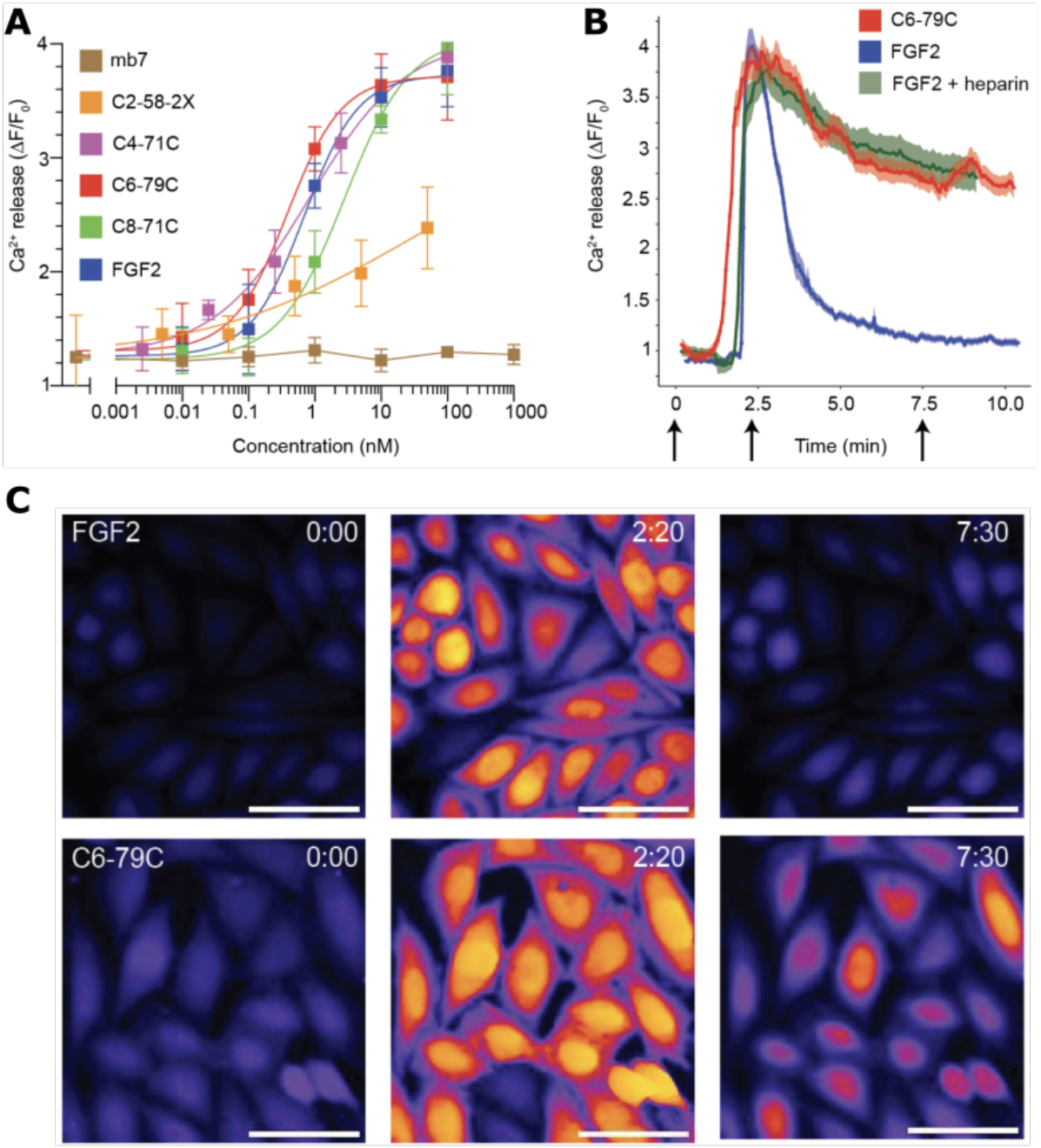

Fig 6: Intracellular Calcium Release. A) Dose-response curves of selected designs, assessed through intracellular calcium release. Error bars represent SEM from three independent biological repeats. B) Comparison of a calcium intensity signaling trajectory after treatment with FGF2 (with or without heparin) or C6-79C_mb7 at 10 nM each. C) Exemplary images comparing the calcium response exhibited in CHO-R1c cells following treatment with FGF2 or C6-79C_mb7 at 10 nM across three different time points (0:00, 2:20, and 7:30 min). Scale bar: 50µm

VASCULAR DIFFERENTIATION WITH DESIGNED AGONISTS

FGF signaling plays an important role during early embryogenesis; the controlled spatiotemporal expression of FGFRs and their ligands drives specification and development of many cell lineages. In the vasculature, mesodermal precursors give rise to endothelial and perivascular cell fates. The role of FGF signaling and the FGFR isoforms in this bifurcation is not currently understood. We investigated the effect of the c-isoform-specific FGFR minibinder oligomers on vascular development by generating endothelial cells and perivascular cells from human induced pluripotent stem cells (iPSCs) through a cardiogenic mesoderm intermediate [Fig 7A]. We replaced the FGF2 (which engages both b- and c-isoforms of FGFRs) in a previously described differentiation media between days 2 and 5 (when mesodermal intermediates first appear) in the protocol with 1 nM C6-79C_mb7 (the most potent synthetic agonist), 100 nM C2-58-2X_mb7 (the weakest agonist), 10 nM mb7, or 10 nM mb7, in combination with 1 nM FGF2 (to specifically activate signaling through the b-isoform), and from day 5 onward allowed the cells to differentiate in normal conditions for 28 days; samples were harvested for single-cell RNA sequencing (scRNA-seq) analysis at days 0, 5, 14, and 28. The sequencing datasets were analyzed using Monocle3 and visualized using uniform manifold approximation and projection (UMAP), which revealed 5 clusters of cells that segregated predominantly by time point and cell type [Fig 7B]; cell types were annotated based on the differential expression of previously published canonical marker genes [Fig 7C].

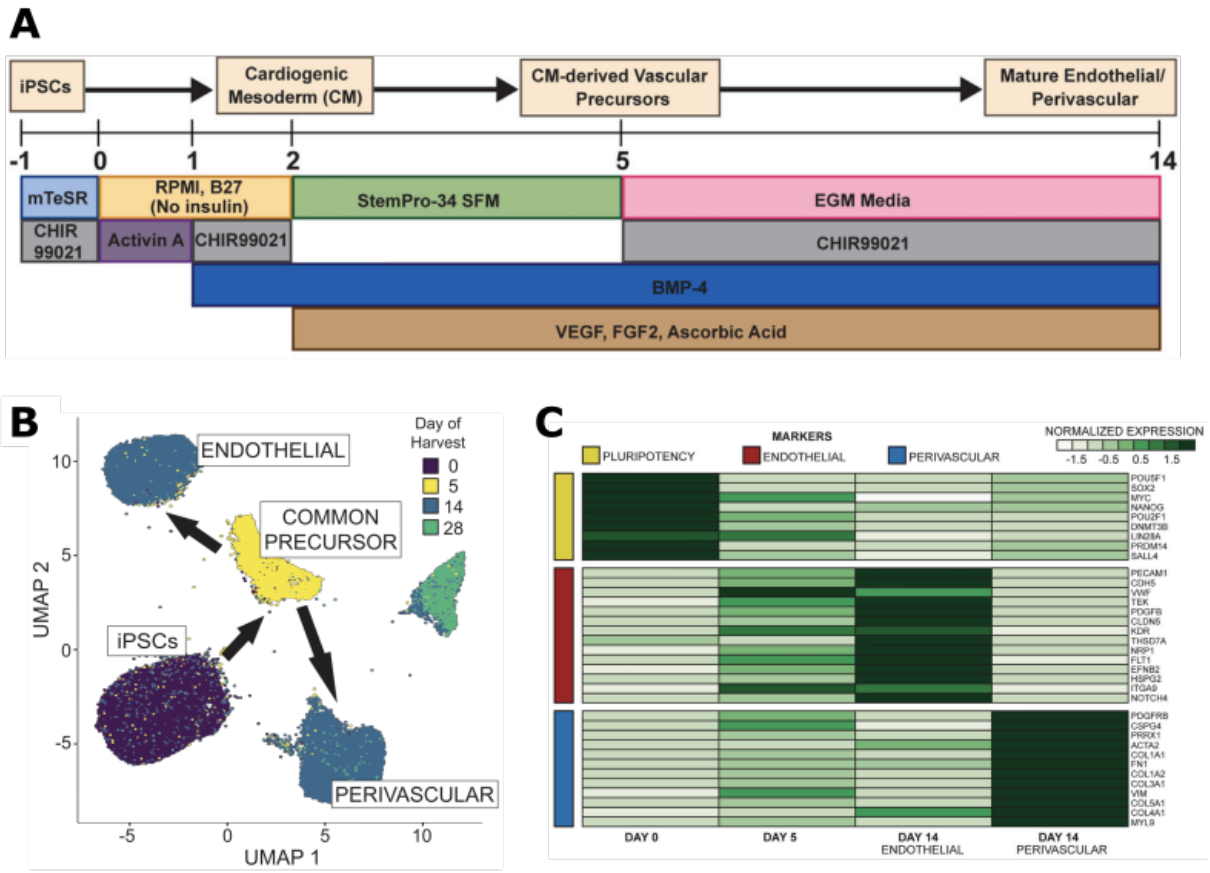

Fig 7: Vascular differentiation using designed agonists. A) Schematic for endothelial cell differentiation from iPSCs through a cardiogenic mesoderm intermediate. B) UMAP embeddings of all sequenced cells colored by day of harvest, along with given cluster annotations. C) Clustered heatmap comparing the normalized expression of selected putative cell markers (iPSCs, endothelial and perivascular) across all obtained clusters along with given annotations.

ENDOTHELIAL VS PERIVASCULAR FATE SPECIFICATION

All treatments (FGF2 and designed agonists) directed iPSCs to differentiate and form a common endothelial-perivascular precursor at Day 5. This common precursor population then bifurcated to form either endothelial cells or perivascular cells at Day 14. The cellular differentiation trajectory was design-dependent and determined by Day 14. Addition of FGF2, C6-79C_mb7, or C2-58-2X_mb7 generated ~60% endothelial cells in all three cases; the remaining population differentiated into perivascular cells. In contrast, the differentiation media without any FGF addition (control) resulted in a population that was only ~34% endothelial (endothelial cell formation is weakly driven in

the absence of any supplemented FGF2, presumably because of low levels of endogenously secreted FGFs). On the other end of the spectrum, cells treated with mb7 showed a marked preference for perivascular lineage, producing only 28% endothelial cells. Cells treated with a combination of mb7 and FGF2 were almost exclusively mesenchymal, producing a population that was 93% perivascular [Fig 8A]. These results suggest that FGFR c-isoform activity is critical for the development of endothelial cells, and specific activation of the b-isoform instead biases the cells toward perivascular fate. Immunostainings of differentiated iPSCs for endothelial (CD31) and perivascular (PDGFR-B) markers at Day 14 confirmed the primary cell fate after treatment with C6-79C_mb7 (FGFR c-isoform-specific signaling) or mb7 together with FGF2 (FGFR b-isoform-specific signaling), which led to the enrichment of endothelial or perivascular cells, respectively [Fig 8B]. We used flow cytometry with endothelial and perivascular cell surface markers to further characterize the cells harvested at Day 14 of differentiation. Populations derived using FGF2 or C6-79C_mb7 were similar in composition, consisting primarily of endothelial cells (VE-cadherin+ cells: 81.2% and 69.9%, respectively; CD31+ cells: 70.1% and 87.2%, respectively; CLND5+ cells: 34.9% and 41.2%, respectively), whereas cells derived using mb7 in combination with FGF2 were overwhelmingly perivascular in identity (PDGFR-B+ cells: 76.2%; NG2+ cells: 33.9%; ACTA2+ cells: 16.2%) [Fig 8C]. These results agree with the trend seen in the transcriptomic data—signaling of FGFRs through their c-isoform is critical for the development of endothelial cells, while b-isoform-specific signaling instead promotes the perivascular lineage.

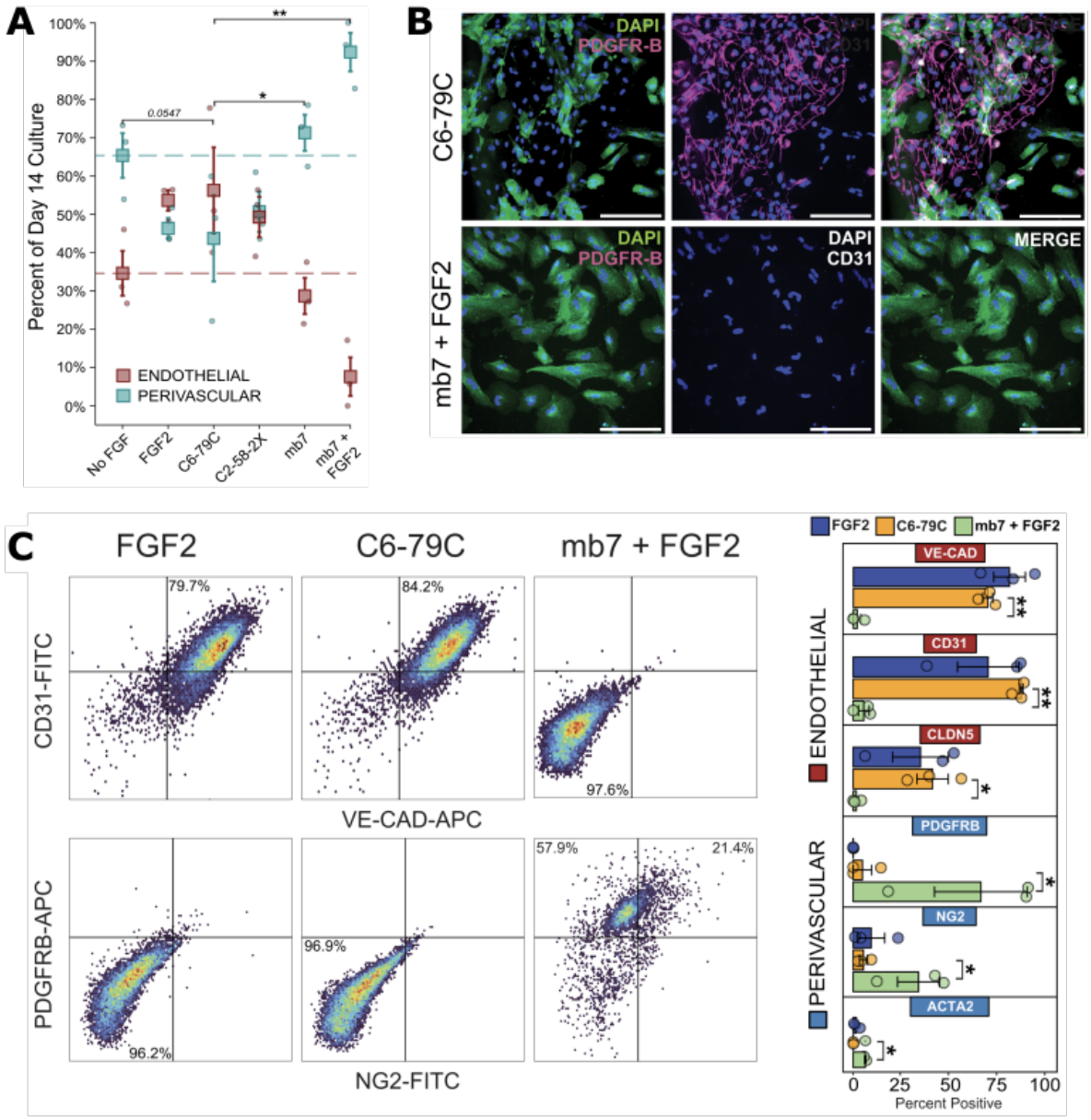

Fig 8: Endothelial vs Perivascular fate specification. A) Proportion of endothelial or perivascular cells generated at day 14 following treatment with FGF2, C2-58-2X_mb7, C6-79C_mb7, mb7 alone, or mb7 in combination with FGF2. Error bars represent SEM from 3 independent biological repeats. B) Immunohistochemical characterization of differentiated cells treated with C6-79C_mb7 or mb7 in combination with FGF2, with PDGFR-B and CD31 to specifically mark perivascular and endothelial cells, respectively. Scale bars: 200 μm C) Quantitative analysis of a select panel of endothelial (VE-cadherin, CD31, and CLND5) and perivascular (PDGFR-B, ACTA2, and NG2) markers using flow cytometry. Left: representative

2D scatterplots; Right: summarized results with mean and SEM from 3 independent biological repeats.

FUNCTIONAL CHARACTERIZATION OF CELLULAR PHENOTYPES

Perivascular cells are contractile cells that are known to play a role in capillary blood flow regulation through the assembly of F-actin bundles;[113] we characterized our cell populations by measuring intracellular actin (using fluorescently labeled phalloidin) at Day 14 of differentiation. Cells derived using mb7 + FGF2 exhibited ~4-fold increase in F-actin assembly over cells derived using FGF2 or C6-79C_mb7 [Fig 9] owing to the robust formation of stress fibers in these perivascular cells.

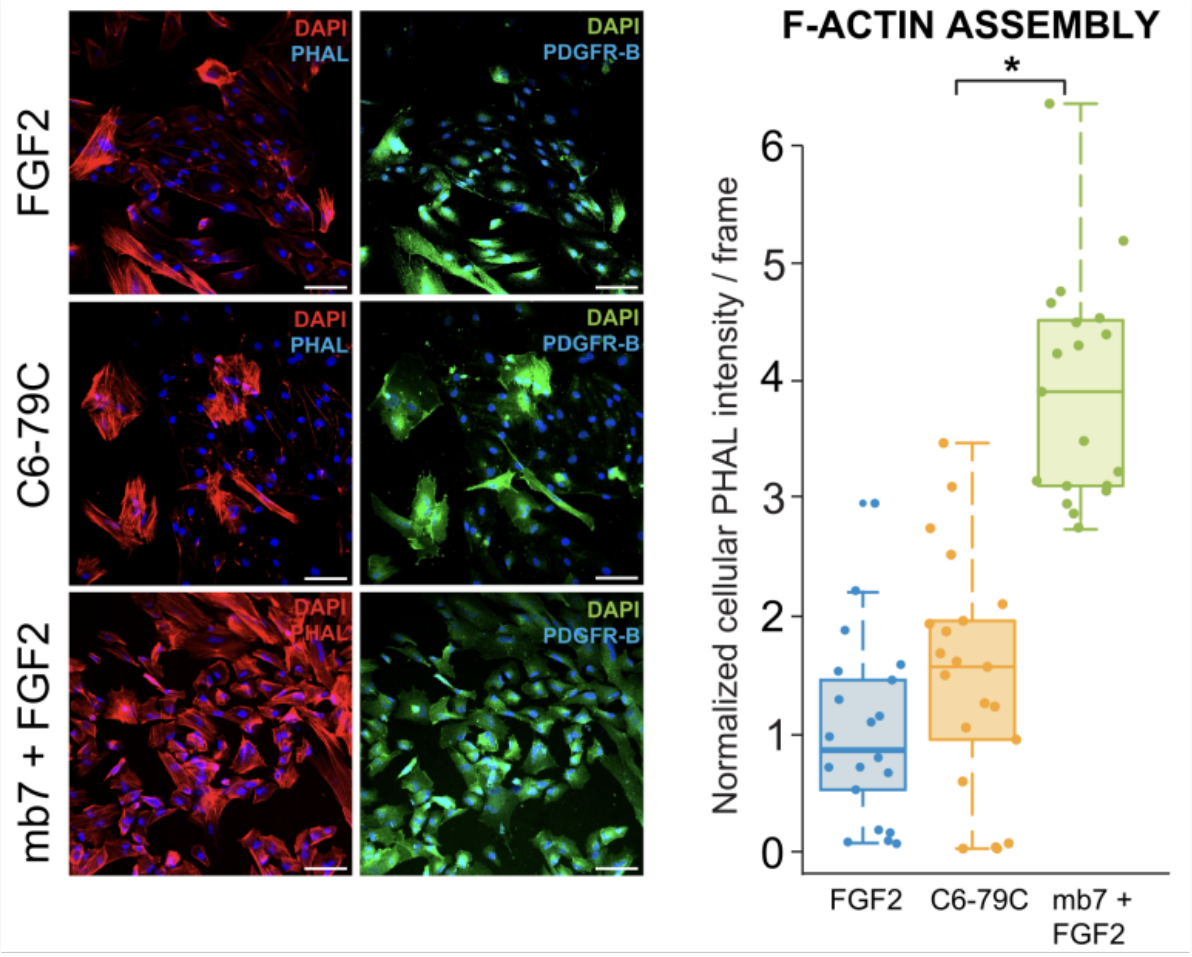

Fig 9: F-actin assembly. Left: representative immunofluorescence images from FGF2, C6-79C_mb7 and mb7 + FGF2-derived cells (PDGFR-B, perivascular cells; PHAL, F-actin). Scale bars: 100 μm. Right: summarized per-cell phalloidin (PHAL) intensity from 3 independent biological repeats (7 randomly chosen field of views from each).

To characterize the functional maturity of the endothelial populations, we used tube formation[114], cell migration[115, 116], LDL uptake[117] and cytokine challenge[118] assays. The capacity to assemble into capillary-like tubules is a hallmark phenotype of endothelial cells and the cells derived via FGFR c-isoform activation demonstrated a robust 2D network formation capacity (measured by numbers of nodes, segments, and meshes in a tube formation assay) [Fig 10]. In addition, these cells readily migrated, completely sealing an inflicted scratch within 24 h [Fig 11].

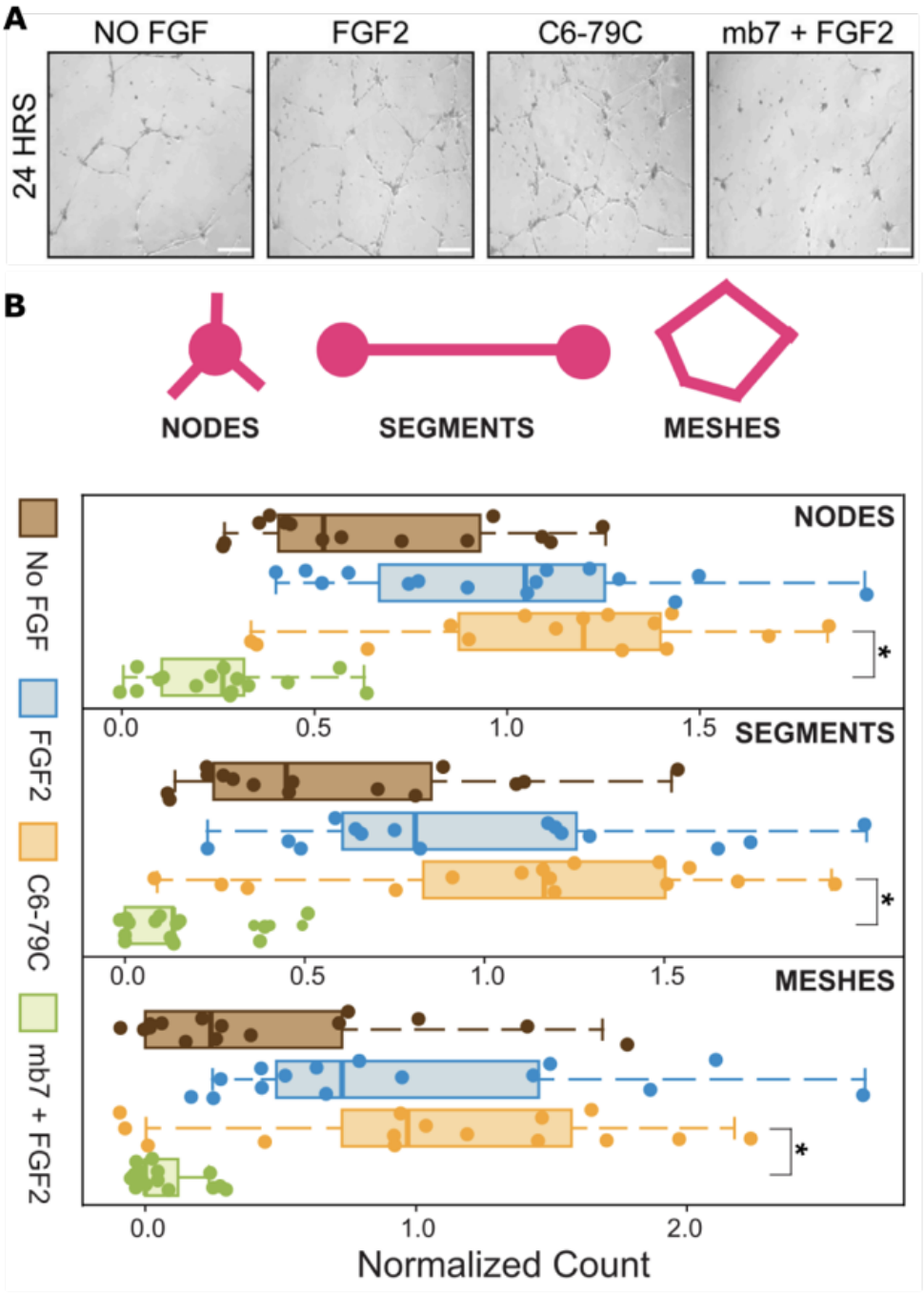

Fig 10: 2D network formation. A) Representative images showing 2D network forming ability in 24 h of cells derived using No FGF, FGF2, C6-79C, or mb7 + FGF2. Scale bars: 100 μm B) Normalized count of nodes, segments, and meshes after 24 h, summarized from 3 independent biological repeats (5 randomly chosen fields of view from each).

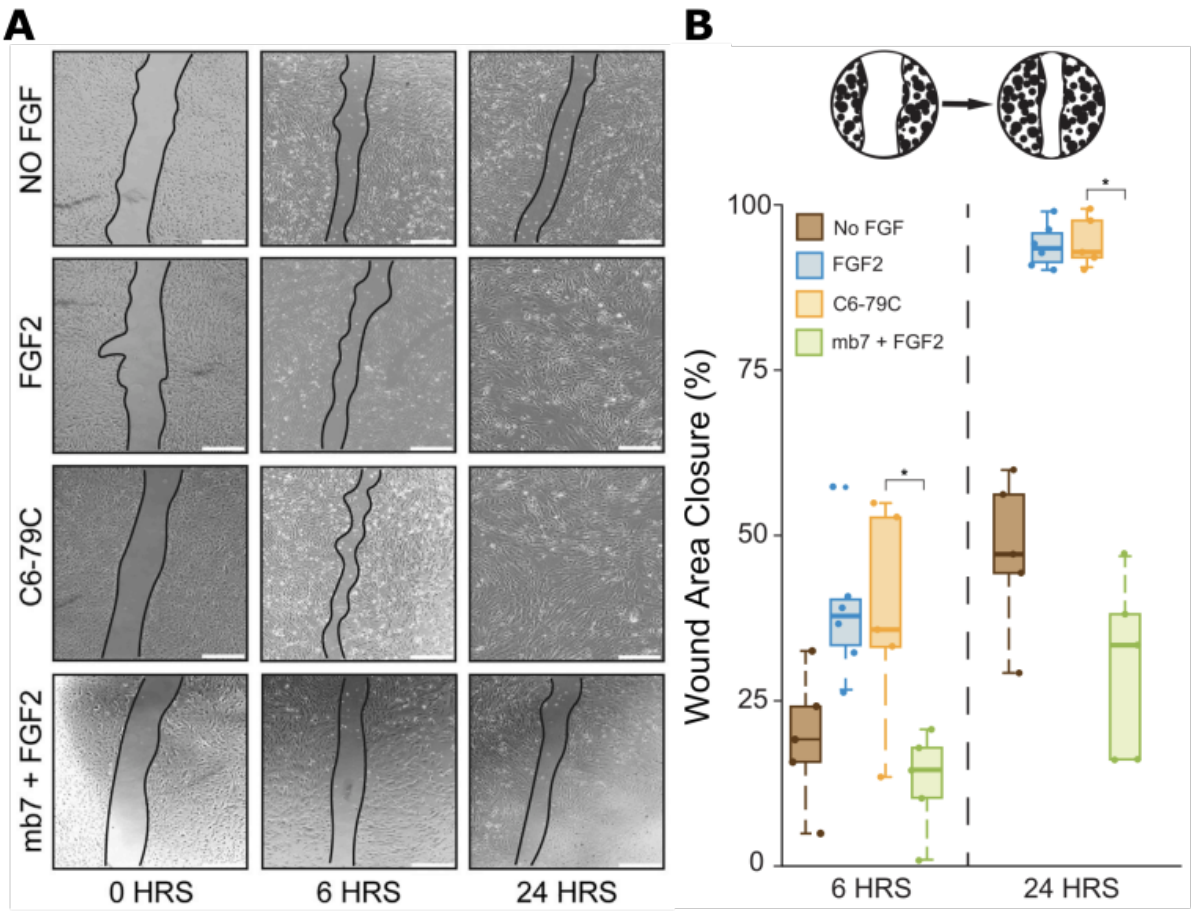

Fig 11: Cell migration. A) Representative images showing migratory capacity of cells derived using No FGF, FGF2, C6-79C, or mb7 + FGF2. Images are taken at 0, 6, and 24 h after inducing the scratch. Scale bars, 150 μm B) Percentage closure of inflicted scratch area after 6 and 24 h, summarized from 3 independent biological repeats

Low-density lipoprotein (LDL) uptake is a critical process observed in endothelial cells to acquire cholesterol and we found that endothelial cells derived using FGF2 and C6-79C_mb7 (but not mb7 + FGF2) exhibited high and comparable levels of receptor-mediated uptake of fluorophore-labeled LDL [Fig 12A]. Finally, endothelial cells are known to upregulate vascular cell adhesion molecule 1 (VCAM-1) (for adhesion and trans-endothelial migration of leukocytes) in response to inflammatory cytokines and we observed that endothelial cells derived using FGF2 and C6- 79C_mb7 (but not mb7 + FGF2), upon exposure to tumor necrosis factor alpha (TNF-a), displayed a significant increase in VCAM-1 expression [Fig 12B]. These results suggest that the endothelial

cells generated via c-isoform activity are functional and mature, with increased endothelial functionality compared with cells derived using the FGFR c-isoform antagonist (mb7 + FGF2), which exhibit more of a perivascular identity.

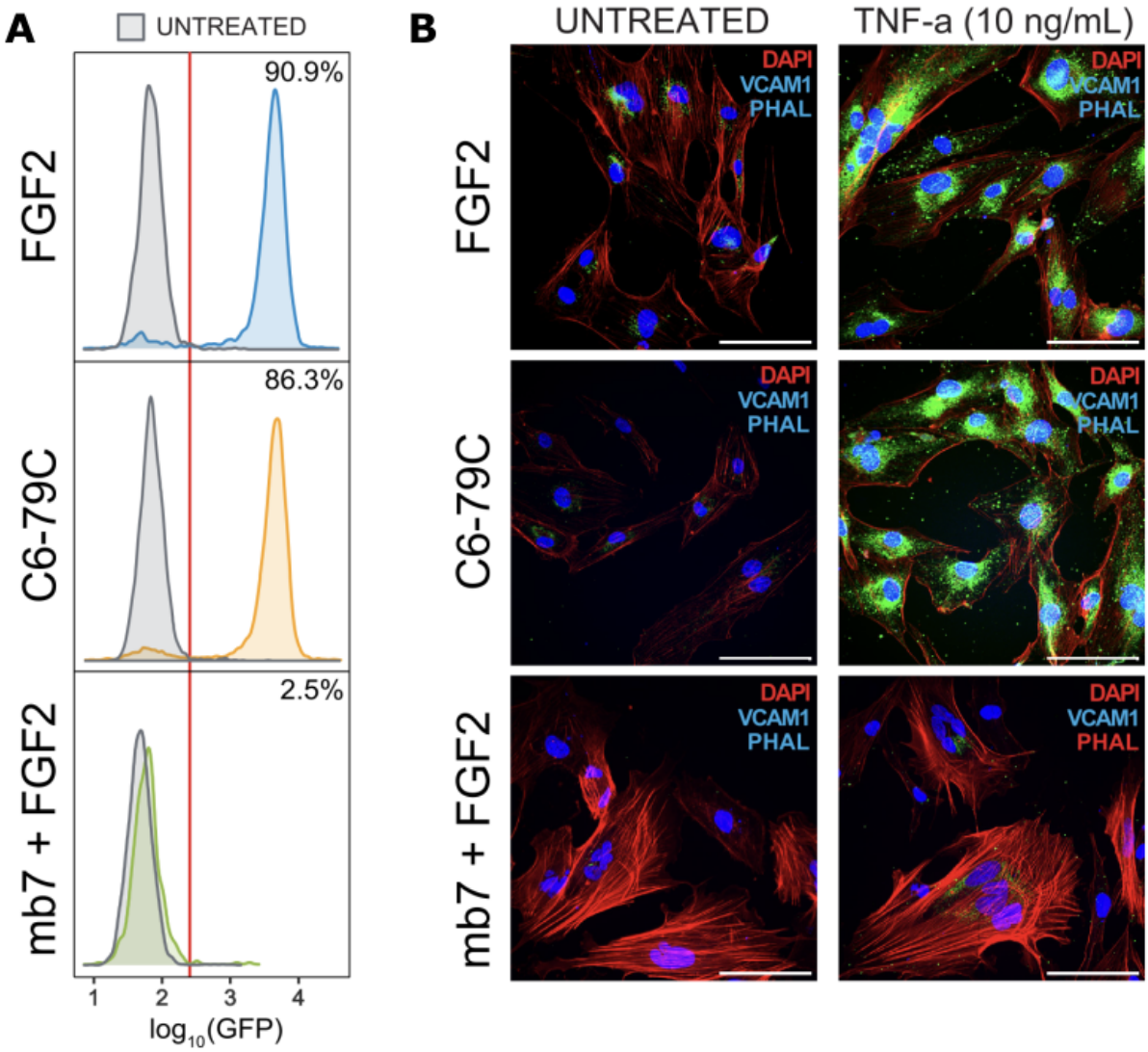

Fig 12: LDL uptake and Cytokine challenge. A) Representative flow cytometry of fluorescently labeled LDL uptake by cells generated using FGF2, C6-79C_mb7, and mb7 + FGF2 after 4 h of treatment. B) Representative immunofluorescence images of cells treated with TNF-a (10 ng/mL) for 24 h (VCAM1, vascular cell adhesion molecule) Scale bars: 100 μm.

ARTERIAL VS VENOUS ENDOTHELIAL FATE SPECIFICATION

Sub-clustering of the Day 14 endothelial expression data suggested that arterial and venous endothelial cells emerged in different ratios with the different treatments. In order to characterize these sub-populations, we compared our endothelial expression data with a previously published RNA-seq dataset from arterial and venous endothelial cells generated from human pluripotent stem cells.[119] We used the genes identified as differentially expressed in arterial and venous cells in this dataset to assign an arteriovenous specificity score for each cell in our endothelial dataset, and classified cells that scored above the median specificity score as arterial, and cells below the score as venous. We found that endothelial cells generated with or without added FGF2 primarily adopted the venous cell fate (68% or 86% venous, respectively), while C6-79C_mb7 induced a strong bias toward an arterial-like endothelial cell fate (64% arterial-like) [Fig 13A]. We hypothesized that the clear emergence of endothelial subtypes at the protein level would require further maturation of the iPSC-derived endothelial cells. To this end, we adapted a previously described protocol for creating self-organizing 3D blood vessel organoids (BVOs) from pluripotent stem cells[120]. These organoids contain the major cell types (endothelial and perivascular cells) that assemble into capillary-like networks, and, importantly, these organoids can be grown and matured for more than 60 days in culture. We replaced FGF2 in the protocol with an equivalent concentration of C6-79C_mb7 between Days 5 and 13, which mimics days 2–5 in 2D culture in respect of the emergence of mesodermal intermediates and promotion of vascular lineages. Organoids were harvested at Day 37 and stained for VE-Cadherin (to observe the formation of vascular networks) and EFNB2 (to detect arterial-like endothelial cells). Cells in organoids derived using C6-79C_mb7 exhibited significantly higher average expression of EFNB2 [Fig 13B], suggesting that c-isoform activation of FGFRs biases endothelial cells toward an arterial fate following maturation. BVOs can form stable vascular networks upon transplantation into immunodeficient mice. To investigate whether organoids generated using C6-79C_mb7 could replicate this phenotype, we transplanted Day 21 C6-79C_mb7-derived and FGF2-derived organoids under the kidney capsule of immunodeficient mice and harvested tissues after 3 weeks. Immunohistochemical analysis revealed the emergence of human

vascular endothelial (hVE-cadherin+ or hCD31+) networks with outgrowths into the surrounding stroma that formed connections with mouse (mCD31+) vascular cells [Fig 13C]. These results highlight the potential of designed proteins as tailored agonists for differentiation of cells into highly specific lineages.

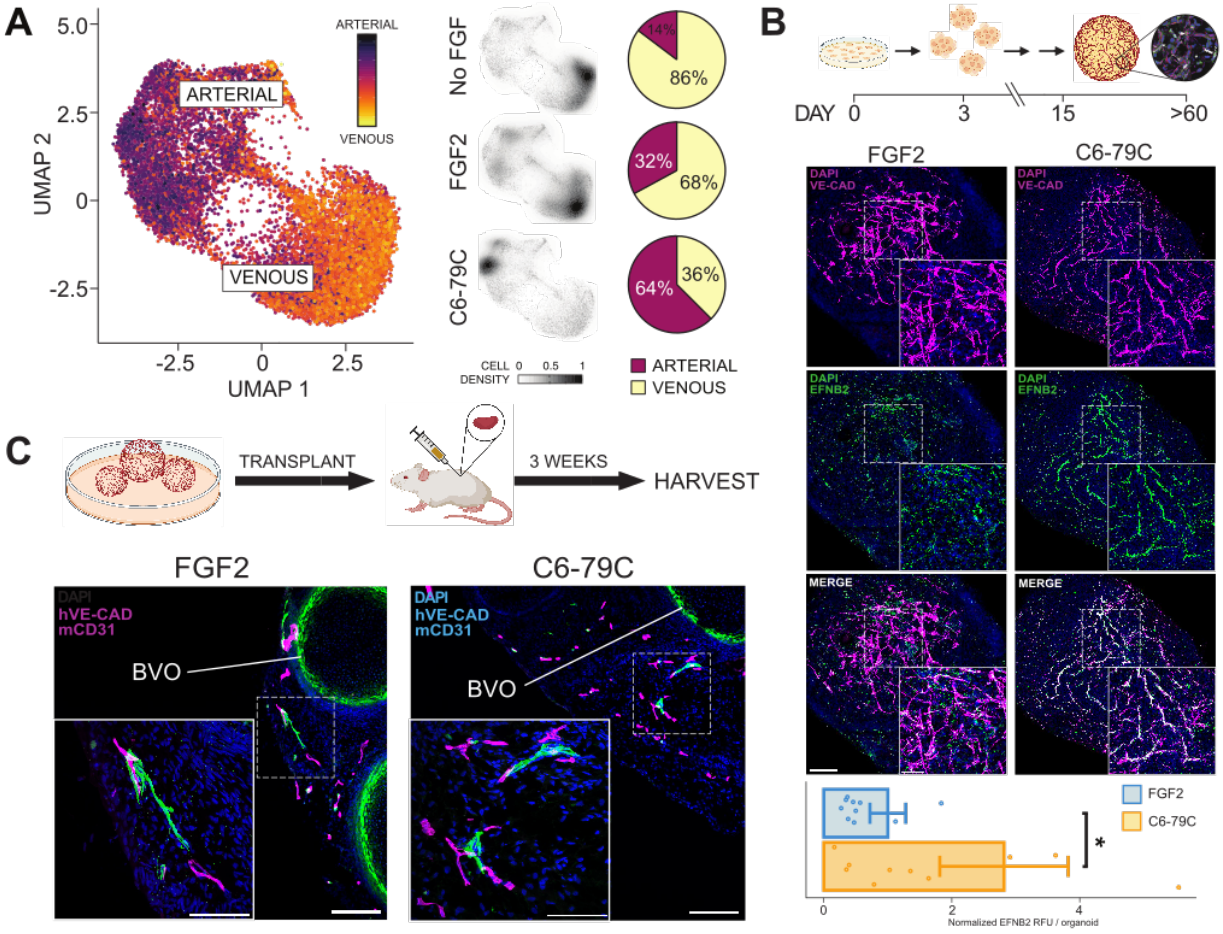

Fig 13: Control over endothelial subtype fate via isoform-specific agonism (A Left: UMAP embeddings of sub-clustered endothelial cells, colored by arteriovenous cell specificity. Middle: density plots showing specific endothelial subtype populations enriched by the individual treatments. Right: proportion of arterial or venous endothelial cells generated at day 14 following treatment with No FGF, FGF2, or C6-79C_mb7. (B Top: representative immunofluorescence images of blood vessel organoids (BVOs) generated using FGF2 or C6-79C_mb7. Vascular networks are marked with VE-cadherin and arterial-like endothelial cells are marked with EFNB2. Scale bars: 200 μm (whole) and 50 μm (inset). Bottom: per-organoid quantification of EFNB2, summarizing 10 independently generated organoids from each treatment. (C

Immunohistochemical characterization of BVOs transplanted under the mouse kidney capsule. Scale bars: 200 μm (whole) and 100 μm (inset).

EPIGENETIC REPROGRAMMING TO SUPPRESS DMG VIABILITY

The use of EBdCas9, a dCas9 fusion with EB, a computationally designed PRC2 inhibitor[134], was investigated to derepress tumor suppressor genes in diffuse midline gliomas (DMGs). This system was employed to target the CDKN2A locus, encoding the p16 tumor suppressor, a critical regulator of cell cycle arrest frequently silenced in gliomas. The mechanism of EBdCas9 relies on its ability to disrupt PRC2 activity at specific genomic loci [Fig 14A]. Polycomb Repressive Complex 2 (PRC2) catalyzes the trimethylation of histone H3 on lysine 27 (H3K27me3), a hallmark repressive epigenetic modification that silences transcription. EBdCas9 is a fusion of dCas9 (a catalytically inactive version of Cas9) with a computationally designed EED-binding domain (EB). When guided to specific genomic loci by a single-guide RNA (sgRNA), EBdCas9 binds EED and inhibits the function of PRC2. This inhibition prevents the deposition of H3K27me3, thereby relieving transcriptional repression and activating target gene expression.

When targeted to the CDKN2A locus, EBdCas9 resulted in a significant upregulation of p16 expression, as quantified by RT-qPCR [Fig 14B]. Cells treated with EBdCas9 and a guide RNA specific to CDKN2A (+g1) displayed a ~45-fold increase in p16 expression compared to untreated controls or cells treated with a non-functional dCas9 (NCdCas9) construct. Importantly, the specificity of this effect was confirmed by the lack of significant p16 upregulation in cells lacking guide RNA (-g).

The functional impact of p16 upregulation was assessed in DMG cell cultures. Bright-field and mCherry fluorescence imaging revealed successful expression of EBdCas9 in DMG cultures [Fig 14C]. Quantitative viability assays indicated that EBdCas9-treated cells exhibited a significant, time-dependent decrease in viability, with ~40%

suppression observed after 48 hours relative to controls [Fig 14D]. In contrast, NCdCas9 treatments had no effect on cell viability.

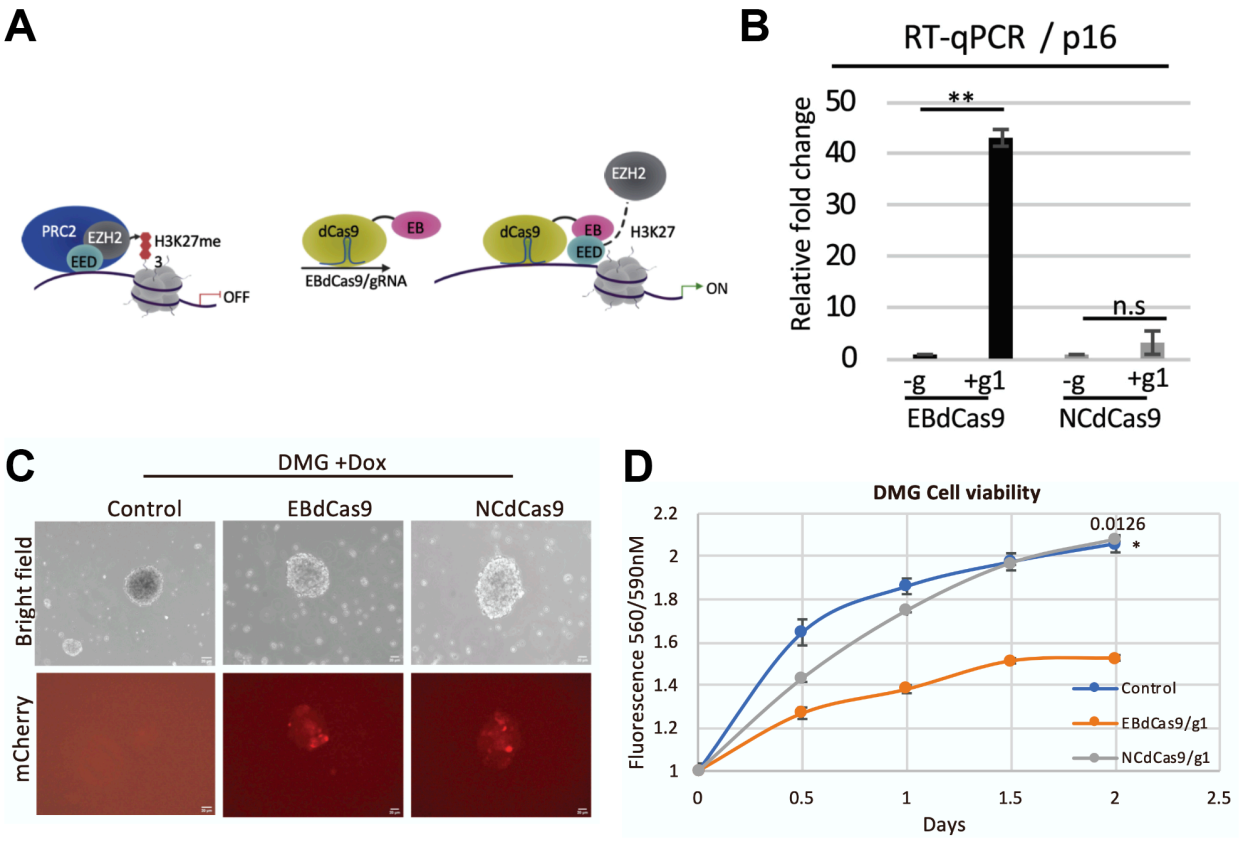

Fig 14: EBdCas9-mediated targeting of PRC2 derepresses p16 and suppresses DMG cell viability. A) Model of EBdCas9 precise elimination of PRC2 activity in targeted loci. B) qRT-PCR of *p16* relative fold change of EBdCas9 and NCdCas9 after 3 days of Dox induction and *p16* g1 transfection. C) DMG transient transfection of either EBdCas9 or NCdCas9 after 3D induction with (2µg/ml) Dox. D) Targeting EBdCas9/ g1 to p16 reduces cell viability and cell replication in DMG cells.

DISCUSSION AND PERSPECTIVES

PLASTICITY BETWEEN ARTERIAL AND VENOUS SUB-TYPES

The loss of arterial fate bias observed in *ex vivo* differentiated endothelial cells following in vivo transplantation highlights the intrinsic plasticity of endothelial cells, which adapt

to their microenvironmental cues. Endothelial plasticity is a well-documented phenomenon influenced by biomechanical forces, systemic signaling gradients, and local microenvironmental conditions. Shear stress, in particular, is a critical determinant of endothelial identity, with high laminar shear stress promoting arterialization through activation of the Notch signaling pathway and upregulation of arterial markers such as Ephrin-B2 and Dll4. Conversely, low or oscillatory flow conditions are associated with venous specification and downregulation of arterial markers.

Systemic signaling molecules further contribute to this plasticity. For example, VEGF, while critical for endothelial proliferation and migration, displays concentration-dependent effects on arterial-venous specification. High VEGF levels bias endothelial cells toward arterial fate by enhancing Notch signaling, whereas lower VEGF concentrations support venous identity. Angiopoietins also play a role, with Ang1 stabilizing arterial identity through Tie2 receptor signaling, while Ang2, in the absence of VEGF, promotes vascular remodeling and venous fate.

This plasticity complicates efforts to maintain stable arterial identities in therapeutic applications. Strategies to address this challenge include pre-conditioning organoids or endothelial cells with arterial-promoting cues prior to transplantation. For example, exposing cells to high laminar shear stress prior to transplantation or treating them with Notch signaling agonists, such as DLL4 mimetics, could pre-program arterial identity. Similarly, the addition of small molecules or growth factors, such as VEGF-A, during ex vivo culture could prime cells toward arterial specification by enhancing arterial marker expression and signaling pathways.

In vivo, modifying the microenvironment to favor arterialization is another promising approach. This could include the localized delivery of Notch agonists, VEGF gradients, or other arterial-promoting factors at the transplantation site. Additionally, engineering biomaterials that mimic the high-shear-stress environment of arteries could provide mechanical cues to reinforce arterial identity during and after transplantation.

Future studies should focus on elucidating the molecular mechanisms underlying endothelial plasticity. Investigating the interplay between biomechanical forces, systemic signals, and local microenvironmental factors will provide deeper insights into how arterial-venous fate is regulated. Omics-based approaches, such as single-cell RNA sequencing and epigenetic profiling, could identify key molecular drivers of plasticity. Furthermore, leveraging computational models of endothelial signaling networks may help predict the effects of specific interventions, aiding in the development of targeted strategies to stabilize arterial identity in therapeutic contexts. These insights will be crucial for advancing the use of engineered endothelial cells and organoids in regenerative medicine.

EXPLORATION OF OTHER SIGNALING PATHWAYS

While this study highlights the role of FGF signaling in vascular development, it is essential to recognize the broader network of signaling pathways that coordinate vascular morphogenesis and homeostasis. Pathways such as VEGF, TGF-β, PDGF, and Wnt play pivotal roles in distinct yet interconnected processes that collectively drive vascular formation and maintenance. For example, VEGF and Notch signaling intricately regulate tip-stalk cell specification during sprouting angiogenesis. VEGF gradients promote the migration of tip cells toward angiogenic cues, while Notch signaling, mediated by Delta-like ligands (e.g., DLL4), suppresses excessive tip cell formation by maintaining adjacent endothelial cells in a stalk-cell phenotype.

Similarly, TGF-β and PDGF-B signaling are critical for endothelial-perivascular cell interactions and vessel stabilization. TGF-β signaling, through its activation of SMAD-dependent pathways, promotes the differentiation of mesenchymal progenitors into vascular smooth muscle cells (vSMCs) and pericytes, which in turn stabilize nascent vessels. PDGF-BB, secreted by endothelial cells, acts as a chemoattractant for pericytes, guiding their recruitment to newly formed vessels and reinforcing vascular integrity. Dysregulation of these pathways often results in vascular pathologies, such as aneurysms or hemorrhages, emphasizing their importance in vascular development and maintenance.

Exploring how synthetic ligands can modulate these pathways offers significant opportunities for expanding the toolkit available for vascular engineering. For instance, designing ligands that target VEGFR and Notch simultaneously could enable precise control over angiogenesis by tuning the balance between tip and stalk cell phenotypes. Similarly, ligands engineered to activate TGF-β and PDGF-B signaling in a spatially restricted manner could facilitate the stabilization of vascular networks, particularly in engineered tissues or organoids.

NON-NATIVE SIGNALING PAIRS TO ELICIT BIASED SIGNALING

One of the inherent limitations of native ligands lies in their inability to elicit biased signaling, as they often activate multiple downstream pathways simultaneously. This lack of specificity can lead to undesired effects, particularly in therapeutic contexts where selective activation of specific pathways is crucial. For example, in the case of receptor tyrosine kinases (RTKs), native ligands such as FGFs and VEGFs often stimulate both the PI3K-AKT and MAPK-ERK pathways, which may result in conflicting biological outcomes, such as promoting survival alongside uncontrolled proliferation. One solution to this limitation could be the use of synthetic heterodimers to selectively activate specific pathways by forcing non-native receptor pairs to form functional dimers.

This concept involves designing heterodimeric ligands that bridge receptors from different pathways, such as FGFR1 and VEGFR2, to induce biased activation of signaling cascades. For instance, a synthetic heterodimer that links FGFR1 with VEGFR2 could preferentially activate the pro-survival PI3K-AKT pathway while avoiding activation of the proliferative MAPK-ERK pathway. This type of pathway-specific activation has significant potential in therapeutic applications, such as controlling inflammation or promoting cell survival in tissue regeneration, without triggering pathways that might lead to oncogenic proliferation or fibrosis.

Precedents for such approaches exist in the context of synthekines, which are engineered ligands capable of creating non-native receptor complexes to achieve selective signaling outcomes. These studies demonstrate that modifying receptor dimer configurations can alter downstream signaling dynamics, providing a foundation for the design of novel heterodimers with biased signaling properties.

Despite its promise, the implementation of this strategy faces several challenges. First, optimizing the binding affinities and geometries of synthetic ligands is critical to ensure efficient receptor dimerization while maintaining specificity. For example, small changes in the spatial arrangement of receptor-binding domains could significantly alter the signaling output. Advanced protein engineering tools, such as computational modeling and directed evolution, will be essential for fine-tuning these parameters

Second, ensuring specificity in complex in vivo environments remains a significant hurdle. Cells express multiple RTKs with overlapping binding affinities for certain ligands, increasing the risk of off-target effects. To address this, future studies should focus on high-throughput screening platforms capable of identifying effective heterodimer pairs and characterizing their downstream signaling profiles under physiologically relevant conditions. Techniques such as single-cell phospho-proteomics could be particularly valuable for dissecting the specific pathways activated by engineered ligands.

STRUCTURAL REQUIREMENTS FOR SIGNALING ACTIVATION

The FGF signaling pathway, while complex, is relatively easy to activate due to its reliance on heparan sulfate proteoglycans (HSPGs) as co-factors and its well-characterized receptor-ligand geometry. However, other receptor tyrosine kinase (RTK) pathways and cytokine systems exhibit more intricate structural requirements for signaling, which pose unique challenges for engineering synthetic ligands.

For instance, transforming growth factor-beta (TGF-β) receptors require ligand-induced heterodimerization between type I and type II receptor subunits to initiate signaling. This assembly is contingent upon precise ligand geometry and specific receptor-ligand

interactions, adding a layer of complexity not seen in simpler RTK systems like FGF. Similarly, Eph receptors, which are critical in processes such as axon guidance and vascular development, depend on cell-cell contact to form signaling clusters. These clusters arise from interactions between membrane-bound ephrin ligands and their corresponding Eph receptors, creating bidirectional signaling outputs that are highly spatially regulated.

The structural requirements of Wnt signaling are even more elaborate. Wnt ligands undergo post-translational lipid modifications that are critical for their activity. These modifications facilitate interactions with Frizzled receptors and co-receptors such as LRP5/6, forming large multi-protein complexes that initiate downstream signaling. The dependency on lipid modifications, along with the assembly of receptor complexes, introduces challenges in designing synthetic ligands capable of precisely mimicking these interactions.

Post-translational modifications, such as lipidation or glycosylation, represent another critical area of focus. For pathways like Wnt, incorporating these modifications into synthetic ligands could enhance their bioactivity and mimic native ligand-receptor interactions. Emerging technologies in protein engineering, including site-specific conjugation methods, could be leveraged to introduce these modifications with high precision.
Furthermore, stabilizing complex receptor-ligand geometries remains a significant challenge. Strategies such as introducing artificial co-factors or designing scaffold proteins to support multi-receptor assemblies could expand the applicability of synthetic ligands beyond FGF signaling. For example, scaffold-based approaches have been explored to stabilize Wnt-receptor interactions and enhance their signaling efficacy in regenerative applications.

Future research should aim to develop a broader toolkit of synthetic ligands capable of addressing the structural intricacies of diverse signaling pathways. By extending the principles of computational protein design to pathways with complex activation

requirements, such as TGF-β, Eph/ephrin, or Wnt systems, researchers can unlock new therapeutic and regenerative possibilities. This approach not only broadens the scope of synthetic biology but also deepens our understanding of the structural underpinnings of cellular signaling.

REFERENCES

1. Schlessinger, Joseph. “Cell signaling by receptor tyrosine kinases.” *Cell*, vol. 103, no. 2, Oct. 2000, pp. 211–225, https://doi.org/10.1016/s0092-8674(00)00114-8.
2. Trumpp, A., et al. “Cre-mediated gene inactivation demonstrates that FGF8 is required for cell survival and patterning of the first branchial arch.” *Genes & Development*, vol. 13, no. 23, 1 Dec. 1999, pp. 3136–3148, https://doi.org/10.1101/gad.13.23.3136.
3. Moon, Anne M., and Mario R. Capecchi. “FGF8 is required for outgrowth and patterning of the limbs.” *Nature Genetics*, vol. 26, no. 4, Dec. 2000, pp. 455–459, https://doi.org/10.1038/82601.
4. Nieto, M. Angela. “The snail superfamily of zinc-finger transcription factors.” *Nature Reviews Molecular Cell Biology*, vol. 3, no. 3, Mar. 2002, pp. 155–166, https://doi.org/10.1038/nrm757.
5. Lamouille, Samy, et al. “Molecular mechanisms of epithelial–mesenchymal transition.” *Nature Reviews Molecular Cell Biology*, vol. 15, no. 3, 21 Feb. 2014, pp. 178–196, https://doi.org/10.1038/nrm3758.
6. Liu, Pentao, et al. “Requirement for wnt3 in vertebrate Axis Formation.” *Nature Genetics*, vol. 22, no. 4, Aug. 1999, pp. 361–365, https://doi.org/10.1038/11932.
7. Wang, Yiping. “Wnt and the Wnt signaling pathway in Bone Development and disease.” *Frontiers in Bioscience*, vol. 19, no. 3, 2014, p. 379, https://doi.org/10.2741/4214.
8. Akram, Khondoker, et al. “Lung regeneration: Endogenous and exogenous stem cell mediated therapeutic approaches.” *International Journal of Molecular Sciences*, vol. 17, no. 1, 19 Jan. 2016, p. 128, https://doi.org/10.3390/ijms17010128.
9. Danopoulos, Soula, et al. “FGF signaling in lung development and disease: Human Versus Mouse.” *Frontiers in Genetics*, vol. 10, 12 Mar. 2019, https://doi.org/10.3389/fgene.2019.00170.

10. Hellström, Mats, et al. “Role of PDGF-B and PDGFR-β in recruitment of vascular smooth muscle cells and pericytes during embryonic blood vessel formation in the mouse.” *Development*, vol. 126, no. 14, 15 July 1999, pp. 3047–3055, https://doi.org/10.1242/dev.126.14.3047.
11. Eswarakumar, V.P., et al. “Cellular signaling by fibroblast growth factor receptors.” *Cytokine & Growth Factor Reviews*, vol. 16, no. 2, Apr. 2005, pp. 139–149, https://doi.org/10.1016/j.cytogfr.2005.01.001.
12. Dhillon, A S, et al. “MAP kinase signalling pathways in cancer.” *Oncogene*, vol. 26, no. 22, 14 May 2007, pp. 3279–3290, https://doi.org/10.1038/sj.onc.1210421.
13. Manning, Brendan D., and Lewis C. Cantley. “AKT/PKB signaling: Navigating downstream.” *Cell*, vol. 129, no. 7, June 2007, pp. 1261–1274, https://doi.org/10.1016/j.cell.2007.06.009.
14. Pawson, Tony. “Specificity in signal transduction.” *Cell*, vol. 116, no. 2, Jan. 2004, pp. 191–203, https://doi.org/10.1016/s0092-8674(03)01077-8.
15. Ornitz, David M., and Pierre J. Marie. “FGF signaling pathways in Endochondral and intramembranous bone development and human genetic disease.” *Genes & Development*, vol. 16, no. 12, 15 June 2002, pp. 1446–1465, https://doi.org/10.1101/gad.990702.
16. Normanno, Nicola, et al. “Epidermal growth factor receptor (EGFR) signaling in cancer.” *Gene*, vol. 366, no. 1, Jan. 2006, pp. 2–16, https://doi.org/10.1016/j.gene.2005.10.018.
17. Ogiso, H., et al. *Crystal Structure of the Complex of Human Epidermal Growth Factor and Receptor Extracellular Domains.*, 16 Oct. 2002, https://doi.org/10.2210/pdb1ivo/pdb.
18. Lemmon, Mark A., and Joseph Schlessinger. “Cell signaling by receptor tyrosine kinases.” *Cell*, vol. 141, no. 7, June 2010, pp. 1117–1134, https://doi.org/10.1016/j.cell.2010.06.011.
19. Roghani, M., et al. “Heparin increases the affinity of basic fibroblast growth factor for its receptor but is not required for binding.” *Journal of Biological Chemistry*, vol. 269, no. 6, Feb. 1994, pp. 3976–3984, https://doi.org/10.1016/s0021-9258(17)41730-3.

20. Hubbard, Stevan R., and Jeffrey H. Till. “Protein tyrosine kinase structure and function.” *Annual Review of Biochemistry*, vol. 69, no. 1, June 2000, pp. 373–398, https://doi.org/10.1146/annurev.biochem.69.1.373.
21. Hubbard, S.R., et al. *Crystal Structure of the Tyrosine Kinase Domain of the Human Insulin Receptor*, 27 Feb. 1995, https://doi.org/10.2210/pdb1irk/pdb.
22. Goh, L. K., and A. Sorkin. “Endocytosis of receptor tyrosine kinases.” *Cold Spring Harbor Perspectives in Biology*, vol. 5, no. 5, 1 May 2013, https://doi.org/10.1101/cshperspect.a017459.
23. Tonks, Nicholas K. “Protein tyrosine phosphatases: From genes, to function, to disease.” *Nature Reviews Molecular Cell Biology*, vol. 7, no. 11, 1 Nov. 2006, pp. 833–846, https://doi.org/10.1038/nrm2039.
24. Azad, Taha, et al. “Hippo signaling pathway as a central mediator of receptors tyrosine kinases (rtks) in tumorigenesis.” *Cancers*, vol. 12, no. 8, 24 July 2020, p. 2042, https://doi.org/10.3390/cancers12082042.
25. Carmeliet, Peter. “Mechanisms of angiogenesis and arteriogenesis.” *Nature Medicine*, vol. 6, no. 4, Apr. 2000, pp. 389–395, https://doi.org/10.1038/74651.
26. Ferrara, N. “The Biology of Vascular Endothelial Growth Factor.” *Endocrine Reviews*, vol. 18, no. 1, 1 Feb. 1997, pp. 4–25, https://doi.org/10.1210/er.18.1.4.
27. Cleaver, Ondine, and Douglas A Melton. “Endothelial signaling during development.” *Nature Medicine*, vol. 9, no. 6, 1 June 2003, pp. 661–668, https://doi.org/10.1038/nm0603-661.
28. Risau, Werner. “Mechanisms of angiogenesis.” *Nature*, vol. 386, no. 6626, Apr. 1997, pp. 671–674, https://doi.org/10.1038/386671a0.
29. Gerhardt, Holger, et al. “VEGF guides angiogenic sprouting utilizing endothelial tip cell filopodia.” *The Journal of Cell Biology*, vol. 161, no. 6, 16 June 2003, pp. 1163–1177, https://doi.org/10.1083/jcb.200302047.
30. Djonov, V., et al. “Intussusceptive angiogenesis.” *Circulation Research*, vol. 86, no. 3, 18 Feb. 2000, pp. 286–292, https://doi.org/10.1161/01.res.86.3.286.
31. Prummel, Karin D., et al. “The lateral plate mesoderm.” *Development*, vol. 147, no. 12, 15 June 2020, https://doi.org/10.1242/dev.175059.

32. Trost, Andrea, et al. “Neural crest origin of retinal and choroidal pericytes.” *Investigative Opthalmology & Visual Science*, vol. 54, no. 13, 5 Dec. 2013, p. 7910, https://doi.org/10.1167/iovs.13-12946.
33. Trost, Andrea, Simona Lange, et al. “Brain and retinal pericytes: Origin, function and role.” *Frontiers in Cellular Neuroscience*, vol. 10, 4 Feb. 2016, https://doi.org/10.3389/fncel.2016.00020.
34. Nelson, Ronald A., et al. “Advances in biomaterials for promoting vascularization.” *Current Stem Cell Reports*, vol. 8, no. 4, 7 Sept. 2022, pp. 184–196, https://doi.org/10.1007/s40778-022-00217-w.
35. Adams, Ralf H., and Kari Alitalo. “Molecular regulation of angiogenesis and lymphangiogenesis.” *Nature Reviews Molecular Cell Biology*, vol. 8, no. 6, June 2007, pp. 464–478, https://doi.org/10.1038/nrm2183.
36. Wigle, Jeffrey T, and Guillermo Oliver. “PROX1 function is required for the development of the murine lymphatic system.” *Cell*, vol. 98, no. 6, Sept. 1999, pp. 769–778, https://doi.org/10.1016/s0092-8674(00)81511-1.
37. Pober, Jordan S., and William C. Sessa. “Evolving functions of endothelial cells in inflammation.” *Nature Reviews Immunology*, vol. 7, no. 10, Oct. 2007, pp. 803–815, https://doi.org/10.1038/nri2171.
38. Armulik, Annika, et al. “Pericytes regulate the blood–brain barrier.” *Nature*, vol. 468, no. 7323, 13 Oct. 2010, pp. 557–561, https://doi.org/10.1038/nature09522.
39. Daneman, Richard, et al. “Pericytes are required for blood–brain barrier integrity during embryogenesis.” *Nature*, vol. 468, no. 7323, 13 Oct. 2010, pp. 562–566, https://doi.org/10.1038/nature09513.
40. Rusnati, Marco, and Marco Presta. “Targeting fibroblast growth factor/fibroblast growth factor receptor system in angiogenesis.” *Antiangiogenic Cancer Therapy*, 25 July 2007, https://doi.org/10.1201/9781420004298.ch8.
41. Augustin, Hellmut G., and Ulrike Fiedler. “Regulation of angiogenesis and vascular homeostasis through the angiopoietin / tie system.” *Tumor Angiogenesis*, pp. 109–120, https://doi.org/10.1007/978-3-540-33177-3_6.

42. Troise, Dario, et al. “Hypoxic inducible factor stabilization in pericytes beyond erythropoietin production: The good and the bad.” *Antioxidants*, vol. 13, no. 5, 27 Apr. 2024, p. 537, https://doi.org/10.3390/antiox13050537.
43. Gerhardt, Holger, and Christer Betsholtz. “Endothelial-Pericyte Interactions in angiogenesis.” *Cell and Tissue Research*, vol. 314, no. 1, 1 Oct. 2003, pp. 15–23, https://doi.org/10.1007/s00441-003-0745-x.
44. Daneman, Richard, and Alexandre Prat. “The blood–brain barrier.” *Cold Spring Harbor Perspectives in Biology*, vol. 7, no. 1, Jan. 2015, https://doi.org/10.1101/cshperspect.a020412.
45. World Health Organization. (2021). Global status report on noncommunicable diseases. *WHO*. https://www.who.int
46. Libby, Peter, et al. “Inflammation in atherosclerosis: transition from theory to practice.” *Circulation Journal*, vol. 74, no. 2, 2010, pp. 213–220, https://doi.org/10.1253/circj.cj-09-0706.
47. Kim, Ann S., et al. “Mechanisms and biomarkers of cancer-associated thrombosis.” *Translational Research*, vol. 225, Nov. 2020, pp. 33–53, https://doi.org/10.1016/j.trsl.2020.06.012.
48. Brownlee, Michael. “The pathobiology of diabetic complications.” *Diabetes*, vol. 54, no. 6, 1 June 2005, pp. 1615–1625, https://doi.org/10.2337/diabetes.54.6.1615.
49. Forbes, Josephine M., and Mark E. Cooper. “Mechanisms of diabetic complications.” *Physiological Reviews*, vol. 93, no. 1, Jan. 2013, pp. 137–188, https://doi.org/10.1152/physrev.00045.2011.
50. Hammes, H.-P. “Pericytes and the pathogenesis of diabetic retinopathy.” *Hormone and Metabolic Research*, vol. 37, Apr. 2005, pp. 39–43, https://doi.org/10.1055/s-2005-861361.
51. Beltramo, Elena, and Massimo Porta. “Pericyte loss in diabetic retinopathy: Mechanisms and consequences.” *Current Medicinal Chemistry*, vol. 20, no. 26, 1 July 2013, pp. 3218–3225, https://doi.org/10.2174/09298673113209990022.

52. Wimmer, Reiner A., et al. “Human blood vessel organoids as a model of diabetic vasculopathy.” *Nature*, vol. 565, no. 7740, Jan. 2019, pp. 505–510, https://doi.org/10.1038/s41586-018-0858-8.
53. Ferrara, Napoleone. “VEGF as a therapeutic target in cancer.” *Oncology*, vol. 69, no. Suppl. 3, 2005, pp. 11–16, https://doi.org/10.1159/000088479.
54. Olsson, Anna-Karin, et al. “VEGF receptor signalling ? in control of vascular function.” *Nature Reviews Molecular Cell Biology*, vol. 7, no. 5, May 2006, pp. 359–371, https://doi.org/10.1038/nrm1911.
55. Tsang, Kit Man, et al. “Embryonic stem cell differentiation to functional arterial endothelial cells through sequential activation of ETV2 and Notch1 signaling by HIF1α.” *Stem Cell Reports*, vol. 9, no. 3, Sept. 2017, pp. 796–806, https://doi.org/10.1016/j.stemcr.2017.07.001.
56. Palpant, Nathan J, et al. “Generating high-purity cardiac and endothelial derivatives from patterned mesoderm using human pluripotent stem cells.” *Nature Protocols*, vol. 12, no. 1, 1 Dec. 2016, pp. 15–31, https://doi.org/10.1038/nprot.2016.153.
57. Shaik, Faheem, et al. “Structural basis for vascular endothelial growth factor receptor activation and implications for disease therapy.” *Biomolecules*, vol. 10, no. 12, 15 Dec. 2020, p. 1673, https://doi.org/10.3390/biom10121673.
58. Wang, Hai U, et al. “Molecular distinction and angiogenic interaction between embryonic arteries and veins revealed by ephrin-B2 and its receptor Eph-B4.” *Cell*, vol. 93, no. 5, May 1998, pp. 741–753, https://doi.org/10.1016/s0092-8674(00)81436-1.
59. Lawson, Nathan D., et al. “Notch signaling is required for arterial-venous differentiation during embryonic vascular development.” *Development*, vol. 128, no. 19, 1 Oct. 2001, pp. 3675–3683, https://doi.org/10.1242/dev.128.19.3675.
60. Jin, Daqing, et al. “VEGFA signaling regulates diverse artery/vein formation in Vertebrate Vasculatures.” *Journal of Genetics and Genomics*, vol. 44, no. 10, Oct. 2017, pp. 483–492, https://doi.org/10.1016/j.jgg.2017.07.005.

61. You, Li-Ru, et al. “Suppression of notch signalling by the coup-TFII transcription factor regulates vein identity.” *Nature*, vol. 435, no. 7038, May 2005, pp. 98–104, https://doi.org/10.1038/nature03511.
62. Williams, Charles, et al. “Hedgehog signaling induces arterial endothelial cell formation by repressing venous cell fate.” *Developmental Biology*, vol. 341, no. 1, May 2010, pp. 196–204, https://doi.org/10.1016/j.ydbio.2010.02.028.
63. Han, Orjin, et al. “The role of BMP signaling in endothelial heterogeneity.” *Frontiers in Cell and Developmental Biology*, vol. 9, 21 June 2021, https://doi.org/10.3389/fcell.2021.673396.
64. Goumans, Marie-José, et al. “TGF-β signaling in vascular biology and Dysfunction.” *Cell Research*, vol. 19, no. 1, 30 Dec. 2008, pp. 116–127, https://doi.org/10.1038/cr.2008.326.
65. Gerety, Sebastian S, et al. “Symmetrical mutant phenotypes of the receptor EphB4 and its specific transmembrane ligand ephrin-B2 in cardiovascular development.” *Molecular Cell*, vol. 4, no. 3, Sept. 1999, pp. 403–414, https://doi.org/10.1016/s1097-2765(00)80342-1.
66. Le Bras, Alex, et al. “Molecular mechanisms of endothelial differentiation.” *Vascular Medicine*, vol. 15, no. 4, 9 July 2010, pp. 321–331, https://doi.org/10.1177/1358863x10371685.
67. Ornitz, David M., and Nobuyuki Itoh. “The fibroblast growth factor signaling pathway.” *WIREs Developmental Biology*, vol. 4, no. 3, 13 Mar. 2015, pp. 215–266, https://doi.org/10.1002/wdev.176.
68. Thisse, Bernard, and Christine Thisse. “Functions and regulations of fibroblast growth factor signaling during embryonic development.” *Developmental Biology*, vol. 287, no. 2, Nov. 2005, pp. 390–402, https://doi.org/10.1016/j.ydbio.2005.09.011.
69. Beenken, Andrew, and Moosa Mohammadi. “The FGF family: Biology, pathophysiology and therapy.” *Nature Reviews Drug Discovery*, vol. 8, no. 3, Mar. 2009, pp. 235–253, https://doi.org/10.1038/nrd2792.

70. Zhang, Xiuqin, et al. “Receptor specificity of the fibroblast growth factor family.” *Journal of Biological Chemistry*, vol. 281, no. 23, June 2006, pp. 15694–15700, https://doi.org/10.1074/jbc.m601252200.
71. Tabin, Cliff, and Lewis Wolpert. “Rethinking the proximodistal axis of the vertebrate limb in the molecular era.” *Genes & Development*, vol. 21, no. 12, 15 June 2007, pp. 1433–1442, https://doi.org/10.1101/gad.1547407.
72. Dorey, Karel, and Enrique Amaya. “FGF signalling: Diverse roles during early vertebrate embryogenesis.” *Development*, vol. 137, no. 22, 15 Nov. 2010, pp. 3731–3742, https://doi.org/10.1242/dev.037689.
73. Turner, Nicholas, and Richard Grose. “Fibroblast growth factor signalling: From development to cancer.” *Nature Reviews Cancer*, vol. 10, no. 2, Feb. 2010, pp. 116–129, https://doi.org/10.1038/nrc2780.
74. Gong, Siew-Ging. “Isoforms of receptors of fibroblast growth factors.” *Journal of Cellular Physiology*, vol. 229, no. 12, 27 Aug. 2014, pp. 1887–1895, https://doi.org/10.1002/jcp.24649.
75. Schlessinger, Joseph, et al. “Crystal structure of a ternary FGF-FGFR-heparin complex reveals a dual role for heparin in FGFR binding and dimerization.” *Molecular Cell*, vol. 6, no. 3, Sept. 2000, pp. 743–750, https://doi.org/10.1016/s1097-2765(00)00073-3.
76. Mohammadi, Moosa, et al. “Structure of the FGF receptor tyrosine kinase domain reveals a novel autoinhibitory mechanism.” *Cell*, vol. 86, no. 4, Aug. 1996, pp. 577–587, https://doi.org/10.1016/s0092-8674(00)80131-2.
77. Marshall, C.J. “Specificity of receptor tyrosine kinase signaling: Transient versus sustained extracellular signal-regulated kinase activation.” *Cell*, vol. 80, no. 2, Jan. 1995, pp. 179–185, https://doi.org/10.1016/0092-8674(95)90401-8.
78. Ornitz, David M., et al. “Receptor specificity of the fibroblast growth factor family.” *Journal of Biological Chemistry*, vol. 271, no. 25, June 1996, pp. 15292–15297, https://doi.org/10.1074/jbc.271.25.15292.
79. Moerlooze, Laurence De, et al. “An important role for the IIIB isoform of fibroblast growth factor receptor 2 (FGFR2) in mesenchymal-epithelial signalling during

mouse organogenesis.” *Development*, vol. 127, no. 3, 1 Feb. 2000, pp. 483–492, https://doi.org/10.1242/dev.127.3.483.

80. Coultas, Leigh, et al. “Endothelial cells and VEGF in vascular development.” *Nature*, vol. 438, no. 7070, 14 Dec. 2005, pp. 937–945, https://doi.org/10.1038/nature04479.
81. Hosaka, Kayoko, et al. “Dual roles of endothelial FGF-2–FGFR1–PDGF-BB and perivascular FGF-2–FGFR2–PDGFRB signaling pathways in tumor vascular remodeling.” *Cell Discovery*, vol. 4, no. 1, 16 Jan. 2018, https://doi.org/10.1038/s41421-017-0002-1.
82. Cross, Michael J, and Lena Claesson-Welsh. “FGF and VEGF function in angiogenesis: Signalling pathways, biological responses and therapeutic inhibition.” *Trends in Pharmacological Sciences*, vol. 22, no. 4, Apr. 2001, pp. 201–207, https://doi.org/10.1016/s0165-6147(00)01676-x.
83. Fish, Jason E., and Joshua D. Wythe. “The Molecular Regulation of arteriovenous specification and maintenance.” *Developmental Dynamics*, vol. 244, no. 3, 26 Feb. 2015, pp. 391–409, https://doi.org/10.1002/dvdy.24252.
84. Garcia-Parajo, M.F., Cambi, A., Torreno-Pina, J.A., Thompson, N., and Jacobson, K. (2014). Nanoclustering as a dominant feature of plasma membrane organization. J. Cell Sci. 127, 4995–5005. https://doi.org/ 10.1242/jcs.146340.
85. Wu, H. (2013). Higher-order assemblies in a new paradigm of signal transduction. Cell 153, 287–292. https://doi.org/10.1016/J.CELL.2013. 03.013
86. Mayer, B.J., and Yu, J. (2018). Protein Clusters in Phosphotyrosine Signal Transduction. J. Mol. Biol. 430, 4547–4556. https://doi.org/10.1016/J. JMB.2018.05.040.
87. Zhang, K., Gao, H., Deng, R., and Li, J. (2019). Emerging Applications of Nanotechnology for Controlling Cell-Surface Receptor Clustering. Angew. Chem. Int. Ed. Engl. 58, 4790–4799. https://doi.org/10.1002/anie. 201809006
88. Pore˛ bska, N., Ciura, K., Chora˛ zewska, A., Zakrzewska, M., Otlewski, J., _ and Opalinski. (2023). Multivalent protein-drug conjugates - An emerging strategy for the upgraded precision and efficiency of drug delivery to cancer cells. Biotechnol. Adv. 67, 108213. https://doi.org/10. 1016/j.biotechadv.2023.108213.

89. Westerfield, J.M., and Barrera, F.N. (2020). Membrane receptor activation mechanisms and transmembrane peptide tools to elucidate them. J. Biol. Chem. 295, 1792–1814. https://doi.org/10.1074/jbc.REV119. 009457.
90. Zhao, Y.T., Fallas, J.A., Saini, S., Ueda, G., Somasundaram, L., Zhou, Z., Xavier Raj, I., Xu, C., Carter, L., Wrenn, S., et al. (2021). F-domain valency determines outcome of signaling through the angiopoietin pathway. EMBO Rep. 22, e53471. https://doi.org/10.15252/embr.202153471.
91. Divine, R., Dang, H.V., Ueda, G., Fallas, J.A., Vulovic, I., Sheffler, W., Saini, S., Zhao, Y.T., Raj, I.X., Morawski, P.A., et al. (2021). Designed proteins assemble antibodies into modular nanocages. Science 372, eabd9994. https://doi.org/10.1126/science.abd9994.
92. Shaw, A., Lundin, V., Petrova, E., Fordos, F., Benson, E., Al-Amin, A., Herland, A., Blokzijl, A., Hogberg, B., and Teixeira, A.I. (2014). Spatial control of membrane receptor function using ligand nanocalipers. Nat. Methods 11, 841–846. https://doi.org/10.1038/nmeth.3025.
93. Mohan, K., Ueda, G., Kim, A.R., Jude, K.M., Fallas, J.A., Guo, Y., Hafer, M., Miao, Y., Saxton, R.A., Piehler, J., et al. (2019). Topological control of cytokine receptor signaling induces differential effects in hematopoiesis. Science 364, eaav7532. https://doi.org/10.1126/science.aav7532.
94. Moraga, I., Spangler, J.B., Mendoza, J.L., Gakovic, M., Wehrman, T.S., Krutzik, P., and Garcia, K.C. (2017). Synthekines are surrogate cytokine and growth factor agonists that compel signaling through non-natural receptor dimers. eLife 6, e22882. https://doi.org/10.7554/eLife.22882.
95. Taga, T., and Kishimoto, T. (1997). Gp130 and the interleukin-6 family of cytokines. Annu. Rev. Immunol. 15, 797–819. https://doi.org/10.1146/annurev.immunol.15.1.797.
96. Martinez-Moczygemba, M., and Huston, D.P. (2003). Biology of common b receptor–signaling cytokines: il-3, IL-5, and GM-CSF. J. Allergy Clin. Immunol. 112, 653–665. https://doi.org/10.1016/S0091.

97. Boulanger, M.J., Chow, D.C., Brevnova, E.E., and Garcia, K.C. (2003). Hexameric structure and assembly of the interleukin-6/IL-6 alpha-receptor/gp130 complex. Science 300, 2101–2104. https://doi.org/10.1126/ science.1083901.
98. Gerben, S.R., Borst, A.J., Hicks, D.R., Moczygemba, I., Feldman, D., Coventry, B., Yang, W., Bera, A.K., Miranda, M., Kang, A., et al. (2023). Design of Diverse Asymmetric Pockets in De Novo Homo-oligomeric Proteins. Biochemistry 62, 358–368. https://doi.org/10.1021/acs.biochem.2c00497.
99. Watson, J.L., Juergens, D., Bennett, N.R., Trippe, B.L., Yim, J., Eisenach, H.E., Ahern, W., Borst, A.J., Ragotte, R.J., Milles, L.F., et al. (2023). De novo design of protein structure and function with RFdiffusion. Nature 620, 1089–1100. https://doi.org/10.1038/s41586-023-06415-8
100. Wicky, B.I.M., Milles, L.F., Courbet, A., Ragotte, R.J., Dauparas, J., Kinfu, E., Tipps, S., Kibler, R.D., Baek, M., DiMaio, F., et al. (2022). Hallucinating symmetric protein assemblies. Science 378, 56–61. https://doi.org/10. 1126/science.add1964.
101. Fallas, J.A., Ueda, G., Sheffler, W., Nguyen, V., McNamara, D.E., Sankaran, B., Pereira, J.H., Parmeggiani, F., Brunette, T.J., Cascio, D., et al. (2017). Computational design of self-assembling cyclic protein homo-oligomers. Nat. Chem. 9, 353–360. https://doi.org/10.1038/ NCHEM.2673.
102. Park, J.S., Choi, J., Cao, L., Mohanty, J., Suzuki, Y., Park, A., Baker, D., Schlessinger, J., and Lee, S. (2022). Isoform-specific inhibition of FGFR signaling achieved by a de-novo-designed mini-protein. Cell Rep. 41, 111545. https://doi.org/10.1016/j.celrep.2022.111545.
103. Schindelin, J., Arganda-Carreras, I., Frise, E., Kaynig, V., Longair, M., Pietzsch, T., Preibisch, S., Rueden, C., Saalfeld, S., Schmid, B., et al. (2012). Fiji: an open-source platform for biological-image analysis. Nat. Methods 9, 676–682. https://doi.org/10.1038/nmeth.2019
104. Carpenter, A.E., Jones, T.R., Lamprecht, M.R., Clarke, C., Kang, I.H., Friman, O., Guertin, D.A., Chang, J.H., Lindquist, R.A., Moffat, J., et al. (2006). CellProfiler: image analysis software for identifying and quantifying cell phenotypes. Genome Biol. 7, R100. https://doi.org/10.1186/ gb-2006-7-10-r100.

105. Srivatsan, S.R., McFaline-Figueroa, J.L., Ramani, V., Saunders, L., Cao, J., Packer, J., Pliner, H.A., Jackson, D.L., Daza, R.M., Christiansen, L., et al. (2020). Massively multiplex chemical transcriptomics at single-cell resolution. Science 367, 45–51. https://doi.org/10.1126/SCIENCE. AAX6234.

106. Hao, Y., Hao, S., Andersen-Nissen, E., Mauck, W.M., 3rd, Zheng, S., Butler, A., Lee, M.J., Wilk, A.J., Darby, C., Zager, M., et al. (2021). Integrated analysis of multimodal single-cell data. Cell 184, 3573–3587.e29. https:// doi.org/10.1016/j.cell.2021.04.048.

107. Ellis, B., Haaland, P., Hahne, F., Le Meur, N., Gopalakrishnan, N., Spidlen, J., Jiang, M., and Finak, G. (2024). flowCore: Basic structures for flow cytometry data. Bioconductor. http://bioconductor.org/packages/ flowCore/.

108. Suarez-Arnedo, A., Torres Figueroa, F., Clavijo, C., Arbela´ ez, P., Cruz, J.C., and Mun˜ oz-Camargo, C. (2020). An image J plugin for the high throughput image analysis of in vitro scratch wound healing assays. PLoS One 15, e0232565. https://doi.org/10.1371/journal.pone.0232565

109. Carpentier, G., Berndt, S., Ferratge, S., Rasband, W., Cuendet, M., Uzan, G., and Albanese, P. (2020). Angiogenesis Analyzer for ImageJ—A comparative morphometric analysis of ‘‘Endothelial Tube Formation Assay’’ and ‘‘Fibrin Bead Assay’’. Sci. Rep. 10, 11568. https://doi.org/ 10.1038/s41598-020-67289-8.

110. Trapnell, C., Cacchiarelli, D., Grimsby, J., Pokharel, P., Li, S., Morse, M., Lennon, N.J., Livak, K.J., Mikkelsen, T.S., and Rinn, J.L. (2014). The dynamics and regulators of cell fate decisions are revealed by pseudotemporal ordering of single cells. Nat. Biotechnol. 32, 381–386. https://doi. org/10.1038/nbt.2859.

111. Los, G.V., Encell, L.P., McDougall, M.G., Hartzell, D.D., Karassina, N., Zimprich, C., Wood, M.G., Learish, R., Ohana, R.F., Urh, M., et al. (2008). HaloTag: A novel protein labeling technology for cell imaging and protein analysis. ACS Chem. Biol. 3, 373–382. https://doi.org/10. 1021/cb800025k.

112. Jaqaman, K., Kuwata, H., Touret, N., Collins, R., Trimble, W.S., Danuser, G., and Grinstein, S. (2011). Cytoskeletal control of CD36 diffusion promotes its receptor and signaling function. Cell 146, 593–606. https:// doi.org/10.1016/j.cell.2011.06.049.

113. Kureli, G., Yilmaz-Ozcan, S., Erdener, S.E., Donmez-Demir, B., Yemisci, M., Karatas, H., and Dalkara, T. (2020). F-actin polymerization contributes to pericyte contractility in retinal capillaries. Exp. Neurol. 332, 113392. https://doi.org/10.1016/j.expneurol.2020.113392.

114. Kubota, Y., Kleinman, H.K., Martin, G.R., and Lawley, T.J. (1988). Role of laminin and basement membrane in the morphological differentiation of human endothelial cells into capillary-like structures. J. Cell Biol. 107, 1589–1598. https://doi.org/10.1083/jcb.107.4.1589.

115. Liang, C.-C., Park, A.Y., and Guan, J.-L. (2007). In vitro scratch assay: a convenient and inexpensive method for analysis of cell migration in vitro. Nat. Protoc. 2, 329–333. https://doi.org/10.1038/nprot.2007.30.

116. Chim, S.M., Qin, A., Tickner, J., Pavlos, N., Davey, T., Wang, H., Guo, Y., Zheng, M.H., and Xu, J. (2011). EGFL6 promotes endothelial cell migration and angiogenesis through the activation of extracellular signal-regulated kinase. J. Biol. Chem. 286, 22035–22046. https://doi.org/10.1074/ jbc.M110.187633.

117. Voyta, J.C., Via, D.P., Butterfield, C.E., and Zetter, B.R. (1984). Identification and isolation of endothelial cells based on their increased uptake of acetylated-low density lipoprotein. J. Cell Biol. 99, 2034–2040. https:// doi.org/10.1083/jcb.99.6.2034.

118. Amersfoort, J., Eelen, G., and Carmeliet, P. (2022). Immunomodulation by endothelial cells - partnering up with the immune system? Nat. Rev. Immunol. 22, 576–588. https://doi.org/10.1038/s41577-022-00694-4

119. Ang, L.T., Nguyen, A.T., Liu, K.J., Chen, A., Xiong, X., Curtis, M., Martin, R.M., Raftry, B.C., Ng, C.Y., Vogel, U., et al. (2022). Generating human artery and vein cells from pluripotent stem cells highlights the arterial tropism of Nipah and Hendra viruses. Cell 185, 2523–2541.e30. https:// doi.org/10.1016/j.cell.2022.05.024

120. Wimmer, R.A., Leopoldi, A., Aichinger, M., Wick, N., Hantusch, B., Novatchkova, M., Taubenschmid, J., Ha¨ mmerle, M., Esk, C., Bagley, J.A., et al. (2019). Human blood vessel organoids as a model of diabetic vasculopathy. Nature 565, 505–510. https://doi.org/10.1038/s41586-018- 0858-8.

121. Smith, Zachary D., and Alexander Meissner. “DNA methylation: Roles in mammalian development.” *Nature Reviews Genetics*, vol. 14, no. 3, 12 Feb. 2013, pp. 204–220, https://doi.org/10.1038/nrg3354.

122. Rando, Oliver J., and Howard Y. Chang. “Genome-wide views of chromatin structure.” *Annual Review of Biochemistry*, vol. 78, no. 1, 1 June 2009, pp. 245–271, https://doi.org/10.1146/annurev.biochem.78.071107.134639.

123. Bannister, Andrew J, and Tony Kouzarides. “Regulation of Chromatin by Histone Modifications.” *Nature News*, Nature Publishing Group, 15 Feb. 2011, www.nature.com/articles/cr201122.

124. Atlasi, Yaser, and Hendrik G. Stunnenberg. “The interplay of epigenetic marks during stem cell differentiation and development.” *Nature Reviews Genetics*, vol. 18, no. 11, 14 Aug. 2017, pp. 643–658, https://doi.org/10.1038/nrg.2017.57.

125. Zaret, Kenneth S, and Susan E Mango. “Pioneer transcription factors, chromatin dynamics, and Cell Fate Control.” *Current Opinion in Genetics & Development*, vol. 37, Apr. 2016, pp. 76–81, https://doi.org/10.1016/j.gde.2015.12.003.

126. Margueron, Raphaël, and Danny Reinberg. “The Polycomb Complex PRC2 and its mark in life.” *Nature*, vol. 469, no. 7330, 19 Jan. 2011, pp. 343–349, https://doi.org/10.1038/nature09784.

127. Huang, Jialiang, et al. “Dynamic control of enhancer repertoires drives lineage and stage-specific transcription during hematopoiesis.” *Developmental Cell*, vol. 36, no. 1, Jan. 2016, pp. 9–23, https://doi.org/10.1016/j.devcel.2015.12.014.

128. Heintzman, Nathaniel D, et al. “Distinct and predictive chromatin signatures of transcriptional promoters and enhancers in the human genome.” *Nature Genetics*, vol. 39, no. 3, 4 Feb. 2007, pp. 311–318, https://doi.org/10.1038/ng1966.

129. Hirabayashi, Yusuke, and Yukiko Gotoh. “Epigenetic control of neural precursor cell fate during development.” *Nature Reviews Neuroscience*, vol. 11, no. 6, June 2010, pp. 377–388, https://doi.org/10.1038/nrn2810.

130. Kim, Kimberly H, and Charles W M Roberts. “Targeting EZH2 in Cancer.” *Nature News*, Nature Publishing Group, 4 Feb. 2016, www.nature.com/articles/nm.4036.

131. Weinberg, Daniel N., et al. “Oncogenic mechanisms of histone H3 mutations.” *Cold Spring Harbor Perspectives in Medicine*, vol. 7, no. 1, 18 Nov. 2016, https://doi.org/10.1101/cshperspect.a026443.

132. Schwartzentruber, Jeremy, et al. “Driver Mutations in Histone H3.3 and Chromatin Remodelling Genes in Paediatric Glioblastoma.” *Nature News*, Nature Publishing Group, 29 Jan. 2012, www.nature.com/articles/nature10833.

133. Bender, Sebastian, et al. “Reduced h3k27me3 and DNA hypomethylation are major drivers of gene expression in K27M mutant pediatric high-grade gliomas.” *Cancer Cell*, vol. 24, no. 5, Nov. 2013, pp. 660–672, https://doi.org/10.1016/j.ccr.2013.10.006.

134. Moody, James D., et al. “First critical repressive h3k27me3 marks in embryonic stem cells identified using designed protein inhibitor.” *Proceedings of the National Academy of Sciences*, vol. 114, no. 38, Sept. 2017, pp. 10125–10130, https://doi.org/10.1073/pnas.1706907114.